THE EFFECTS OF STIFFENERS ON THE BUCKLING OF CYLINDERS WITH MODERATE WALL THICKNESS

Thesis by

Henry T. Ponsford

In Partial Fulfillment of the Requirements

for the Degree of

Doctor of Philosophy

California Institute of Technology

Pasadena, California

1953

ACKNOWLEDGMENTS

On this first page of my thesis, I take pleasure in expressing my heartfelt thanks to the many people whose efforts have helped to make this study possible:

To Dr. Ernest Sechler, the Chairman of my committee, for his unfailing faith and guidance throughout the project.

To Dr. Donald Hudson and Dr. Harold Lurie, for their many helpful suggestions.

To Mr. Milton Wood, for the long hours he spent assembling the specimens and assisting with the experiments.

To the RAND Corporation, particularly Dr. James Lipp, for granting many of the hours I used on this study.

To my father, Mr. H. J. Ponsford, for his continued encouragement and assistance.

To Mrs. Marjorie Mowatt, for her draftmanship on the figures.

And, finally, to my wife, Marian, for her excellent secretarial work, and most importantly, for her devotion.

ABSTRACT

A series of 25 complete cylinders was tested experimentally to determine the effects of stiffening elements on the buckling of cylinders with moderate wall thickness, and to present a physical basis for an understanding of the mechanism of cylinder buckling.

It was found that both axial and circumferential stiffeners spaced at distances comparable to the buckle wave length of the unstiffened cylinder will raise the buckling stress, reduce the wave length, and alter the shape of the buckling waves. It was shown that for cylinders of D/t = 400, the addition of axial stiffening as little as 2% or 3% of the cylinder wall material can raise the buckling stress by 30% over the unstiffened case.

The experiments of this study lend support to a theory developed by Donnell and Wan which ascribes the reduction of the buckling stress of a real cylinder below the classical theoretical value to the initial imperfections of construction in the real cylinder. Conversely, the results cast doubt on the validity of the theory which explains the "premature" failure on the basis of external energy disturbances present in the testing laboratory.

It was shown that the buckling waves of a reasonably well-made cylinder develop with extreme rapidity without the necessity of a change in cylinder length, and are fully developed in their lateral dimensions throughout the buckling process. Some previous results of Kanemitsu and Nojima which exhibited an essentially different buckling mechanism were explained as the consequence of excessive initial imperfection.

A brief study of the vibrations of a cylinder under axial load demonstrated an approximate correlation between the vibration and buckling modes of the cylinder.

TABLE OF CONTENTS

TABLE OF CONTENTS (Cont.)

LIST OF FIGURES

LIST OF FIGURES (Cont.)

LIST OF FIGURES (Cont.)

LIST OF FIGURES (Cont.)

LIST OF FIGURES (Cont.)

LIST OF FIGURES (Cont.)

LIST OF FIGURES (Cont.)

LIST OF TABLES

EXPLANATION OF SYMBOLS

a	Buckle half-wave length in the x direction
b	Buckle half-wave length in the y direction as used in the von Kármán-Tsien equation for W; also cylinder panel width (circumferential direction) for a stiffened cylinder, inches
D	Cylinder diameter, measured from the mid-thickness of the skin, inches
E	Young's modulus, psi; without subscript, E is the Young's modulus of the cylinder skin
F	The Airy stress function
f_o, f_1, f_2	Arbitrary constants in the von Kármán-Tsien buckle wave equation
h	Cylinder panel height (axial direction), inches
I	Moment of inertia of the cross-section of a stiffening element, in^4
K	Dimensionless constant in Donnell's equation, used to define the degree of initial imperfection
L	Cylinder length, inches
m	Arbitrary constant, see f_o
N	Number of axial stiffeners on a cylinder
n	Arbitrary constant, see f_o
R	Cylinder radius (=D/2), inches
t	Cylinder skin thickness, inches
U	Dimensionless "unevenness coefficient" defined by Donnell $\left(= \frac{w_o \pi^2 t}{a^{3/2} b^{1/2}}\right)$

EXPLANATION OF SYMBOLS (Cont.)

W	Strain energy in one complete buckle, in-lb
w	Deflection coordinate normal to a plane tangent to the cylinder, positive inwards, inches
x	Axial coordinate, inches
y	Circumferential coordinate, inches
μ	Poisson's ratio of the cylinder skin material
σ	Tension or compression stress, psi
σ_B	Buckling stress, psi
σ_{cy}	Yield stress in compression, psi
σ_x	Stress in the x direction, psi
σ_y	Stress in the y direction, psi
τ_{xy}	Shear stress in the x,y plane, psi
$( )_f$	Pertaining to frames
$( )_{st}$	Pertaining to stiffeners

PART I - INTRODUCTION

The objective of this study was the examination of a type of aircraft structure which is coming into increasing use: the cylinder of moderate wall thickness. In the past, the aircraft stress analyst has been required to deal with two widely separated types of cylindrical structures: cylinders of large diameters and thin walls, such as metal skinned fuselages; and cylinders of small diameters and thick walls, such as struts and structural tubing. Both types could be simplified for analysis under compressive stresses; the thin walled cylinder buckles at low stresses so the structure could be considered as a group of stiffeners acting as columns, whereas the thick wall cylinder does not experience local buckling in the usual cylinder failure sense, and could also be treated as a simple column.

With the present trend toward sonic speeds, new factors are changing the structure of the past. On the one hand, higher speeds require smaller frontal areas and larger fineness ratios; on the other hand, the high speeds produce larger air loads. The combination of these effects leads both to increased bending moments, and to smaller diameters which decrease the structural resistance to bending. In addition, less skin buckling can be tolerated if the degree of smoothness required for high

speed flight is to be attained. These design trends must be countered with increased skin thicknesses, and so a new type of cylindrical structure emerges which is intermediate between the two of the past. This structure may be envisaged in practice as the fuselage of a high speed fighter aircraft or guided missile.

Unfortunately, the new structure poses problems to the stress analyst which are as yet not completely solved. In a cylinder of high D/t (diameter/thickness) ratio, subjected to bending or compressive loads, the skin buckles at a stress far below the material working stress, and most of the load is actually carried by stiffeners acting as columns, aided by small strips of skin immediately adjacent to them. As a consequence, the stress analyst has not been required to calculate the local buckling stress of the skin to any great accuracy. In the new type of structure, however, the cylindrical shell must carry the major part of the loads, and yet it cannot be allowed to buckle because this would involve, at the least, an intolerable roughening of the external surface of the aircraft, and possibly a complete collapse of the structure.

The present study was consequently made to obtain a better understanding of the problems involved in analyzing the intermediate type of structure; that is, cylinders

with moderate D/t ratios (approximately 300 to 750 for aluminum alloys) which fail by the formation of buckling waves in the skin. In addition, the cylinders considered were too short to fail as Euler columns. Though only the local or panel type of instability was studied, the formulation may properly be generalized to include the general instability (frame failure) case as well.

PART II - OUTLINE OF THE STUDY

Because the many aspects of the cylinder buckling problem are so interrelated, it is difficult to discuss one facet without reference to the other sides of the problem. To facilitate the detailed treatment of each individual sub-problem considered in the thesis, a synopsis of the entire project will be presented first to serve as a frame of reference.

A literature survey showed that the study of the cylinder buckling problem dated back many years, but that it was still a subject of controversy. Several investigators developed theoretical solutions for this problem in the earlier part of the present century using the small deflection stability concepts of classical elasticity. Although their results generally agreed with each other, they showed poor agreement with early experimental tests, being somewhat non-conservative. Kanemitsu and Nojima carried out experiments in 1939 to study realistic buckling wave patterns, since experimental patterns did not conform to the ones used in the classical theories. Kanemitsu and Nojima also found in certain cases that the buckling started as very small waves and grew to the full sized final pattern as strain increased. Using a wave shape similar to the results of Kanemitsu and Nojima, von Kármán and Tsien developed an approximate theoretical

solution for a perfect unstiffened cylinder using a non-linear, large deflection type of analysis, which showed that a cylinder could be maintained in a buckled state by stresses very much less than the theoretical buckling stress. The mechanism by which an experimental cylinder jumped "prematurely" into the buckled state was still a matter of conjecture, several explanations having been put forth by investigators. In 1942, Leggett and Jones refined the von Kármán-Tsien work in an extensive calculation leading to detailed quantitative results.

One result of Leggett's work was a prediction that the number of circumferential waves at buckling would be approximately $0.3\sqrt{D/t}$. If D/t were about 500, the number of waves would be 6 or 7, and so the preferred wave length would be of the order of the radius of the cylinder. The author proposed that the buckling stress of a cylinder of these proportions might be raised significantly by the use of a reasonably small number of light stiffeners spaced to interfere with the normal wave pattern of the unstiffened cylinder. Kanemitsu and Nojima's experimental results concerning buckle growth threw some doubt on the effectiveness of this general structural device when applied to cylinders, and, because of the many doubts connected with the discrepancies between theory and experiment, a small experimental program was carried out to determine whether

the effect did in fact exist. The results of the experiments showed an unmistakable increase in the cylinder buckling stress as a result of the presence of stiffeners, and this increase in stress was associated with a systematic change in wave pattern.

Since the experiments succeeded in adding another paradox to the larger uncertainty, a brief attempt was made to analyze the stiffened cylinder problem by theoretical methods. The most logical starting point was the von Kármán-Tsien theory, but this theory made use of two simplifying assumptions (the use of an approximate wave shape and the neglecting of all boundary conditions) which were unfortunately not justified in the problem at hand. Since these assumptions had made von Kármán and Tsien's solution feasible from a mathematical standpoint, a more elegant effort proved impractical, and a more comprehensive experimental program seemed the next logical step. In view of the generally incomplete understanding of the entire cylinder buckling problem, several objectives were set for the program:

(a) A study of the effects of several physical parameters on the buckling stress increase caused by stiffeners.

(b) A check on the effect of experimental errors in load application on the stress distribution in cylinders

under test.

(c) A study of "frozen" buckling in cylinders of moderate D/t to be compared with Kanemitsu and Nojima's similar work on cylinders of high D/t.

(d) An attempt by continuous observation of all experimental effects to formulate a mechanism of buckling which would serve as a physical model for further theoretical work.

(e) A brief study of cylinder vibration modes as related to the buckling problem. This experiment was initiated late in the thesis program to verify a corollary of the physical model developed under objective (d).

Because of the time and expense required to carry out an experimental program, it was necessary for a number of specimens to serve more than one purpose. For this reason, the several lines of investigation were actually carried out concurrently, and their interaction will be seen as each is discussed separately.

PART III - SUMMARY OF PREVIOUS INVESTIGATIONS PERTINENT TO THE STUDY

The classical theory of cylinder buckling was developed earlier in the present century by Timoshenko[1], Southwell[2], Lorenz[3,4], Robertson[5], and others, using the small deflection linear theory of elasticity on perfect cylinders. The buckling wave pattern used by these investigators varied, since the actual shape was not easily predictable on the basis of intuition. Some used a radially symmetric bellows wave; others used either undefined wave shapes or types which have never occurred in experiment. In spite of the diversity of approach, a generally accepted equation for the buckling stress resulted:

$$\sigma_B = \frac{2E}{\sqrt{3(1-\mu^2)}} \frac{t}{D} \qquad [1]$$

where σ_B = buckling stress

E = Young's modulus

μ = Poisson's ratio

or, if $\mu = 0.27$, the familiar

$$\sigma_B = 1.2\, E \frac{t}{D} \qquad [2]$$

In the meantime, experimental workers such as Donnell[6], Lundquist[7], Wilson and Newmark[8], and others performed experimental tests on cylinders, and found that buckling stresses were much lower than predicted by the classical equation. Donnell[6] attempted to show theoret-

ically that the discrepancy was caused by small initial imperfections in the cylinder. He derived two equations using a large deflection, non-linear theory which satisfied the compatibility and equilibrium conditions completely in terms of the Airy stress function, F. These equations were

$$\left(\frac{\partial^2}{\partial x^2}+\frac{\partial^2}{\partial y^2}\right)^2 F = EK\left[\left(\frac{\partial^2 w}{\partial x\,\partial y}\right)^2 - \frac{\partial^2 w}{\partial x^2}\frac{\partial^2 w}{\partial y^2}\right] - \frac{E}{R}\frac{\partial^2 w}{\partial x^2} \qquad [3]$$

$$\frac{Et^2}{12(1-\mu^2)}\left(\frac{\partial^2}{\partial x^2}+\frac{\partial^2}{\partial y^2}\right)^4 w + \frac{E}{R^2}\frac{\partial^4 w}{\partial x^4}$$

$$= \left(\frac{\partial^2}{\partial x^2}+\frac{\partial^2}{\partial y^2}\right)^2\left[\frac{\partial^2 F}{\partial y^2}\frac{\partial^2 w}{\partial x^2} - 2\frac{\partial^2 F}{\partial x\,\partial y}\frac{\partial^2 w}{\partial x\,\partial y} + \frac{\partial^2 F}{\partial x^2}\frac{\partial^2 w}{\partial y^2}\right] \qquad [4]$$

where x = axial coordinate

y = circumferential coordinate

w = deflection coordinate normal to a local tangent to the cylinder

K = factor proportional to initial imperfection

R = cylinder radius

Unfortunately, no exact general solution of these equations has ever been found. Donnell worked out an approximate solution which was of insufficient accuracy to produce significant results. Flügge[9] attempted to explain the discrepancy between theory and experiment on the basis that the theoretically assumed cylinder end conditions were not duplicated in experimental work, but von Kármán and Tsien[10]

pointed out that this approach could not explain such large differences.

In 1939, Kanemitsu and Nojima[11] correlated all experimental work performed to that time, together with their own results, into an empirical relationship

$$\frac{\sigma_B}{E} = 9\left(\frac{t}{R}\right)^{1.6} + 0.16\left(\frac{t}{L}\right)^{1.3} \qquad [5]$$

for $500 < R/t < 3000$

$0.1 < L/R < 1.5$

where L = cylinder length

This equation described the actual performance of cylinders, and was a notable illustration of the discrepancy between theory and experiment. In addition, Kanemitsu and Nojima performed special tests on several cylinders for the purpose of determining visually the mechanism of buckling. They designed test equipment which gave very close control of applied end shortening, and "froze" the buckling process of several cylinders with D/t = 3740. In these experiments, they were able to develop the buckles slowly under good control, and were also able to take the buckles out of the skin by reducing the end shortening. They found that the buckles tended to form initially as small elliptical dimples, shifting about and growing in both area and depth as end shortening was increased, until they eventually formed a characteristic regular "diamond" pattern of the larger final buckles. They attempted similar experiments on cylinders

of D/t = 2500, but found that the final buckle pattern formed very suddenly over a considerable area, and the buckling process was not amenable to control. They speculated that more "refined" ("rigid", perhaps?) equipment would give them the control which they lacked over the stronger cylinders. The "diamond" buckle pattern described by Kanemitsu and Nojima formed a physical model for theoretical work carried out shortly thereafter by von Kármán and Tsien, and the observed buckle "growth" mechanism eventually influenced the experimental program of the author's study.

Von Kármán and Tsien started with Equation [3], the first of the two large deflection non-linear equations developed by Donnell, but converted it to the case of a perfect cylinder by deleting the initial imperfection factor, K. They were successful in solving the modified equation by an energy method which gave sufficient accuracy to define the essential features of the problem[12,13]. They established an equation for a buckling wave pattern which defined a surface approximately similar to the diamond buckling pattern of Kanemitsu and Nojima in terms of five undetermined coefficients:

$$\frac{w}{R} = \left(f_0 + \frac{f_1}{4}\right) + \frac{f_1}{2}\left(\cos\frac{mx}{R}\cos\frac{ny}{R} + \frac{1}{4}\cos\frac{2mx}{R} + \frac{1}{4}\cos\frac{2ny}{R}\right) + \frac{f_2}{4}\left(\cos\frac{2mx}{R} + \cos\frac{2ny}{R}\right) \qquad [6]$$

where f_0, f_1, f_2, m, and n are the arbitrary coefficients. This equation represented a set of cosine waves parallel and perpendicular to the cylinder axis superimposed on a second set running at arbitrary angles to the first. If it is substituted into the modification of Equation [3], the stresses in the cylinder can be evaluated in terms of the arbitrary coefficients. An expression can be written for the strain energy, W, in one complete wave:

$$W = \frac{t}{2E} 4\int_0^a\int_0^b \left[(\sigma_x + \sigma_y)^2 - 2(1+\mu)(\sigma_x\sigma_y - \tau_{xy}^2)\right] dx\,dy + \frac{t^3 E}{24(1-\mu^2)} 4\int_0^a\int_0^b \left[\left\{\frac{\partial^2 w}{\partial x^2} + \frac{\partial^2 w}{\partial y^2}\right\}^2 - 2(1-\mu)\left\{\frac{\partial^2 w}{\partial x^2}\frac{\partial^2 w}{\partial y^2} - \left(\frac{\partial^2 w}{\partial x\,\partial y}\right)^2\right\}\right] dx\,dy \qquad [7]$$

where

a = buckle half-wave length in the x direction, inches

b = buckle half-wave length in the y direction, inches

σ_x = stress in the x direction, psi

σ_y = stress in the y direction, psi

τ_{xy} = shear stress in the xy plane, psi

The first integral of Equation [7] gives the strain energy of extension of the mid-surface; the second, the strain energy of bending out of the plane of the sheet. The arbitrary coefficients of the buckling wave expression can be determined by substituting the cylinder stresses determined from the modified Equation [3] into the equation for strain energy, Equation [7], and minimizing the resulting expression with respect to these coefficients, without references to boundary conditions. Von Kármán and Tsien fixed three of the coefficients on the basis of judgment and minimized the strain energy to obtain the other two. The resulting solution gave a buckling stress equal to the classical value, but, in addition, described the post-buckle equilibrium states which are shown in Figure 1 as the curve labeled "perfect cylinder". The existence of a second set of equilibrium states with the same values of strain as the unbuckled cylinder but at much lower stresses showed the cylindrical shape to have a buckling mechanism essentially different from other common

structures. It gave a strong clue to the possibility of "premature" buckling, but left undefined the mechanism by which cylinders tested in the laboratory were moving into the post-buckle equilibrium state without first going up to the buckling stress for perfect cylinders. Von Kármán and Tsien speculated that the premature buckling was caused by a weakness resulting from initial imperfections, or by random exitations from vibrations present in the laboratory which increased the strain energy of a cylinder momentarily, or both. Upper and lower bounds were placed on the buckling stress by von Kármán and Tsien on the basis of energy considerations which bracketed experimental values. These bounds were later extended on the basis of a more extensive study by Tsien[14,15]. Leggett and Jones[16] carried the von Kármán-Tsien work further by a simultaneous variation of four undetermined coefficients of the buckling pattern instead of two, providing more accurate quantitative results within the assumptions of the theory.

During the same years, a number of investigators[17] [18,19,20] performed experiments on curved panels to provide empirical information useful in aircraft design. Most of this work concerned panels of the higher D/t values characteristic of aircraft fuselages of the past, and did not throw light directly on the problem of this study.

The work of Welter[21,22,23], however, was an interesting variation. He tested a number of curved panels of fairly high D/t value which were mutilated by a variety of defects, such as round holes, slits running both circumferentially and axially, dents made by forcing small diameter steel spheres into the skin, and even ragged holes made by firing bullets through the panels. A general result of Welter's work was that mutilations extending across a distance comparable to, or greater than, a buckling wave length, produced significant reductions in the buckling stress, but small imperfections, even though severe, had little effect. Cox and Pribram[24] presented a paper in 1948 which, although its purpose was different from the present study, gave an excellent synopsis of the history described in the preceding pages.

In 1950, Donnell and Wan[25] carried out a theoretical analysis of unstiffened cylinders with initial imperfections by combining Donnell's original general large deflection, non-linear equation (Equation [3]) with the von Kármán-Tsien buckle wave form (Equation [6]), and solved for all five undetermined coefficients simultaneously by minimizing strain energy. The only initial imperfections considered to be significant in the analysis were deviations of the same wave length and amplitude distribution as the buckle pattern. The imperfect cylinder

stress-strain characteristics are shown in Figure 1, which was taken directly from Donnell's paper, for various amounts of initial imperfection. In this figure, Donnell showed that initial imperfections have a profound effect in reducing the buckling stress below that of a perfect cylinder. It should be noted that this theory explained the lower buckling stresses by a mechanism which allowed the cylinder to remain in equilibrium until after the buckling had begun. In contrast, the "energy barrier" theory required the cylinder to leave the equilibrium state (defined by the inclined straight line of Figure 1) and hurdle an adjacent higher energy state under external exitation in order to reach the buckled state. No experimental evidence was available, however, to prove or disprove the validity of either theory as a proper explanation of the premature buckling.
Towards the end of the thesis project, an unpublished English translation of a paper by Yoshimura[26] came into the possession of the author. Although the paper was concerned primarily with a study of long cylinders, it presented a geometrical concept of the cylinder buckling wave pattern which was of considerable interest to the problem at hand. Yoshimura proved the existence of a geometric family of concave polyhedrons which are developable from an unbuckled cylinder without distortion, and are remarkably similar in configuration to observed buckle waves. The physical existence of this family can easily

be demonstrated by the construction of models from single pieces of cardboard, and two such models are illustrated in Figures 76 and 77. This concept will be discussed further in Part VII.

PART IV - THE POSSIBILITY OF LARGE GAINS FROM SMALL STIFFENERS

An inspection of Leggett's numerical results showed that as the D/t ratio of an unstiffened cylinder decreased, the preferred wave size increased. For the D/t range of interest in this study, the number of waves around the circumference was predicted to be 6 or 7. This result suggested to the author the possibility of using a reasonably small number of light stiffening elements to raise the buckling stress by interfering with the preferred wave pattern. This hope was based on the fundamental consideration that a structure will always fail in the mode which has the lowest associated failing stress, but if failure in that mode is made more difficult by external means, the structure will choose a different mode which must have a higher failing stress than the first. It should be emphasized that the proposed additional elements were truly stiffeners in that their primary action was to interact with the skin, rather than to serve as load-carrying columns in their own right.

A survey of previous work on cylinders to prove or disprove the effectiveness of this proposal was inconclusive. The theoretical work based on the von Kármán-Tsien method considered only unstiffened shells without boundary conditions, and gave no clue to the changes which

might result from distorting the wave pattern, either from its true shape or from the approximate shape assumed by von Kármán and Tsien. Considerable experimentation has been carried out on stiffened panels to aid aircraft designers, but these tests were performed on panels of D/t ratios higher than those of interest in this study, and, as a result, the panel widths were considerably larger than the buckle wave lengths.

The only careful qualitative experiments found which seemed to throw light on the problem were the "frozen" buckling tests of Kanemitsu and Nojima. Their work indicated that buckles began at places of local weakness with a wave length somewhat smaller than that of the final pattern, and then spread in lateral dimension while moving over the surface to fill in the complete pattern. If this behavior were typical of all cylindrical structures, then stiffeners which were separated by distances of the order of the wave length of the final buckle pattern might have spacings much larger than the initial wave length, and thus would exert little or no effect on the initiation of failure.

In spite of this negative indication, it was decided to test a family of four cylindrical specimens in the laboratory to see whether stiffeners were effective in interfering with the buckling process. A description of

the specimens and test procedures is presented in detail in Part VI-A, and the results of the tests are discussed in Part VI-B. It will be sufficient at this point to state that these preliminary results constitute 4 of the 8 specimens on Figure 113, which figure indicates a definite increase in the buckling stress with increasing number of stiffeners. Furthermore, the increase in number of stiffeners was associated with a continuous change in the buckle wave pattern in the direction of smaller wave lengths. As this experimental evidence was in conflict with what might be predicted from the work of Kanemitsu and Nojima, it was clear that further study was necessary to an understanding of the problem.

PART V - THEORETICAL BACKGROUND OF THE EXPERIMENTAL STUDY

Because of the similarities between the stiffened cylinder problem and the theoretical work of Donnell, von Kármán, and Tsien, a natural starting point was to examine their methods for suitability to the present problem. The formulation of the differential equations of a cylindrical shell by Donnell was general, and would give a correct solution for the stiffened case if the equations could be solved and the appropriate boundary conditions substituted. Unfortunately, no way of solving these equations could be found, and so recourse was made to approximate solutions using minimum energy methods. This procedure was extremely laborious, and unless it could be simplified to a considerable extent, was prohibitive. Von Kármán and Tsien were able to find two valuable simplifications for the unstiffened problem:

(a) A useful approximate expression for the wave pattern was developed which contained only 5 undetermined coefficients, and,

(b) It was not necessary to include any effects of boundary conditions because the buckle wave length was small compared to the cylinder dimensions.

Neither of these simplifying assumptions was permissible in the stiffened cylinder problem. It was not useful to assume a uniform approximate wave shape in a problem

where an essential feature was the distortion of the wave shape by external influences such as stiffeners. Similarly, the boundary conditions in the realistic problem were in themselves extremely complicated. Because of the axial compression present throughout the structure, the stiffener had to act as a column, but if it were also to exert virtual transverse forces on the skin to interfere with buckling waves, it would then become a beam-column subjected to a number of possible distributed side loads depending on the many wave patterns available to the skin. One line of approach to an analysis of the skin behavior would have been to assume idealized boundary conditions, such as simply supported or clamped edges. Unfortunately, this procedure would have ignored a study of the stiffener itself, which was an essential part of the problem. The practical value of using stiffeners in this way depended on the minimum size of stiffener required to achieve effective interference, as their presence represented a weight penalty which might be utilized in other ways, e.g., increasing the skin thickness.

An additional difficulty in approaching the problem was the possibility that stiffeners might have no effect on the buckling of perfect cylinders, but that they might have a considerable influence on the factors which cause "premature" buckling. Donnell's paper[25] accounted for the effect of initial imperfections of unstiffened cylin-

ders in an approximate manner, but again, since small differences in buckling patterns resulting from the presence of stiffeners were of primary importance, a more accurate approach was probably necessary to obtain significant results.

It was realized at this point that no useful theoretical solution of the problem was feasible with the state of knowledge available at the time. As a basis for a future theoretical solution which might account for more of the realistic complications, an experimental program was laid out which had two principal objectives: first, a descriptive parameter variation study of the effect of stiffeners on buckling; and, second, a group of special experiments to obtain a better understanding of the physical mechanism of buckling, of the discrepancies between a perfect cylinder with perfect loading and a real cylinder subjected to a disturbing environment, and of possible errors arising from the experimental methods themselves which might tend to confuse the comparison between perfection and experiment.

In an attempt to simplify the experimental parameter variation study, the stiffened cylinder problem was considered briefly from the point of view of dimensional analysis[27]. On the basis of physical intuition, it would seem that the significant parameters of the problem included: buckling stress (σ_B), yield stress of the skin

in compression (σ_{cy}), modulus of elasticity of the skin (E), cylinder diameter (D), skin thickness (t), panel height (h), panel width (b) or number of stiffeners (N), flexural stiffness of a stiffener $(EI)_{st}$, and flexural stiffness of a frame $(EI)_f$. Unfortunately, these variables do not lend themselves readily to reduction by the principles of dimensional analysis because they are so numerous and so uniform in dimensional character. It was not possible to investigate the effects of all the parameters within the time and effort available to this experimental program. The particular variables which were not considered and the extent to which the others were investigated will be discussed in the following section.

PART VI - EXPERIMENTAL PROGRAM

A. General Experimental Equipment and Test Procedures

The first objective of the experimental program was to investigate by parameter variation the effect of stiffeners on the buckle pattern and the buckling stress. From the theoretical consideration, it was clear that an indispensable requirement of the specimen design was to achieve realistic boundary conditions for each panel of the cylinder. For this reason, it was felt necessary to use specimens which were complete cylinders assembled with aircraft rivets, instead of the more economical curved panels with artificial supports which have been used by several other investigators.

A drawing of a typical specimen is presented in Figure 2. Stiffening elements of rectangular cross section were used in order to insure accurate determination of flexural rigidities. The frames were placed on the outside of the cylinder and the axial stiffeners on the inside to eliminate the necessity of notching at points of intersection. Although this arrangement was not the best aerodynamic design, it essentially duplicated the structural properties of typical aircraft construction. The rivets were spaced in every case to prevent skin buckling between rivets. The ends of the cylinders were milled flat after assembly by mounting the cylinder on a

precision turntable and rotating it under a milling cutter in order to insure as nearly perfect radial symmetry in load application as possible, and to minimize any local bending moments on the ends of the cylinders.

The method of applying compressive loads is illustrated in Figure 79. The actual loading surfaces were two mild steel plates 18" in diameter and 2¼" thick. The flat surfaces of these plates were finished by grinding. The lower plate rested on a spherical seat (radius of the sphere was 4") to permit the lower loading plate to align itself and thus prevent eccentric load application. The upper loading plate was simply bolted against the loading head of the testing machine in the four preliminary tests, but an examination of the results of those tests showed that the plate was bending slightly under load because of high spots on the lower surface of the machine loading head. As a result, a plaster shim was cast between the machine loading head and the upper loading plate (see Figure 93, for example) for the remainder of the test program. The effectiveness of this shim is discussed in Part VI-C. The testing machine was manufactured by Baldwin-Southwark, and equipped with an Emery capsule type weighing system. The load was applied by means of a hydraulic piston, and the indicating scale had ranges of 12,000 lb, 60,000 lb, and 300,000 lb.

In order to sample the distribution of stress around

the circumference of each specimen, four strain gauges of the SR-4 type were mounted on the mid-height cross section, as shown in Figures 79 through 107. These strain gauges were read by means of a Leeds and Northrup slide wire potentiometer through a suitable bridge circuit consisting of a 6-volt automobile battery, a switching panel, and dummy gauges of the same type as were mounted on the cylinders. The test equipment, including the strain gauge measuring apparatus, is illustrated in Figure 78. Cylinder deflections were measured by Federal dial gauges mounted at equidistant points around the circumference. These gauges were marked with divisions of 0.001", and readings were estimated to 0.0001".

The proportions and size of the specimens are given in Table 1. The specimen design was the result of several compromises with practical considerations. The maximum cylinder height which could be machined in the milling machine-turntable installation was 10". It was felt imperative to have a "buffer" section on each end of the cylinder in order to prevent any minor concentrated end loads from crippling the cylinder, and a test panel h/D ratio of 0.5 was considered to be as low as could be tolerated, so the maximum cylinder diameter was automatically determined to be about 13". In order to provide reasonable freedom from initial imperfections, a minimum sheet thickness for good workmanship was set at 0.020". The

combination of maximum diameter and minimum thickness set a practical upper limit on the D/t ratio of about 650. The minimum D/t ratio was limited only by the onset of plastic failure.

Because of the large number of parameters in the stiffened cylinder problem, it was necessary to restrict the experimental variation to several which seemed interesting and informative. Accordingly, it was decided to use only one material, limiting the parameters σ_y, E, E_{st}, and E_f to one value. The material chosen was 24S-T, but some of the later specimens had to be manufactured from 24S-T Alclad because of material shortage. A correction was used in the data reduction to account for the Alclad coating. In addition, it was decided always to use frames of sufficient stiffness to eliminate the possibility of frame failure and thus reduce the problem to one of "local" buckling, eliminating I_f as a variable. The method of selecting the frame size to achieve this result was proposed by Shanley[28], based on work by Dunn[29], and was successful in all specimens. These decisions left D, t, h, b or N, and I_{st} as remaining independent variables. The first three of these variables were arbitrarily set in dimensionless form as D/t and h/D, N was chosen over b as a variable because of its dimensionless character and because it was more convenient in the limiting case of an unstiffened cylinder, and I_{st} was kept in its original

dimensional form because of the large number of tests which would be required to determine which of the other dimensions formed the physically valid dimensionless variable in combination with the stiffener moment of inertia.

The specimens were grouped into families as follows (see Table 1): Nos. 1-4 were the original preliminary specimens which formed a group with $D/t \doteq 400$, $h/D \doteq 0.5$, $I = 0.001648$ in^4, and N as the independent variable. Specimen No. 6 was later added to make this group more complete. Specimen No. 5 was also included, even though its value of I was different, because it formed a logical member of the family. Specimens Nos. 1A and 5A were duplicates of Specimens Nos. 1 and 5, respectively, to check the amount of experimental scatter, and also became members of this complete 8-specimen family. Specimens Nos. 7-10, together with Specimen No. 6, formed a family with common $D/t \doteq 400$, $h/D \doteq 0.5$, and $N = 6$, with I as the independent variable. The purpose of this group was to determine the effectiveness of different values of I in raising the buckling stress. Specimens Nos. 11, 12, and 13, together with 5 and 5A, formed a group with common values of $D/t \doteq 400$, $N = 2$, and $I = 0.000061$ in^4, with h/D as the independent variable. The objective of this group was to determine the effect of h/D on buckling stress and buckling wave pattern. It was similar in purpose to

the first group, except that the effect of frame spacing was to be investigated instead of axial stiffener spacing. Specimens Nos. 14-17 were a family with $D/t \doteq 670$, $h/D \doteq 0.5$, and $I = 0.001648$ in^4, with N as the independent variable. Specimens Nos. 19-22 were a group with $D/t = 352$, $h/D \doteq 0.5$, and $I = 0.001648$ in^4, with N as the independent variable. These last two groups were similar in purpose to the first group, but different values of the common D/t ratio were used in order to give an understanding of the effects on buckling stress and wave pattern resulting from a variation of both D/t and N. Specimens Nos. 14-22 were made of Alclad sheet; all others were of uncladded material.

Specimen No. 18 (the unlucky specimen) was built as a result of a shop error and was accidentally damaged during test, so it did not form a logical partnership with any of the other cylinders. The test of this specimen is discussed in Part VI-C-3. Specimen No. 5B was also a special case, and is discussed in Part VI-C-4.

The test procedure was straightforward; the load was increased by desired increments, and strain gauge and dial gauge readings were taken at each load. The testing machine load indicator was equipped with a maximum-reading indicator which permitted the measurement of buckling loads, even though the load dropped very

rapidly without warning when buckling took place. It was not feasible to obtain dial gauge readings at buckling in the same manner that load readings were taken, and so a certain amount of fairing and interpolation was necessary to establish the stress-strain curves near buckling. A circumferential coordinate system was established with 0^{o} corresponding to geographical North in the testing laboratory, reading clockwise in the normal manner of the compass. The points 0^{o}, 90^{o}, 180^{o}, and 270^{o} were labeled on each specimen, together with the serial number of the specimen, to facilitate interpretation of the test photographs (Figures 79 through 111).

B. Experimental Results of the Parameter Variation Study

The data obtained from the experimental tests are presented in Figures 3 through 111. Figures 3 through 27 show the familiar stress-strain curves for all of the specimens; Figures 28 through 50 show a sampling of the distribution of stress around the circumference of all cylinders tested with strain gauges. Figures 51 through 75 present a symbolic representation of the buckle pattern of each cylinder, and Figures 76 through 111 are photographs which show the actual characteristics of many of the buckle patterns of the program. The several figures which describe each particular specimen are interrelated by means of small code numbers (1, 2, etc.) which denote the order in which the various buckles appeared. For example, Figure 52 shows that the buckles in Specimen No. 1A appeared in three successive groups: the first from approximately 30° to 200°, the second from 260° through 0° to 30°, and the third from 200° to 270°. The stress and strain associated with each of these states are labeled 1, 2, and 3 on Figure 4, and a photograph of the specimen at the third state is given in Figure 80.

The basic data have been combined to show the variation of important parameters within families in Figures 112 through 117.

Much can be learned from a thorough study of this large body of information. Some of the more interesting points will be mentioned here. In considering the stress-strain curves (Figures 3 through 27), it is seen that the general character of the curves is similar to the results of the von Kármán-Tsien theory, assuming premature buckling from some cause, and of the Donnell theory with the same reservations. One interesting point not readily apparent is the fact that the unbuckled portions of the stress-strain curves are not exactly straight lines as predicted by the perfect cylinder theory. The initial concave-upward curvature in the vicinity of the origin is, of course, the result of taking up the slack in the specimen and test equipment, but a careful comparison of the curves shows that the upper portion of the unbuckled curve is slightly concave downwards. This curvature is so small that it might be well overlooked if the data from only one specimen were being plotted, but is unmistakable because it repeats identically in specimen after specimen. It will be shown in Part VII that this curvature was most probably not a result of plastic deformation. An interesting point to note is that Donnell's curves for imperfect cylinders, Figure 1, show this same concave-downward tendency prior to buckling.

After buckling, the stress-strain curves of the typical cylinder tests give little information of any real quantitative value. The magnitude of the first drop after buckling was a function not only of the strain at which the buckling of the imperfect specimen took place, but was also a function of the remaining strength of the stiffeners, which varied considerably from specimen to specimen. In the stress-strain curves of Specimens 14 through 17 (Figures 19-22), which had the largest stiffeners in comparison with their sheet of any specimens, it can be seen that the stiffeners continued to carry load after buckling almost without faltering when the skin gave up its full share of the burden. It should also be remembered that these cylinders of moderate wall thickness experienced plastic deformation after the buckle waves became severe.

Figures 28 through 50 show that the circumferential stress distribution exhibited a scatter above and below the average stress. In these figures, the ordinate is the reduced strain gauge data at four equally spaced points around the circumference, whereas the abcissa is the average stress obtained by dividing test machine load by the measured cross-section area of the specimen. These two stresses were not exactly comparable because the experimental errors associated with measuring strain

gauge data, specimen dimensions, and testing machine loads were independent of each other, and influenced the two stresses differently. An additional error in the strain gauge stresses occurred in Specimens Nos. 19 through 22, where the high stresses of these tests went beyond the proportional limit of the Alclad material, and the stress indicated by the strain gauges appeared higher than its real value. This apparent increase was a complex result of the action of the cladding when subjected to stresses above its proportional limit, but has not been considered important enough to the study to warrant elaborate correction of the strain gauge data.

If the experimental stress distributions were radially symmetric, Figures 28 through 50 should consist of four coincident straight lines. An examination of the figures shows that the curves are never coincident, but are usually straight. The reasons for the scatter are discussed in detail in Section VI-C-1. The curves are mentioned here because the highest stress existing around the circumference at buckling may be considered as a measure of the buckling stress as well as the average stress over the cylinder.

Figures 112 through 117 present the effects of the various parameter variations. In these figures, both average stress and maximum stress around the circumference

at buckling have been plotted for each specimen. It was found that the trends given by the two buckling stress criteria are similar in character. Figures 112 through 114 show the effect of variation of N on the buckling stress for the three values of D/t. It is seen that there was a significant increase in stress with number of stiffeners in every case. Although there was considerable scatter in the data, clear trends were established. Figure 113, representing a D/t of approximately 400, has been filled in more completely, whereas Figures 112 and 114 serve to check the same trend for the lower and higher values of D/t. Figure 115 is a modified cross plot of the average stress curves of Figures 112 through 114, with D/t as the independent variable instead of N. The ordinate has been modified from σ/E to $(\sigma/E)(D/t)$ to accentuate the relationship. Since the theoretical buckling stress of a perfect unstiffened cylinder varies inversely with D/t, one might expect $(\sigma/E)(D/t)$ to be invariant with D/t. The experimental deviation from this behavior is of interest. It is apparent that σ/E suffered a greater reduction from the theoretical value at the higher values of D/t than at the lower ones. This effect is well known, and has been demonstrated by Kanemitsu and Nojima[11], Donnell and Wan[25], and Batdorf, Schildcrout, and Stein[30]. Figure 115 also indicates, however, that the presence of stiffeners appeared to have more

effect on the cylinders of higher D/t, which were the weakest without stiffening.

The curvature of the lines in Figure 115 is probably not reliable, as the D/t values at approximately 350 and 670 were obtained from tests of Alclad specimens. According to tests carried out by Moore[31], an Alclad sheet has the same buckling properties as an uncladded sheet up to the yield point of the cladding, and to an uncladded sheet 93% as thick above the yield point of the cladding. The test specimens have been classified according to this approximate rule by assuming that the full thickness of the 0.020" thick Alclad sheet was effective because of the low buckling stresses of these specimens (Nos. 14 through 18), whereas the thickness of the 0.040" thick Alclad sheet was reduced by 7% since these specimens (Nos. 19 through 22) buckled at stresses clearly above the yield point of the cladding. It is well to mention at this point that tests by Atchison and Miller[32] showed that the proportional limit of 24S-T is 28,000 psi in transverse compression, and ANC-5a[33] lists the yield point for the same type of loading as 47,000 psi, so it is believed that the 24S-T material was substantially free of plastic effects at buckling throughout the study.

It should be noted in Figure 113 that Specimen No. 5

(N = 2) exhibited a buckling stress much higher than would be expected from the performance of the other seven members of its family. Specimen No. 5A was built and tested in an attempt to duplicate this performance, but Specimen No. 5A fell right in line with its fellows. The performance of Specimen No. 5 will be discussed further in Part VII.

A systematic comparison of Figures 51 through 75 shows that there was a regular change of wave shape with the number of stiffeners, the waves decreasing in size as the number of stiffeners became larger. Specimens Nos. 1-4 (see Figures 51, 53, 54, 55, 79, 81, 83, and 84) were a typical example. Specimen No. 1 exhibited a characteristic buckle extending the full height of the cylinder panel, with a circumferential wave length of one-eighth of the circumference. In Specimen No. 2, the wave size became noticeably smaller in the axial direction, and there were three waves in each of the four quadrants. It is interesting to note that the circumferential wave length did not decrease to the same extent as the axial wave length, since there were still the equivalent of 8 waves around the circumference, but these waves crowded the stiffeners much more closely than the waves in Specimen No. 1 crowded each other. In Specimen No. 3, the waves were spaced in diagonal pairs within the octants. The wave length was noticeably less than one-eighth of the circumference, since

one wave clearly did not fill the width of an octant. In Specimen No. 4, the waves had no choice but to occupy one-twelfth of the circumference or less. In some panels, waves of this size appeared. In others, the wave shape was very much distorted (see Figure 84). It was clear that 12 stiffeners around the circumference for $D/t \doteq 400$ caused a very great inhibiting action on the formation of the usual wave pattern. A similar search through the figures shows that the wave size also decreased as D/t increased.

Figure 116 shows that buckling stress was increased by a reduction in h/D below approximately 0.5, and that this effect increased rapidly for the smaller values of h/D. An inspection of Figures 64-66 and 93-95 shows, however, that the wave pattern adjusted more readily to a close spacing of circumferential stiffeners than to a similar interference from axial stiffeners. Figure 93 shows particularly that the waves could be compressed considerably in the axial direction while still maintaining their original circumferential dimensions.

Figure 117 shows that buckling stress appeared insensitive to variation in stiffener moment of inertia down to extremely low values. This insensitivity was all the more remarkable since the intercept of σ/E vs. N at $N = 0$ was at a value of $\sigma/E = 1.8$, as shown on Figure 113. The utility of this considerable effectiveness of very light

stiffeners will be discussed quantitatively in Part VII.

C. Special Experimental Studies

1. Radial Symmetry of Load Application

Flügge[9] suggested that imperfections involved in the end conditions of experimental cylinder tests might reduce the buckling load below that of perfectly assumed conditions. One of the purposes of the study was to verify experimentally whether or not, with reasonable technique, the stress distribution actually did exhibit radial symmetry, or whether circumferential regions of stress concentration existed which would cause premature buckling. Towards this end, each specimen was provided with four strain gauges spaced equally around the circumference to sample the distribution of stress.

It is well at this point to review the precautions which were taken in constructing the specimens and test equipment to insure radial symmetry of loading. In the preliminary tests, the cylinders were milled off on a turntable, taking care not to clamp any deformations into the cylinder during machining. Similarly, the surfaces of the loading plates were ground flat on a large capacity grinding machine, and were supported under conditions of radial symmetry, the lower resting on a centrally located spherical seat and the upper on a circular pad on the bottom of the test machine loading head.

The first four specimens showed characteristically

curved line variations of local stress versus average stress (Figures 28, 30, 31, and 32), and the slopes of the four lines in each specimen were not consistent. This curvature suggested a change in the errors of loading with magnitude of loading and could only be caused by deflections in the loading plates. It had previously been believed that the 2¼" thickness of the upper loading plate would be sufficient to overcome any minor irregularities on the bottom of the loading machine head; however, after testing the first four specimens, a plaster shim was cast between the upper loading plate and the test machine loading head to fill in any existing minor irregularities of contact. An examination of the circumferential stress distribution figures for Specimens No. 5 and up indicates that this shim was effective in eliminating the curvature of the lines and in bringing them to approximately the same slope. The consistent vertical scatter of the lines suggests an initial uneveness in the load application on each cylindrical element by its matching loading plate surface.

The differences between maximum and minimum circumferential stress at buckling for every cylinder have been determined and are presented in Table 2 both as absolute errors and as percentages of the average buckling stresses. The median values of these discrepancies were 3,440 psi and 16.9%. These figures represent significant errors,

which could easily have caused appreciable scatter in the test results even if no other inaccuracies existed in the problem.

The stress variation of 3,500 psi on the 10-inch long cylindrical elements would correspond to a deflection variation of approximately 0.0035". This spread might also be regarded as representing a ±0.0017" error in the contact of the loading plates and cylinder end surfaces around the circumference. When it is remembered that this error was the sum of errors resulting from the variation of cylinder element lengths, variation of flatness of each loading plate, and unsymmetrical deformations of the loading plates under load, it is seen that errors which were small from a machinist's standpoint were significant in the cylinder buckling tests.

It is interesting to compare the averages of the four strain gauge readings with the average stresses computed from the test machine loads. Table 3 presents the error between the average strain gauge stress and the average test machine stress as a function of test machine stress for the 23 specimens which were equipped with strain gauges. It can be seen from Table 3 that a typical error between two average stresses was of the order of 1% to 2% for the uncladded specimens, and 6% to 8% for the uncorrected Alclad specimens. If the scatter between the four

strain gauge readings (mean error of 16.9%) were principally a result of experimental error or local bending in the sheet, one would expect that the averages of these readings would still differ somewhat from the test machine average stress. Table 3 shows, however, that the agreement between the two average stresses was markedly better than the agreement among the strain gauge readings themselves. It was concluded from this comparison that the strain gauge stress variation around the circumference was, in fact, the result of an actual variation of stress rather than experimental error.

One of the experimental results of this circumferential variation of stress was to cause some of the specimens to buckle on only a part of the circumference. This effect can be seen in Figures 51 through 75.

2. Study of Cylinder Behavior Immediately Following Buckling

Kanemitsu and Nojima[11] performed an interesting experiment on the mechanism of buckling by testing a cylinder in a special set-up which guaranteed a very close control over axial deflection. For cylinders of D/t = 3740, they were able to stop the buckling process at any point in the formation of the buckles, and even to reverse the process, taking the buckles in and out of the skin at will by controlling the end shortening. They found that the buckles started as small indentations, apparently in the vicinity of imperfections in the skin, and became larger as end shortening was increased, moving about until they formed a regular buckling pattern. A similar experiment was attempted on cylinders of D/t = 2500, but no success was attained in "freezing" the buckling process, the buckles forming very rapidly in a complete pattern. They surmised in their discussion that the lack of control over cylinders of D/t = 2500 resulted from a lack of rigidity in their test equipment, and, that with more powerful equipment, they could duplicate the buckling control which they had over the thinner cylinders.

An understanding of the formation mechanism of the buckles, particularly of the question as to whether buckles form with a small initial wave length and increase in size,

or whether they have a large wave length from their beginning, is important when one attempts to interfere with these waves with stiffeners. Consequently, an experimental attempt was made to repeat the phenomenon found by Kanemitsu and Nojima with the cylinders of moderate D/t considered in this work. Three jacks (Nos. 1, 2, and 3) were designed as shown in the upper half of Figure 118 to be spaced equally around the circumference of Specimen No. 5 during loading (see Figure 85). The jacks were to be kept firmly compressed between the loading plates so that when the cylinder buckled the jacks would resist the released potential energy of the testing machine, and would not permit this energy to crush the cylinder. A very high spring constant and a very fine degree of control were needed in these jacks, and they were designed accordingly. The combined spring constant of Jacks Nos. 1, 2, and 3 was 8,030,000 lb per inch, and the combined yield load, using a yield stress of 36,000 psi from ANC-5a[33], was 72,000 lb. In addition, it was possible, by turning the jack shaft a few degrees with a wrench, to change its length under load by small fractions of 0.001". These jacks were first used in the test of Specimen No. 5 as shown in Figure 118. Each jack was equipped with two strain gauges located diametrically opposite each other on the jack shaft. The strain gauges were wired in series to cancel out the effect of any

bending moments which the jack might experience, and, before the jacks were used in a cylinder test, a calibration run was made for each jack, from which a plot of load vs. strain gauge reading was obtained. A typical graph of this type is shown in Figure 119, and it may be seen from the consistency of the data that the jack was a very reliable load measuring device.

The test procedure used with Specimen No. 5 was as follows: The specimen was loaded without the jacks until a stress of 14,700 psi was reached. At this point, the jacks were installed as shown in Figure 118, and the jack loading cycle was begun. The machine load was raised 2000 lb with the jacks firmly in place. Because of the relative spring constants of the jacks and cylinder (5.1 to 1), most of this load increment would be carried by the jacks. Each jack was then backed off in turn to zero load, the drop in machine load being made good after each jack was backed off. In this way, the 2000 lb load increment was gradually shifted from jacks to cylinder, and at the end of the cycle, the jacks were pressed firmly against the upper loading head preparatory to receiving the load increment of the next cycle. An admitted weakness in this procedure was the lack of radial symmetry in load when one jack was unloaded and the others were not, but the eccentricity was small if small load increments were used. At any time during the test, the actual load which the cylinder was carrying could easily be

obtained by subtracting the sum of the three jack loads from the test machine load. The accuracy of this type of indirect measurement of the cylinder load is demonstrated in Figure 8, where the points on the unbuckled section of the curve above a stress of 14,000 psi exhibit no appreciable scatter. Every other one of these points was determined indirectly.

After several loading cycles with the jacks in place, the cylinder buckled violently at the first slight attempt to unload the first of the three jacks after raising the testing machine load. This was a very fortunate point in the cycle for buckling to occur, because all three jacks were firmly compressed between the loading plates by a load of approximately 500 lb each. When the cylinder buckled, it shifted large loads to each of the three jacks, which loads were determined by strain gauge measurements. From this point, the end shortening of the cylinder was gradually increased by adjusting the jacks. The stress-strain curve of the test is shown in Figure 8. The gradual development of the buckling waves reported by Kanemitsu and Nojima on cylinders of high D/t was not obtained; in fact, the violence of buckling in this specimen was as great as that of any other specimen in the experimental tests.

When the jacks were backed down until free, a very unexpected result was observed: each of the three jacks had

apparently sustained permanent compressive set, as the strain gauge readings did not return to zero. Since a total static load of 15,900 lb was transferred to the jacks during buckling, this would represent a stress magnification of approximately five-fold. Two explanations of the apparent compressive set have been proposed: (1) the strain gauges were damaged during buckling in a way which disturbed the strain gauge zeros (or, in other words, there was no permanent set as indicated); (2) a stress magnification was obtained from a dynamic phenomenon which involved the test machine masses and spring constants. The first explanation was refuted to some extent by the dial gauge deflection data taken before and after buckling, which indicated a drop more in agreement with a permanent set than with elastic deformation in the jacks. The second explanation could not be confirmed because of a lack of data concerning the testing machine characteristics, and remained as a speculation without proof.

After ten specimens had been tested, it was apparent that the buckling stress of Specimen No. 5 was considerably higher than would be expected from comparison with the other specimens. It was suspected that the presence of the jacks in this test may have had a supporting effect which the others did not receive, and so duplicates of Specimens Nos. 1 and 5 were tested with jacks in an attempt to repeat

the result. In addition, three new jacks (Nos. 1L, 2L, and 3L) were made which were similar to the previous set in design (see the lower half of Figure 118), but which had a combined spring constant of 16,300,000 lb per inch and a yield load of 171,000 lb in order to reduce the chance of permanent set in the jacks. In addition, the test procedure for operating the jacks was modified in order to keep all jacks continually under a much larger load to insure that any slack would be taken up before buckling.

The new test procedure was as follows: The cylinder was first raised to a load conveniently below the anticipated buckling load. The jacks were then placed in the test machine, and were tightened up firmly by hand between the loading plates. The jacks were given a pre-load by several cycles in which the machine load was increased and the jacks were then adjusted to take up this increase, until each jack was carrying 4,000 lb of pre-load and the load on the cylinder was the same as before the jacks were inserted. The cylinder load was then increased by increments as in the test of Specimen No. 5. The amount that each jack was backed off after each load increment was determined by setting the voltage reading equivalent to the desired load reduction on the strain gauge potentiometer, and then adjusting the jack until its load corresponded to the desired load.

Cylinder No. 1A buckled when the first jack had been unloaded to its standard 4,000 lb pre-load, and the second jack was in the process of being unloaded. The total load on the cylinder was thus slightly eccentric, although the increment being transferred was small compared to the total load. After buckling, the jacks were unloaded as before to increase the axial strain of the cylinder. The resulting stress-strain curve is shown in Figure 4. The jacks returned substantially to zero load at the end of the test, and apparently did not experience permanent set. A significant result of the test of Specimen 1A is that its buckling load was approximately the same as Specimen No. 1 in spite of the presence of the jacks.

Specimen No. 5A was then tested by the same procedure used for Specimen No. 1A. Buckling occurred in Specimen No. 5A at the same point in the cycle as in Specimen No. 1A. Jack No. 1L registered a very large load immediately after buckling, more than the entire load registered by the test machine, but the readings of the other two jacks seemed reasonable. The dial gauges indicated no unusual eccentricity of deflection, and it was assumed that the strain gauge in Jack No. 1L had been damaged during buckling in a manner which shifted its zero reading. The jack unloading part of the test of Specimen No. 5A was controlled from the readings of the dial gauges rather than the jack strain

gauges, as the jacks were not considered reliable indicators. At the end of the test, Jacks Nos. 2L and 3L returned substantially to their original zeros, but Jack No. 1L continued to register a very large load even when completely free. Jack No. 1L was recalibrated immediately after the test of Specimen No. 5A and proved in perfect order based on the new zero. Its recalibration graph is shown in Figure 119, and is very consistent. The stress-strain curve of the cylinder was computed using the final zero of Jack No. 1L, and appeared reasonable. It is presented in Figure 9.

No really satisfactory solution is presented for the peculiar behavior of the jack zeros in these tests. It is felt with some assurance that the small jacks actually experienced permanent set because of the correlation between the residual load reading and the end shortening measured during buckling. The extreme zero shift in Jack No. 1L during the test of Specimen No. 5A remains unexplained. This jack operated satisfactorily during the test of Specimen No. 1A, as did Jacks Nos. 2L and 3L in both tests. Fortunately, the zero shifts did not prevent the calculation of stress-strain curves for the cylinders, since it was possible to calculate the post-buckling loads using the final jack zeros instead of the original ones. Neither Specimen No. 1A nor 5A exhibited the high buckling stress of Specimen No. 5, so its superior performance was probably not

a result of the presence of jacks in the test.

The original goal of these specially restrained tests, a duplication of the Kanemitsu-Nojima control over the formation of buckling waves, was clearly not attained. In view of the fact that the tests of Specimens Nos. 1A and 5A involved jacks with spring constants ten times that of the cylinders being tested, it would seem that further increase in the stiffness of the jacks would be of little avail, and other factors must be studied to explain the phenomenon. It is mentioned in passing that the ratio of jack stiffness to cylinder stiffness in the Kanemitsu-Nojima tests was 3.9 to 1 for the "controlled" tests at $D/t = 3740$, and 2.7 to 1 for the "uncontrolled" tests at $D/t = 2500$.

A very interesting by-product of these restrained tests is apparent from an examination of the stress-strain curves of Specimens Nos. 1A and 5A (Figures 4 and 9). There is a short section of these two curves immediately following the first buckle in which the curve rises once more with a slope substantially equal to the original stiffness before buckling. After a short rise, there is evidence of a secondary weakening in the stress-strain curve, and the cylinder then exhibits the characteristic lethargic post-buckling performance of the other cylinders in the program. The physical counterpart of this behavior was as follows: In the initial

buckling failure, Specimens Nos. 1A and 5A did not fail entirely around the circumference as did Specimen No. 5 (see Figures 52, 56, and 57). As the strain was increased still more by adjusting the jacks, Specimens Nos. 1A and 5A carried greater loads for a short time, and then the remaining sections failed. After the entire circumference had buckled, the cylinders evidenced little remaining stiffness.

It would seem that the imperfectly loaded cylinders buckled first on one side at some maximum load point, and the resulting collapse crushed the entire cylinder. If jacks were present to support the loading head after the first buckle, the unbuckled section was saved and exhibited its original strength until a higher local stress was reached. This behavior was one of the strongest experimental verifications in the program of the contention that lack of radial symmetry in load application caused a reduction of the apparent average buckling stress of the cylinder.

3. The Effects of Gross Imperfections

Three specimens of the program sustained accidental damage before they were tested which resulted in gross initial imperfections, in contrast to the minor initial imperfections which existed in every well-made cylinder. Two of the specimens, Nos. 17 and 20, sustained dents of significant size during construction when the pneumatic rivet gun slipped off a rivet head and dented the sheet nearby. The dent on No. 17 was near an axial stiffener at approximately 115°, midway from top to bottom on the cylinder. The dent on No. 20 was on a center panel in the corner formed by the axial stiffener at 0° and the frame which defines the upper boundary of the center panel. Specimen No. 18 sustained serious damage at the very beginning of its test when a "pilot error" of the testing machine operator resulted in a very rapid increase in applied load which buckled the cylinder before the surge could be checked. The load was returned to zero, and the cylinder was found to have sustained permanent set in the form of small ridges outlining the buckling waves.

All three of these specimens were tested subsequent to their damage, and stress-strain curves for the three are given in Figures 22, 23, and 25. It is interesting to note the effects of the damage on the cylinder performance. No. 17 reacted normally under load until a stress of 12,000

psi was reached, at which point the rivet gun dent increased noiselessly in depth and width to form a small but definite buckle in the skin, illustrated in Figure 100. An inspection of Figure 46 shows that the local stress at 90° increased more rapidly than at the other three points from that stress until failure, indicating that the sections adjacent to the dent were picking up the extra load which was refused by the damaged section. This dent, however, did not bring on markedly premature buckling, as Figure 114 shows that Specimen No. 17 was fairly consistent with the other members of its family, perhaps a trifle low but not grossly out of line. The rivet gun dent in Specimen No. 20 produced no noticeable effect on the performance of the specimen. There was no apparent rearrangement of stress noticeable in the strain gauge data (Figure 48), as compared with Specimen No. 17. There was no increase in size of the dent prior to overall buckling, and the buckling stress appeared satisfactory when plotted with the other members of the family in Figure 112.

Specimen No. 18 was tested after its initial buckling and was found to have a stress-strain curve markedly different from all the other specimens. This curve, shown in Figure 23, has a strong similarity to the curve for $U\frac{D}{t} = 0.4$ of Donnell's imperfect cylinder analysis (Figure 1), if proper allowance is made for compression of the abscissa scale.

4. Vibration Tests as Related to Buckling

Towards the end of the study, it became apparent that some experimental information concerning the configuration of an infinitesimal wave pattern immediately after the beginning of buckling was essential to a confident understanding of the mechanism of wave growth. As it was felt impractical under the circumstances to obtain high-speed motion pictures of a buckle actually taking place, an indirect investigation into the configuration of infinitesimal waves was made by studying the vibration modes of a cylinder.

The specimen used for these tests was No. 5B, a duplicate of 5 and 5A. The cylinder was mounted in the previously used test set-up, but was vibrated by a mechanical oscillator installed as shown in Figure 108. This oscillator, which was similar in construction to one used in a flat plate vibration study by Lurie[34], was a modification of a high power, low fidelity, Navy surplus loudspeaker commonly known as a "Bull Horn." The loudspeaker cone was cut away except for four narrow strips which served as flexure links to maintain alignment of the remaining center of the cone. A light aluminum rod was cemented to the center of the loudspeaker and screwed securely to the cylinder, as shown in Figure 108. Power to operate the speaker was obtained from a Model 200-D Hewlett Packard variable frequency audio oscillator through a 30-watt

amplifier.

The cylinder was subjected to a moderate axial load, full power was applied to the vibrator, and the audio oscillator frequency was tuned through its entire range from 7 to 70,000 cps in a search for resonant frequencies. Several minor responses were obtained from the cylinder, but one unmistakable resonance was found near 1,000 cps, in which the entire circumference of the cylinder vibrated strongly. It was possible to detect the nodal lines of this vibration mode with considerable accuracy simply by running one's fingernail across the surface of the cylinder to detect the "dead" zones. The node lines were marked directly on the surface of the cylinder with grease pencil as they were found, and the pattern of these lines is illustrated in Figure 109. The exact curvature of the lines in Figure 109 is probably not significant, as the location of the node lines was rather vague towards the top and bottom of the center panel. The location of the lines as they crossed the mid-height of the cylinder, however, was extremely sharp. There were 16 node lines around the circumference of the cylinder; their mid-height cross section is plotted in Figure 120. These points have been compared with the location of 16 equally spaced points, and the average angular deviation of a node from the perfect pattern was found to be 2^{o}. Since each cycle of a serpentine wave contains two node lines, the cylinder was vibrating in a wave

pattern containing 8 circumferential waves. The resemblance of this pattern to the buckle patterns of Specimens Nos. 1, 1A, and 5A (Figures 51, 52, 57, 79, 80, 86, and 87) is striking.

After the node pattern was located, a brief study of the effect of variation of load on the vibration mode was made. It was found that the node pattern was invariant with changes in load, but that the resonant frequency showed a definite response. The square of the resonant frequency is plotted against load in Figure 121 as a matter of interest to others who may wish to study this problem further. The shape of this curve is dissimilar to comparable curves obtained in flat plate experiments by Lurie[34]. The sharpness of the resonant frequency was generally very marked, and it was possible to locate this frequency within close limits by ear. The lack of scatter in Figure 121 confirms this sensitivity. It is interesting, however, that the resonance peak flattened considerably at loads below 2,000 lb, and no particular resonance was discernible at zero load.

As a final test, the load was raised by increments until the cylinder buckled. At each increment, the exciting frequency was adjusted to resonance so that the cylinder was always subjected to a strong disturbing vibration favorably situated to cause buckling. It was readily apparent that this vibration was much greater in magnitude and in its

resulting effect on the cylinder than any random disturbance experienced during the test program. Nevertheless, the failing load of Specimen No. 5B while subjected to resonant vibrations was 33,000 lb, a value intermediate between the failing loads of the identical Specimens Nos. 5 and 5A.

PART VII - DISCUSSION

The data obtained in the experimental program were adequate to establish trends which throw a great deal of light on the important factors of the buckling of cylinders with moderate wall thickness, both unstiffened and stiffened.

It is apparent in the various figures that the presence of stiffeners on a cylinder produced a reduction in the buckle wave length, both in the axial and circumferential directions, a change in the shape of the wave resulting from the necessity of the wave to conform to the undeflected boundary condition at the stiffener, and an increase in the buckling stress. The effect of axial stiffeners seemed to be more pronounced than that of frames, possibly because the wave length was less readily compressed in the circumferential direction than in the axial direction (see Figures 84 and 93).

Figure 117 shows that the strength of stiffener required to interfere effectively with the buckling mechanism was very small. The increased buckling stress of the solid line in Figure 117 as compared with the N=0 intercept of the solid curve in Figure 113 is approximately 30%. The corresponding percentage increase in cross-section area of Specimen No. 7 over Specimen No. 1 was 20%. Specimen No. 7, however, contained stiffeners

of a cross-sectional shape which would never be used in an operational design. If solid rectangular stiffeners with a depth/width ratio of 2 were used instead of the corresponding ratio of 1/3 used in Specimen No. 7, the same stiffener moment of inertia could be obtained with a weight increase over the unstiffened cylinder of only 3%. This type of stiffener would lend itself readily to integral construction by extrusion. If the cylinder were fabricated, aircraft type stiffeners such as those described by Dow and Hickman[35] could be used, in which case the stiffener moment of inertia of Specimen No. 7 could be obtained with a weight penalty of less than 1% of the weight of the skin.

The effectiveness of stiffeners which constitute such a minor fraction of the total material is rendered more credible if one remembers that even a small stiffener has a moment of inertia much larger than the thin sheet adjacent to it, and can thus exert a real stiffening action to resist any potential buckle formation. A design principle yielding advantages of this magnitude is certainly worthy of considerable future investigation. The particular cylinder proportions represented in the specimens in this study did not represent any extensive attempt to obtain optimum proportions of skin and stiffener. The effect of variation in D/t on the amount of stiffening required to interfere successfully with

buckling was not determined; indeed, it is not certain that a curve of $\frac{\sigma_B}{E}$ vs. I would have the same flat characteristics for other values of D/t. There is no reason, however, to expect that the effect illustrated in Figure 117 would not hold true for values above and below a D/t of 400, and an experimental program somewhat larger than the present one could undoubtedly establish a family of optimum structures in which the concept of interference between stiffener and sheet buckles is used to advantage. The plot of $(\sigma/E)(D/t)$ vs. D/t in Figure 115 tends to indicate that D/t's higher than 400 may prove a more fruitful field for stiffened cylinder research than the lower values.

It will be emphasized again that this effect is essentially different from the use to which stiffeners have been put in aircraft fuselages up to the present time. The stiffeners of Specimen 7 did not act as load-carrying columns; in fact, if compressed without the skin, they would fail as fixed-end Euler columns at a stress of only 11,000 psi, less than half the actual buckling stress of the specimen. Their only value at the higher stresses is the stiffening which they exert on the skin adjacent to them.

A study of the circumferential stress distributions (Figures 28 through 50) and the results of the jack tests

shows that lack of radial symmetry of load application in experimental tests had the effect of introducing a scatter of approximately 10% into cylinder buckling stresses. As von Karman and Tsien[10] reported, this scatter was not sufficient to explain the discrepancies between the theoretical buckling load of a perfect cylinder and experimental results, but it served as a contributing factor to the uncertainty which has prevailed concerning the disagreement between theory and experiment. It was possibly not coincidental that Specimen No. 5, which was the only cylinder in the entire program that failed in a buckling pattern of perfect radial symmetry, was the only specimen with a buckling stress so high that it was clearly out of line when plotted with other members of its family.

A model of the mechanism of cylinder buckling will be set down and discussed in connection with experiments performed in this study and the work of others. The most important factor in the buckling of a cylinder was discovered theoretically by von Karman and Tsien: a cylinder reasonably free of initial perfection exhibits a stress-strain curve which is double valued for strains immediately below the strain corresponding to buckling. The physical counterpart of this theoretical result is explained by Yoshimura's concept of the two alternative

developable surfaces, one unbuckled, and the other buckled. No other common type of structure exhibits a stress-strain behavior of this type. The consequence of this double choice is that cylinders have the ability to jump from the unbuckled state to a buckled configuration without the possibility of restraint either from an applied load or an applied end shortening. This buckling mechanism peculiar to the cylinder was referred to as "Durchschlag" by von Kármán. English-speaking investigators have referred to the mechanism of "Durchschlag" as "oil canning", which seems a weak and inaccurate term to the author. The phrase "escape jump" is proposed instead; possibly not so satisfying as "Durchschlag", but perhaps as accurate.

Real cylinders invariably execute their escape jump at stresses somewhat below that predicted by theory for a perfect cylinder because of a sensitivity to certain physical factors not usually under the direct control of the laboratory investigator. For this reason, experimental data on cylinder buckling have tended to degenerate into a statistical mass, and theoretical conjectures on the factors causing the "premature" failure have remained without experimental substantiation or rebuttal.

Two basic causes for the "premature" jump have been suggested by various investigators: 1) the presence of

initial imperfections, and 2) the effect of random disturbances which add strain energy momentarily to the cylinder, permitting it to hurdle energy barriers to a buckled lower energy state beyond. The tests performed in this study can be grouped into an array according to the degree of the two proposed weakening factors:

Energy Disturbances	Initial Imperfections: Medium	Initial Imperfections: Large
Low	Specs. No. 1A, 5, &5A (medium buckling stress)	—
Medium	majority of tests (medium buckling stress)	Spec. No. 18 (low buckling stress)
High	Spec. No. 5B (medium buckling stress)	—

The definitions of the terms used in the array are as follows:

(1) Energy disturbances. Low disturbance is assumed to exist in a test in which considerable precaution is taken to shield the specimen against the effects of any disturbances which may be present in the laboratory from accidental causes. Medium disturbance is the normal random vibration present in a laboratory resulting from the operation of the structural testing machine, or from other equipment in the same building. Large disturbances result from a deliberate attempt in the test to excite the specimen.

(2) Initial imperfections. Medium initial imperfections are those deviations from a perfect cylinder which result inevitably in careful shop practice. Large imperfections are the result of deliberate or accidental damage to the specimen.

(3) Regions of buckling stress are defined qualitatively as follows: High buckling stresses are those approaching closely to a perfect cylinder. Medium buckling stresses are $\frac{1}{2}$ to 2/3 of the classical value, and low buckling stresses are $\frac{1}{4}$ to 1/3 of the classical value.

It can be argued that some of the experiments performed in this study fall into four of the six regions

defined by the above array:

(a) Low energy disturbance, medium imperfection. Specimens Nos. 1A, 5, and 5A fall within this category, particularly 1A and 5A. During their entire test, the three specimens were in physical contact only with the atmosphere of the room and the end plates of the loading machine which placed them in compression. There were no noticeable atmospheric disturbances during the tests such as strong winds, explosions, or the like, so it can safely be said that the only possible random energy disturbances which may have entered these cylinders had to come through the loading plates of the test machine. From Hooke's Law, any disturbance transmitted to the cylinder from the loading plates would have to be associated with an additional end shortening in order to transmit the force. These loading plates were supported by jacks which had a combined spring constant several times that of the cylinder, however, so any accidental reduction of the distance between the loading plates would have been resisted much more vigorously by the jacks than by the cylinder. As a result, the cylinder would receive considerable protection from accidental loading; in fact, a ten-fold attenuation might be expected in any disturbances affecting Specimens Nos. 1A and 5A.

Yoshimura[26] has stated that the energy barrier of a typical cylinder is about 7% of the total strain energy

in the vicinity of the lower buckling limit under a rigid test machine loading, and that this barrier decreases to zero at the theoretical buckling stress of a perfect cylinder. It is thus seen that any disturbance large enough to cause failure, even at a stress somewhat above the lower buckling limit, through the insulation provided by the jacks must be a very large disturbance indeed. Since no disturbances of this magnitude were observed during the tests of Specimens Nos. 1A, 5, and 5A, it is concluded that these cylinders experienced an environment of a low energy disturbance level. The buckling stresses of these cylinders were found to be in the buckling stress regime labeled as medium.

(b) Moderate energy disturbance, moderate imperfection. The majority of the tests in the program, which were performed without special equipment, were in this category, as can be seen from the definitions. Measurements made to determine the accuracy of construction of the specimens showed that the ellipticity of a single specimen was approximately $\pm\frac{1}{4}\%$ of the diameter. In addition, there were random deviations from the approximate elliptical cross-sections whose amplitudes were usually less than t, and deviations from straight cylindrical elements which were much less than t. The buckling stresses of these cylinders were within the stress region described as medium.

(c) High energy disturbance, moderate imperfection. The test of Specimen No. 5B clearly fell within this category. The specimen was excited by a vibrator of considerable power output operating in a direction perpendicular to the cylinder surface, tuned to the natural frequency of cylinder vibration, and causing a resonant vibration of the cylinder of appreciable amplitude. The disturbance provided in this test was far greater than any random disturbance observed during the other tests of the study. The buckling stress in the vibration test of Specimen No. 5B was in the medium category.

(4) Moderate energy disturbance, high initial imperfection. Specimen No. 18 falls within this category, since the initial accidental buckling of the cylinder resulted in a permanent set taking the characteristic shape of the actual buckling waves, the type of imperfection considered most significant in Donnell's analysis. The stress-strain performance of this cylinder when tested was so far below those of the other cylinders, that it can easily be placed in the low buckling stress regime.

An examination of the completed array indicates that the magnitude of disturbing vibrations had no significant effect on the buckling stresses of the cylinders, since all of the tests grouped in the first column (medium initial imperfection) buckled in the medium regime.

There is no clearer way of observing this insensitivity than to compare the results of Specimens Nos. 5A and 5B. These two specimens were identical in design, and were as nearly alike in construction as careful shop practice could make them. Specimen No. 5A was tested under the insulating protection of three jacks having ten times its stiffness, and buckled at a load of 32,100 lb. On the other hand, Specimen No. 5B was tested under the disturbing effect of a powerful vibrator tuned to its resonant frequency at the moment of buckling. Its failing load was 33,000 lb. There was obviously no severe weakening effect suffered by Specimen No. 5B in contrast with Specimen No. 5A.

Although the present program did not include a complete investigation of the effect of initial imperfections, a study of the array, together with the results of Welter[22,23] covering imperfections of the order of size of the buckling waves, shows clearly that initial imperfections had a marked weakening effect on the buckling stress. Two similarities between the experimental results of this work and the theoretical analysis of Donnell (Figure 1) were noted. The first is the slight reduction in slope of the stress-strain curves of the various cylinders just before buckling; the second is a very striking similarity between the stress-strain curve of Specimen No. 18 (Figure 23) and Donnell's curve for

$\cup \frac{D}{t} = 0.4$ (Figure 1). These similarities strongly support the contention that initial imperfections are the principal cause of the reduction in buckling stress of a real cylinder as compared to a perfect one. The performance of Specimens Nos. 17 and 20 also support Donnell's contention that imperfections somewhat smaller than the buckling wave length do not enter into the overall buckling process.

It has been argued that external disturbances could be much more decisive in operational experience than in the laboratory because of the general transient nature of airloads, and because they correspond more nearly to dead weight loading than to testing machine loading. According to the energy barrier theory, the lower buckling limit for dead weight loads is less than half that for rigid test machine loading. A test program using dead weight loading should be very enlightening in the comparison between the two theories. If the energy barrier theory were valid, it would be expected that buckling stresses with dead weight loading would be much reduced as compared to testing machine loading, whereas if the initial imperfection theory is the significant one, the two types of loading should give similar buckling stresses. Unfortunately, no dead weight tests on metal cylinders of a reasonable size have ever been performed

to the knowledge of the author.

The theoretical curves for imperfect cylinders derived by Donnell can be used to resolve the difference in buckling mechanism between the tests carried out by Kanemitsu and Nojima on cylinders of D/t = 3740, and the tests carried out by the author and by Kanemitsu and Nojima on cylinders of lower D/t. Donnell's curves show that differences in the degree of initial imperfection of a cylinder can cause an essential change in the buckling behavior. A cylinder with relatively small imperfections has inherently the same characteristic as a perfect cylinder; that is, a double-valued function of stress vs. strain for values of strain immediately below buckling. As the degree of imperfection increases, however, a point is reached at which the stress-strain curve becomes single-valued at all points. Such a cylinder does not have the ability to perform an escape jump, and fails by a continuous process.

Although the author has not measured the initial imperfections of cylinders with widely varying D/t ratios, it can be argued that such imperfections, expressed in terms of the skin thickness, increase as the D/t ratio increases. It is obvious that a constant absolute error in manufacturing is larger for cylinders of higher D/t ratio if expressed as a function of the skin thickness.

In addition, the absolute manufacturing error could well be larger for cylinders of higher D/t ratio, since it is well known to shop mechanics that satisfactory working of thin metal sheets becomes more difficult as the thickness decreases.

If these arguments are valid, one can then say qualitatively that the cylinders of D/t = 3740 tested by Kanemitsu and Nojima probably had larger initial imperfections than the other cylinders considered in the "frozen" buckling tests. The cylinders tested by the author and Kanemitsu and Nojima's cylinders of D/t = 2500, which corresponded to Donnell's nearly perfect cylinders, definitely had the ability to perform an escape jump from the higher-stress unbuckled equilibrium condition to the lower-stress buckled configuration. On the other hand, if the initial imperfections of the cylinders of D/t = 3740 were large enough to produce the single-valued stress-strain characteristic, a control over the behavior of the cylinder would have been obtained which was not present in the previous case. By sufficiently small variations in strain, the cylinder could be compressed through its highest stress value and lowered gradually by degrees into a completely buckled configuration, or, if desired, a buckled configuration could be eased back up over the stress hump to an unbuckled configuration. Both

of these phenomena were actually achieved by Kanemitsu and Nojima with the cylinders of D/t = 3740.

The physical counterpart of this mathematical explanation can also be considered. If the weakening effect of the initial imperfections be sufficient to cause an essential change in the character of the buckling process of the cylinder, it should be expected that the buckles begin at these imperfections and spread outwards across the cylinder, as was observed and reported by Kanemitsu and Nojima. On the other hand, if the effect of the initial imperfections is insufficient to cause an essential change in the mechanism of buckling, then it should be expected that the buckling waves form in a complete and regular pattern dictated by the physical parameters of the cylinder itself, rather than by the random nature of any existing imperfections.

Kanemitsu and Nojima believed that their lack of control over the cylinders of lower D/t was a result of insufficient rigidity in their testing equipment. The present explanation would indicate that this lack of control was not a function of the testing machine, but rather the result of a new avenue of escape opened up to the more nearly perfect cylinder.

It is believed that the demonstration of two different types of buckling behavior also resolves the apparent

paradox between the original contention that widely spaced stiffeners could not raise the buckling stress of a cylinder because the waves were small at their beginning, and the observed experimental fact that such stiffeners were actually effective.

Several experiments tended to show that the buckle pattern of a nearly perfect cylinder progressed to a deeply buckled configuration by means of waves which were shallow but fully developed in lateral extent, rather than by waves of small lateral extent which were more nearly similar to the final wave shape in terms of the amplitude divided by the wave length. Firstly, the vibration test of Specimen No. 5B showed that the natural vibration mode of this cylinder consisted of waves whose dimensions were comparable to the wave lengths of the buckled configuration of identical cylinders. Inasmuch as these cylinders preferred similar dimensions for both infinitesimal and deep buckle waves, it is implausible to suggest that some radically different wave size existed at intermediate amplitudes.

Secondly, in the cylinders tested in this program, the buckling stresses were sufficiently near the yield stress of the material so that after buckling took place, the material experienced a noticeable amount of permanent set in the regions of smallest radius of curvature of the

buckling pattern. This effect was observed even in the thinnest cylinders with the lowest buckling stresses; for example, the damage observed in Specimen No. 18 after the accidental buckling. If the usual buckling mechanism of cylinders were an initial formation of small waves of sharp curvature, which spread laterally into a final pattern with large wave length, the regions of the skin which momentarily formed the sharply curved edges of the small buckles would experience permanent set, and small ridges would be noticeable in the relatively flat intermediate regions of the final wave pattern. In none of the cylinders tested, however, were any such discontinuities observed in the intermediate portions of the buckling waves, and their absence indicated that these regions never constituted the sharply curved edges of smaller waves which might have existed momentarily during the buckling process.

Thirdly, the fact that stiffeners spaced the order of the final wave length apart had a pronounced effect on the initiation of buckling indicated that the initial buckling wave size must also have been of the same order.

This discussion of buckling would not be complete without a few words on the future value of Yoshimura's developable concave polyhedrons. His concept should prove invaluable in obtaining equations which define the buckle

surface to a greater degree of accuracy than those of the past, both for stiffened and unstiffened cylinders. The surfaces illustrated in Figures 76 and 77 could never represent buckled cylinders exactly because they contain bends of zero radius of curvature, which are not possible in metal sheets of finite thickness. A comparison of Figure 95 with Figure 76 shows unmistakably, however, that the cylinder is striving within its limitations to attain the developable surface. A theoretical analysis of buckled surfaces by energy methods in which the wave shape is made to approach the developable polyhedron as closely as possible should prove very instructive. The polyhedron shown in Figure 77 illustrates the most extreme example of the family, a three-sided cross section. It is of interest to mention that the author has seen several small cylinders of $D/t = 60$ from an anonymous experimental project which actually buckled in this triangular mode.

PART VIII - CONCLUSIONS

The following conclusions are presented as consequences of the study:

1. The buckling behavior of cylinders with moderate wall thickness under axial compression is significantly affected by stiffening elements spaced at distances of the order of the unstiffened buckling wave length. The presence of stiffeners raises the buckling stress, reduces the wave length, and alters the shape of the waves. These effects can be produced by stiffeners which are economically small in size.

2. The tendency of a real cylinder to buckle at a stress somewhat below that of a comparable perfect cylinder is primarily the result of minor imperfections in construction. External disturbances and vibrations are not believed to be a major contributing factor to the "premature" buckling of cylinders in the laboratory.

3. The buckling waves in a reasonably well-made cylinder form with extreme rapidity without regard to the imposed load or axial shortening, and are fully developed in lateral extent from their inception. The controlled formation of very small buckles obtained by Kanemitsu and Nojima was a result of excessive initial imperfection resulting from the extreme thinness of their cylinder wall material.

4. The variation of circumferential stress distribution in an experimental cylinder test resulting from dimensional errors which are very small by machine shop standards can cause a 5-10% scatter in the apparent buckling stress of experimental tests.

5. The natural modes of vibration of a cylinder are approximately similar in configuration to the buckling waves of the same cylinder.

REFERENCES

1. Timoshenko, S., Theory of Elastic Stability, McGraw-Hill Book Company, Inc., New York, N. Y., (1936).

2. Southwell, R. V. "On the General Theory of Elastic Stability," Philosophical Transactions of the Royal Society of London, England, Series A, Vol. 213, p. 187, (1914).

3. Lorenz, R., "Achsensymmetrische Verzerrungen in dünnwandigen Hohlzylinderen", Zeitschrift des Vereines deutscher Ingenieure, Vol. 52, p. 1706, (1908).

4. _____, "Die nicht achenssymmetrische Knickung dünnwandiger Hohlsylinder", Physikalische Zeitschrift, Vol. 13, p. 241, (1911).

5. Robertson, A., "The Strength of Tubular Struts", Proceedings of the Royal Society of London, England, Series A, Vol. 121, p. 558, (1928).

6. Donnell, L. H., "A new theory for the buckling of thin cylinders under axial compression and bending", A. S. M. E. Trans., Vol. 56, No. 11, (November, 1934).

7. Lundquist, E. E., "Strength tests of thin-walled duralumin cylinders in compression.", N. A. C. A., Report No. 473, (1933).

8. Wilson, W. M., and Newmark, N. M., "The Strength of Thin Cylindrical Shells", Bulletin No. 255, University of Illinois, (1933).

9. Flügge, W., "Die Stabilität der Kreiszylinderschale", Ingenieur Archiv, Vol. 3, p. 463, (1932).

10. Von Kármán, Th., and Tsien, H.-S., "The Buckling of Spherical Shells by External Pressure", Journal of the Aeronautical Sciences, Vol. 7, No. 2, p. 43, (Dec., 1939).

11. Kanemitsu, S., and Nojima, N., Axial Compression Test of Thin Circular Cylinders, (A) Length Effect, and (B) Visual Study of Buckling, Thesis, California Institute of Technology, (1939).

REFERENCES (Cont.)

12. Von Kármán, Th., Dunn, L. G., and Tsien, H.-S., "The Influence of Curvature on the Buckling Characteristics of Structures", Journal of the Aeronautical Sciences, Vol. 7, No. 7, p. 276, (May, 1940).

13. Von Kármán, Th., and Tsien, H.-S., "The Buckling of Thin Cylindrical Shells under Axial Compression", Journal of the Aeronautical Sciences, Vol. 8, No. 8, p. 303, (June, 1941).

14. Tsien, H.-S., "A Theory for the Buckling of Thin Shells", Journal of the Aeronautical Sciences, Vol. 9, No. 10, p. 373, (Aug., 1942).

15. _____, "Lower Buckling Load in the Non-Linear Buckling Theory for Thin Shells", Quarterly of Applied Mathematics, Vol. V, No. 2, pp. 236-7, (July, 1947).

16. Leggett, D. M. A., and Jones, R. P. N., "The Behaviour of a Cylindrical Shell under Axial Compression when the Buckling Load Has been Exceeded", Aeronautical Research Council Reports and Memoranda No. 2190, (August, 1942).

17. Crate, and Levin, "Data on buckling strength of curved sheet in compression.", N. A. C. A., Adv. Restr. Rept. No. 3104, (October, 1943).

18. McPherson, Fienup, and Zibritosky, "Effect of developed width on strength of axially loaded curved sheet stringer panels.", N. A. C. A., Adv. Restr. Rept. No. 4H08, (November, 1944).

19. Ramberg, Levy, and Fienup, "Effect of curvature on strength of axially loaded sheet-stringer panels.", N. A. C. A., Tech. Note No. 944, (August, 1944).

20. Stowell, "Critical compression stress for curved sheet supported along all edges.", N. A. C. A., Restr. Bul. No. 3107, (1946).

21. Welter, G., "Curved Aluminum-Alloy Sheets in Compression for Monocoque Constructions", Journal of the Aeronautical Sciences, Vol. 12, No. 3, p. 357, (July, 1945).

REFERENCES (Cont.)

22. _____, "Influence of Different Factors on Buckling Loads of Curved Thin Aluminum-Alloy Sheets for Monocoque Constructions", Journal of the Aeronautical Sciences, Vol. 13, No. 4, p. 204, (April, 1946).

23. _____, "The Effect of Radius of Curvature and Preliminary Artificial Eccentricities on Buckling Loads of Curved Thin Aluminum-Alloy Sheets for Monocoque Constructions", Journal of the Aeronautical Sciences, Vol. 13, No. 11, p. 593, (Nov., 1946).

24. Cox, H. L., and Pribram, E., "The Elements of the Buckling of Curved Plates", Journal of the Royal Aeronautical Society, Vol. 52, No. 453, p. 551, (Sept., 1948).

25. Donnell, L. H., and Wan, C. C., "Effect of Imperfections on Buckling of Thin Cylinders and Columns under Axial Compression", Journal of Applied Mechanics, Vol. 17, No. 1, p. 73, (March, 1950).

26. Yoshimura, Y., "On the Mechanism of Buckling of a Circular Cylindrical Shell Under Axial Compression.", Rep. Inst. Sci. Tech., Tokyo Univ., Vol. 5, No. 5, (1951).

27. Langhaar, H. L., Dimensional Analysis and Theory of Models, John Wiley & Sons, Inc., N. Y., (1951).

28. Shanley, F. R., "Simplified Analysis of General Instability of Stiffened Shells in Pure Bending", Paper P-82, The RAND Corp., Santa Monica, Calif., (May, 1949).

29. Dunn, L. G., "Some Investigations of the General Instability of Stiffened Metal Cylinders, Part IX", N. A. C. A., Tech. Note 1198, (Nov., 1947).

30. Batdorf, S. B., Schildcrout, M., and Stein, M., "Critical Stress of Thin-Walled Cylinders in Axial Compression", N. A. C. A., Report No. 887, (1947).

31. Moore, R. L., "Some Comparative Tests of Plain and Alclad 24S-T Sheet", N. A. C. A., Tech. Note No. 821, (August, 1941).

REFERENCES (Cont.)

32. Atchison, C. S., and Miller, J. A., "Tensile and Pack Compressive Tests of Some Sheets of Aluminum Alloy, 1025 Carbon Steel, and Chromium-Nickel Steel", N. A. C. A., Tech. Note No. 840, (Feb., 1942).

33. Munitions Board Aircraft Committee., "Strength of Metal Aircraft Elements", Document No. ANC-5a, (Revised, May, 1949).

34. Lurie, H., "Lateral Vibrations as Related to Structural Stability", Journal of Applied Mechanics, Vol. 19, No. 2, p. 195, (June, 1952).

35. Dow, N. F., and Hickman, W. A. "Design Charts for Flat Compression Panels Having Longitudinal Extruded Y-Section Stiffeners and Comparison with Panels having Formed Z-Section Stiffeners", N. A. C. A., Tech. Note No. 1389, (August, 1947).

Table 1 - Description of Specimens

Specimen	D in	t	D/t	Area in^2	N	Stiffener Thickness in	Stiffener Width in	I $in^4 x 10^{-4}$	h/D
1	12.99	0.032	406	1.320	0	-	-	-	~0.5
1A	12.97	0.033	393	1.356	0	-	-	-	~0.5
2	13.06	0.032	408	1.888	4	0.375	0.375	16.48	~0.5
3	13.10	0.032	409	2.455	8	0.375	0.375	16.48	~0.5
4	13.08	0.032	409	3.016	12	0.375	0.375	16.48	~0.5
5	13.02	0.033	395	1.460	2	0.125	0.375	0.61	0.498
5A	13.11	0.033	397	1.466	2	0.125	0.375	0.61	0.494
5B	13.03	0.033	395	1.464	2	0.125	0.375	0.61	~0.5
6	12.98	0.033	393	2.203	6	0.375	0.375	16.48	~0.5
7	12.97	0.033	393	1.638	6	0.125	0.375	0.61	~0.5
8	12.97	0.033	393	1.712	6	0.156	0.375	1.19	~0.5
9	13.08	0.033	396	1.790	6	0.188	0.375	2.06	~0.5
10	13.10	0.033	397	1.933	6	0.250	0.375	4.88	~0.5
11	13.04	0.033	395	1.465	2	0.125	0.375	0.61	0.247
12	12.97	0.033	393	1.452	2	0.125	0.375	0.61	0.374
13	13.08	0.033	396	1.466	2	0.125	0.375	0.61	0.735
14	13.02	0.0194	671	1.363	4	0.375	0.375	16.48	~0.5
15	12.97	0.0194	669	1.643	6	0.375	0.375	16.48	~0.5
16	13.07	0.0194	674	1.929	8	0.375	0.375	16.48	~0.5
17	13.04	0.0194	672	2.493	12	0.375	0.375	16.48	~0.5
18	13.06	0.0194	673	1.179	8	0.125	0.375	0.61	~0.5
19	12.99	0.0369	352	1.731	2	0.375	0.375	16.48	~0.5
20	13.00	0.0369	352	2.199	4	0.375	0.375	16.48	~0.5
21	13.00	0.0369	352	2.482	6	0.375	0.375	16.48	~0.5
22	13.00	0.0369	352	2.762	8	0.375	0.375	16.48	~0.5

Table 2

Maximum Variation of Stress around Specimen Circumference at Buckling

Specimen	σ_B psi	$\sigma_{max} - \sigma_{min}$ psi	$\frac{\sigma_{max} - \sigma_{min}}{\sigma_B}$ (%)
1	15,080	7,770	51.5
1A	15,470	3,360	21.7
2	20,660	5,250	25.4
3	24,440	10,150	41.5
4	24,870	8,240	33.1
5	17,780	3,000	16.9
5A	19,100	2,360	12.4
6	24,960	2,540	10.2
7	24,420	3,200	13.1
8	23,360	3,440	14.7
9	22,350	2,750	12.3
10	25,870	4,133	16.0
11	24,570	1,840	7.5
12	22,040	2,690	12.2
13	21,830	1,920	8.8
14	11,740	1,490	12.7
15	10,960	4,690	42.8
16	14,520	3,960	27.3
17	14,440	4,270	29.6
19	26,000	6,670	25.7
20	27,280	6,190	22.7
21	26,190	2,740	10.5
22	27,150	5,210	19.2
	MEAN VALUE	3,440	16.9

Table 3

Difference between Average Strain Gauge Stress and Load/Area Stress as a Function of σ

Specimen	Approximate Stress Difference (psi)
1	$240 - 0.030\sigma$
1A	$-130 + 0.005\sigma$
2	$40 - 0.017\sigma$
3	$125 - 0.038\sigma$
4	$470 - 0.056\sigma$
5	$80 - 0.014\sigma$
5A	$140 - 0.017\sigma$
6	$60 + 0.040\sigma$
7	$135 - 0.008\sigma$
8	$210 - 0.005\sigma$
9	$180 - 0.011\sigma$
10	$-220 + 0.005\sigma$
11	$400 - 0.044\sigma$
12	$140 + 0.013\sigma$
13	$110 - 0.011\sigma$
14	$110 + 0.050\sigma$
15	$90 + 0.103\sigma$
16	$500 + 0.096\sigma$
17	$170 + 0.048\sigma$
19	$-0.028\sigma + 2.3 \times 10^{-6}\sigma^2$
20	$0.029\sigma + 3.2 \times 10^{-6}\sigma^2$
21	$0.032\sigma + 2.2 \times 10^{-6}\sigma^2$
22	$-0.026\sigma + 6.3 \times 10^{-6}\sigma^2$

Figure 1

Donnell's Solution of

Stress vs. Strain for Imperfect Cylinders

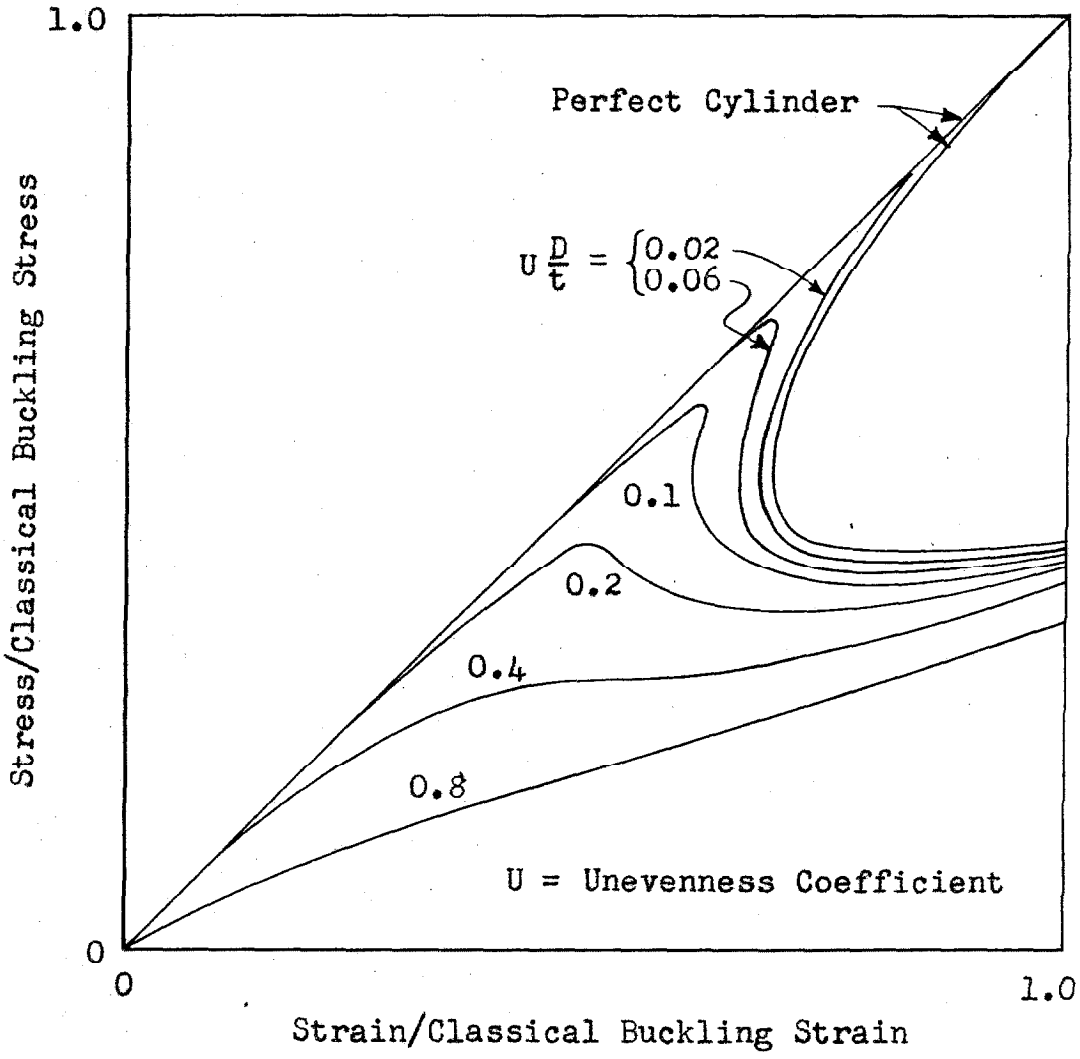

Figure 2

Details of a Typical Specimen (No. 14)

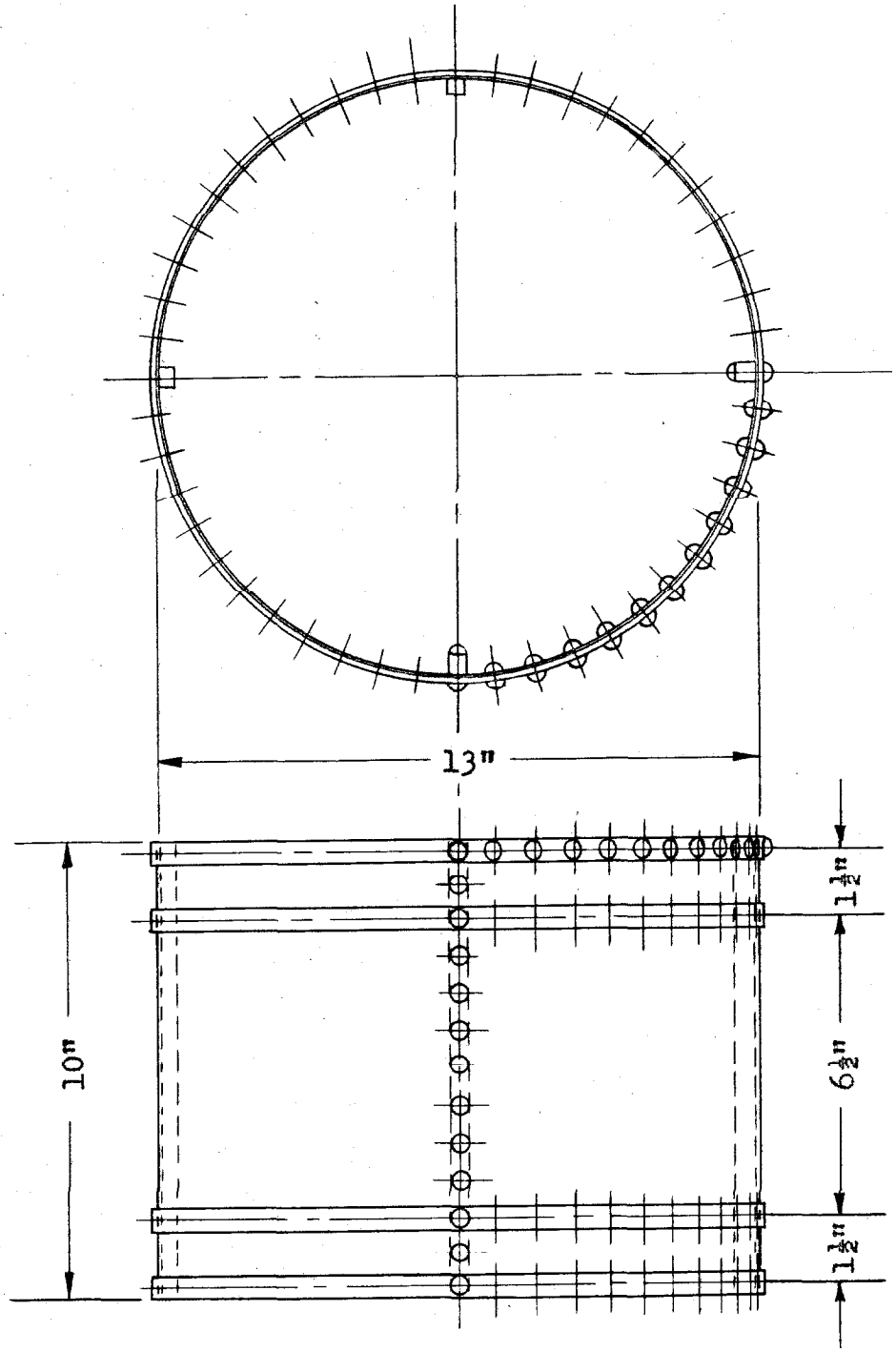

Figure 3

Average Stress vs. Strain for Specimen No. 1

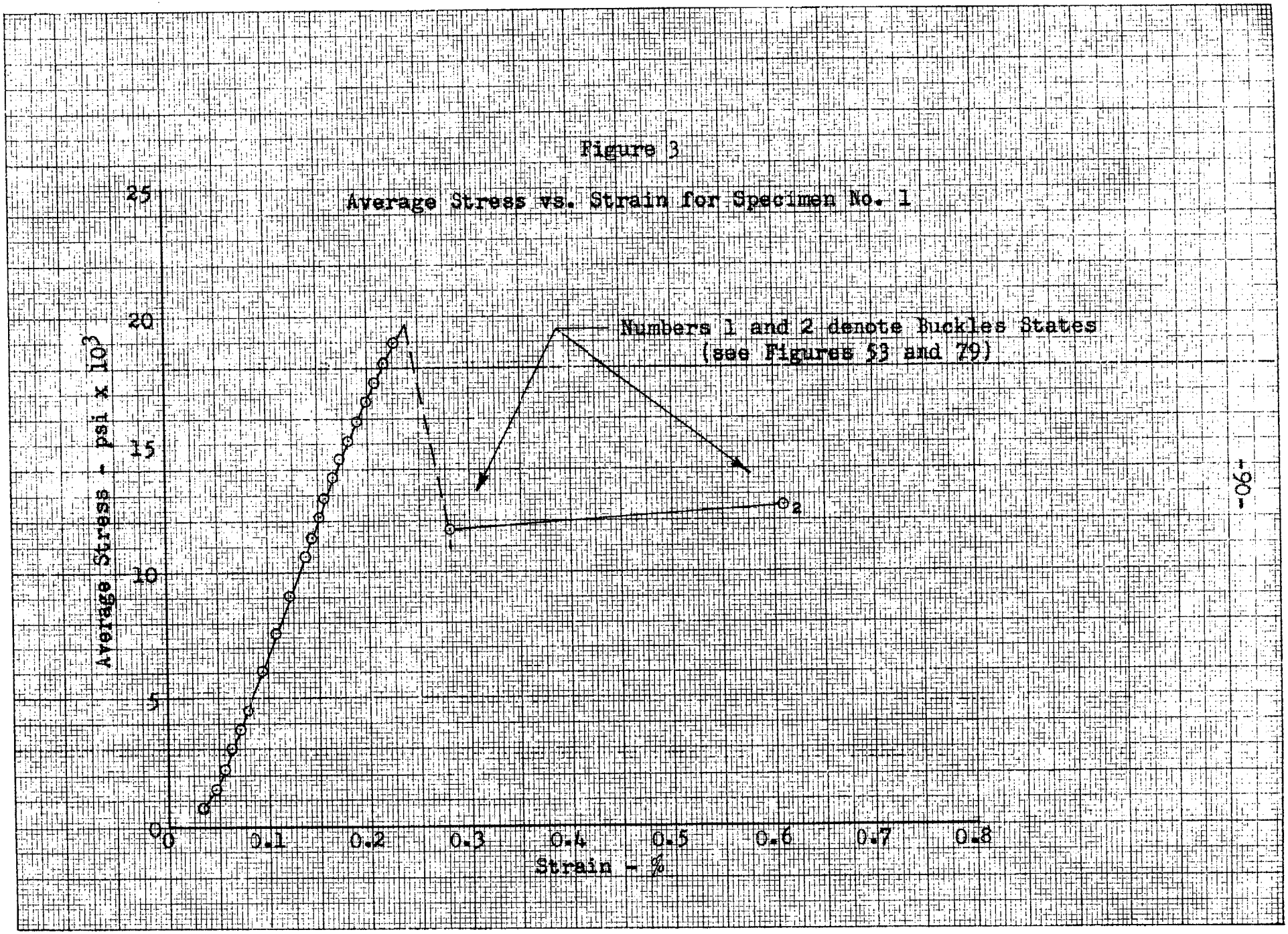

Figure 4

Average Stress vs. Strain for Specimen No. 1A

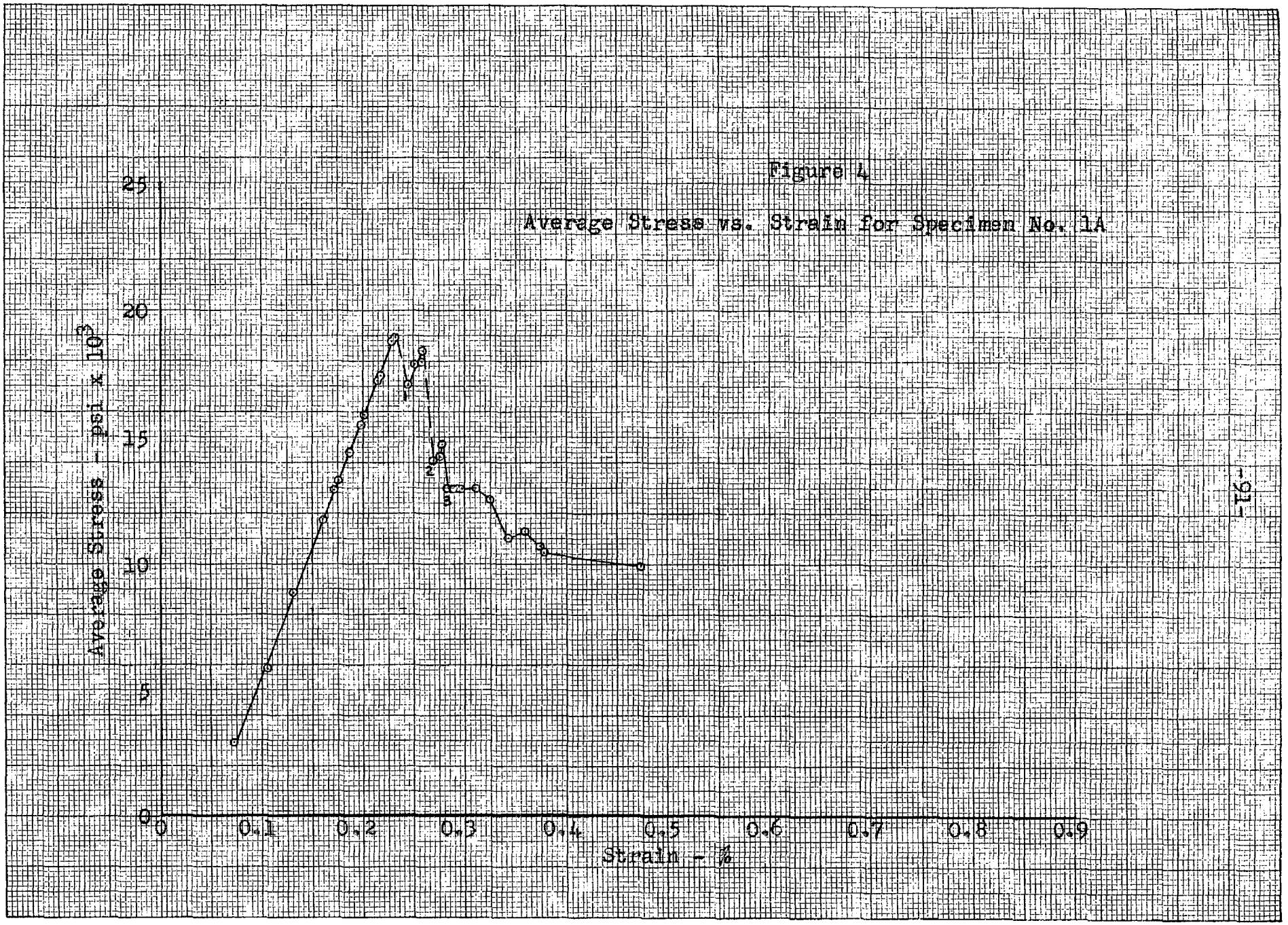

Figure 5

Average Stress vs. Strain for Specimen No. 2

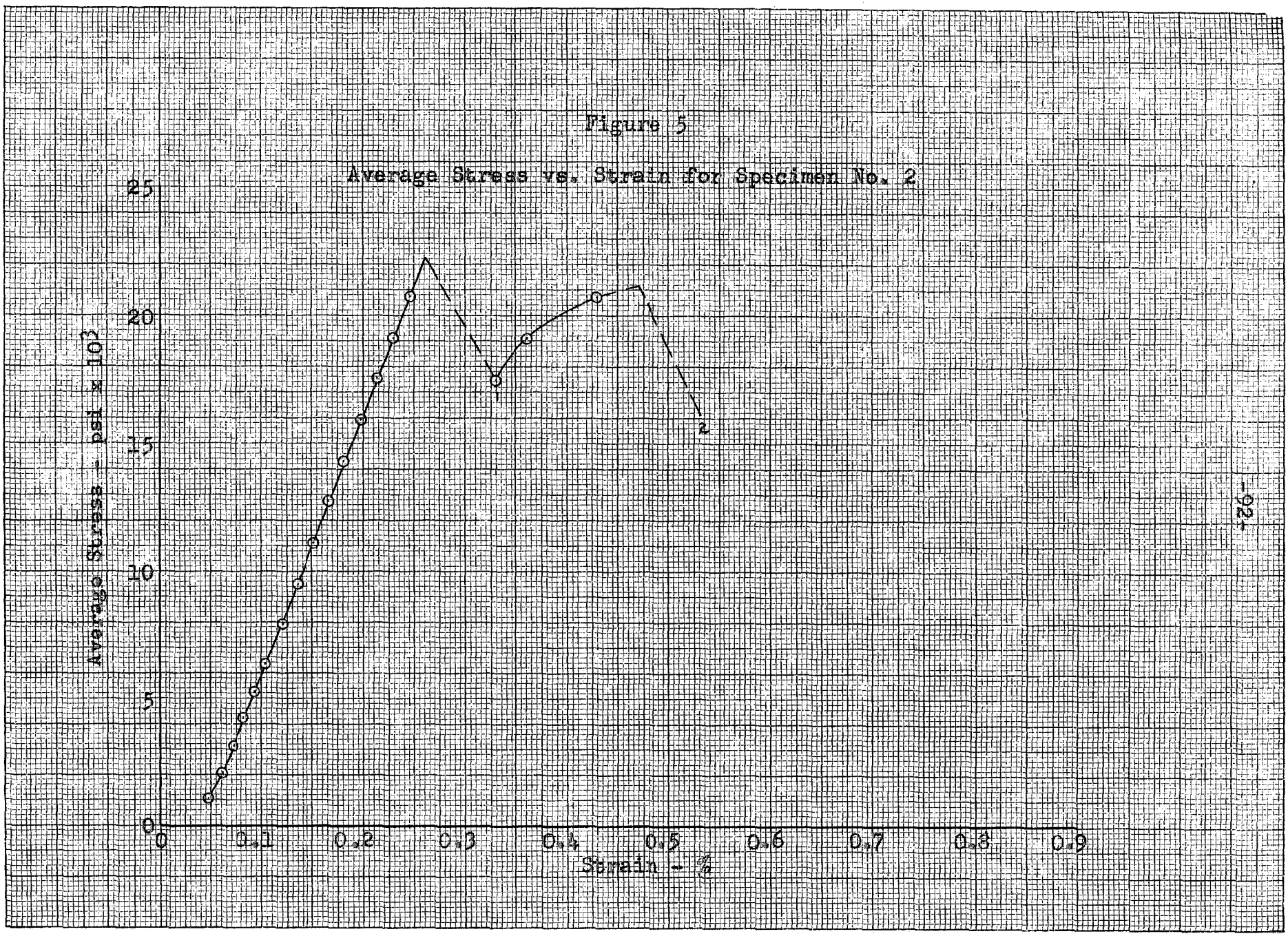

Figure 6

Average Stress vs. Strain for Specimen No. 3

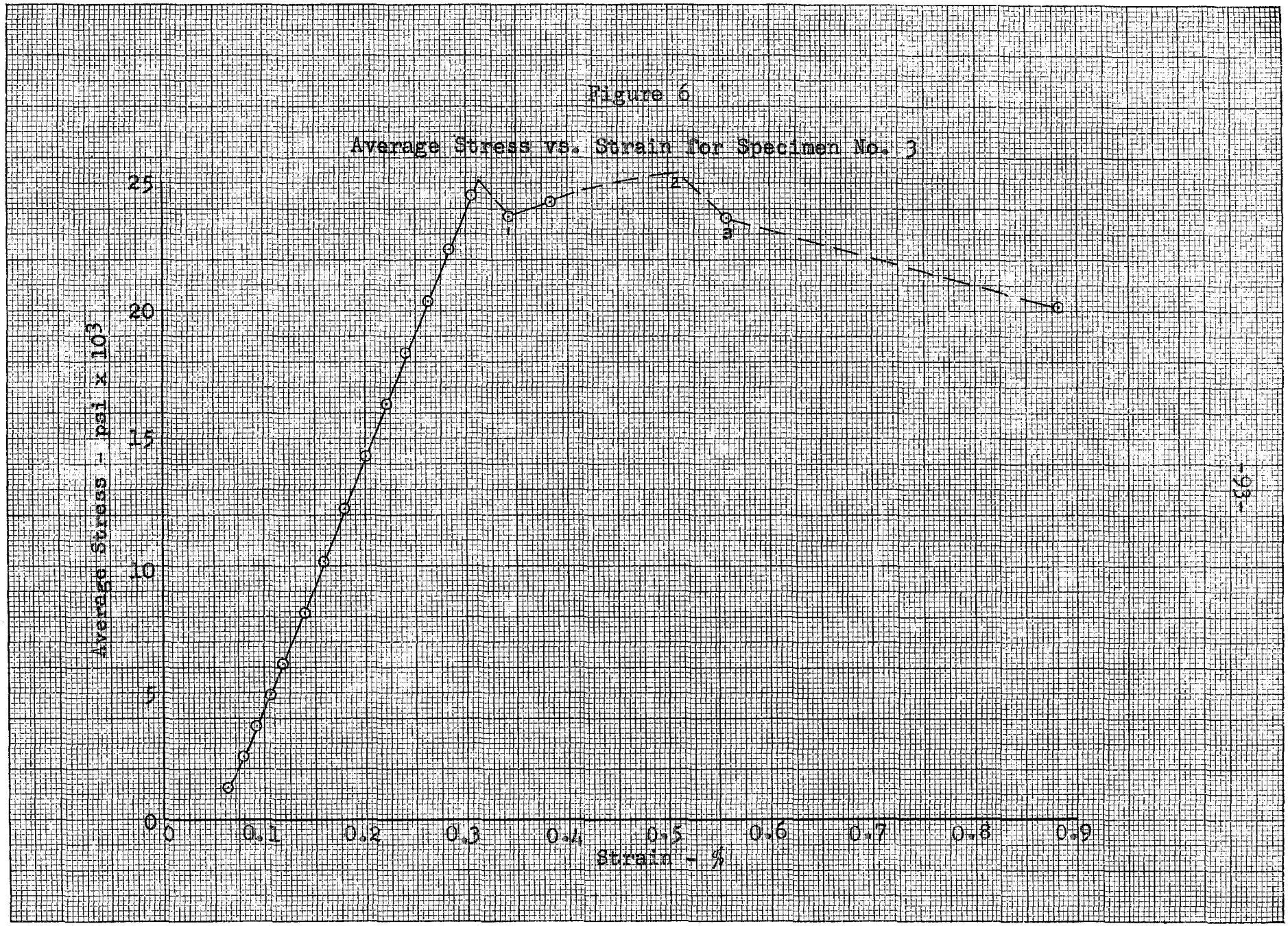

Figure 7 Average Stress vs. Strain for Specimen No. 4

Figure 8

Average Stress vs. Strain for Specimen No. 5

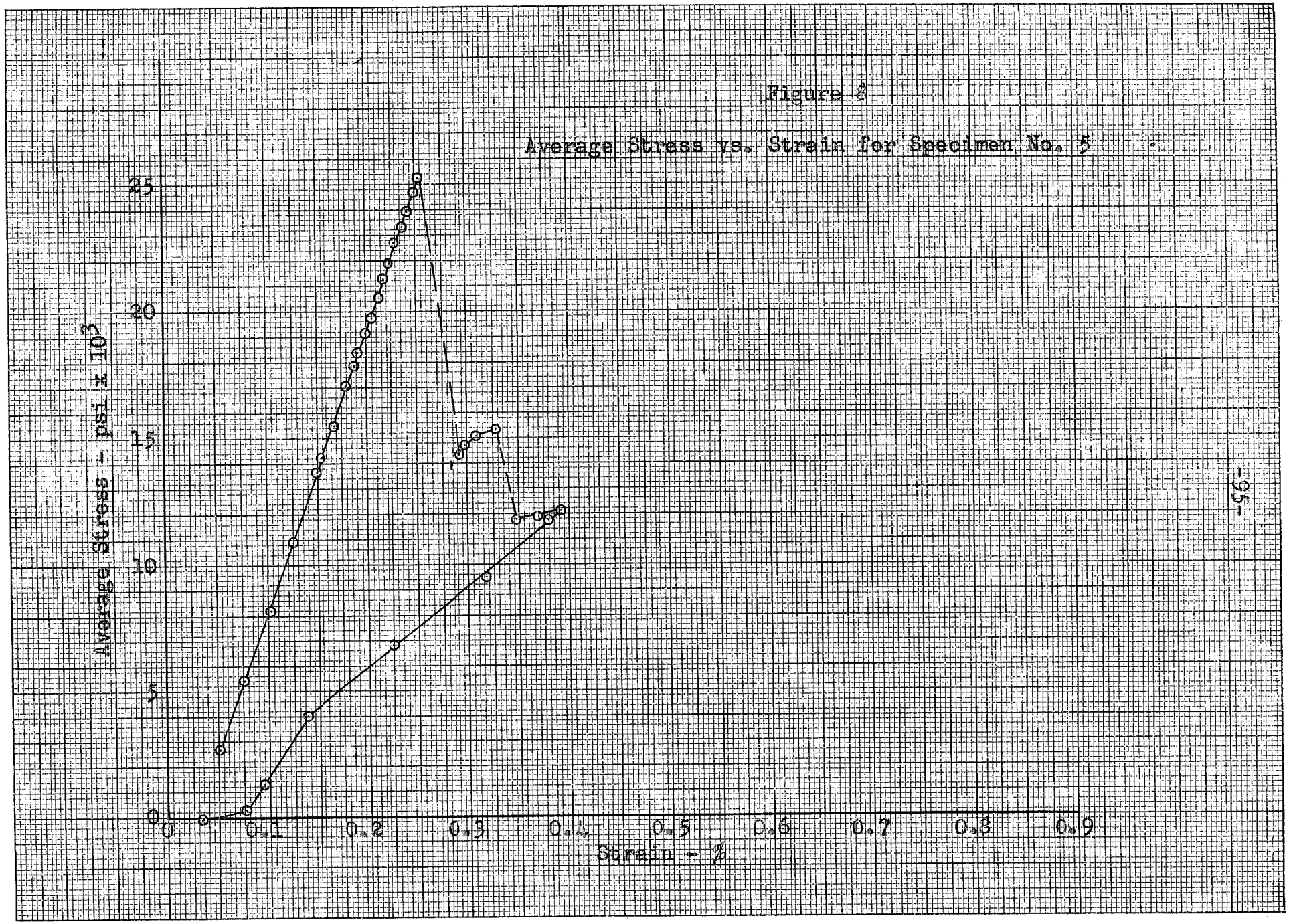

Figure 9

Average Stress vs. Strain for Specimen No. 5A

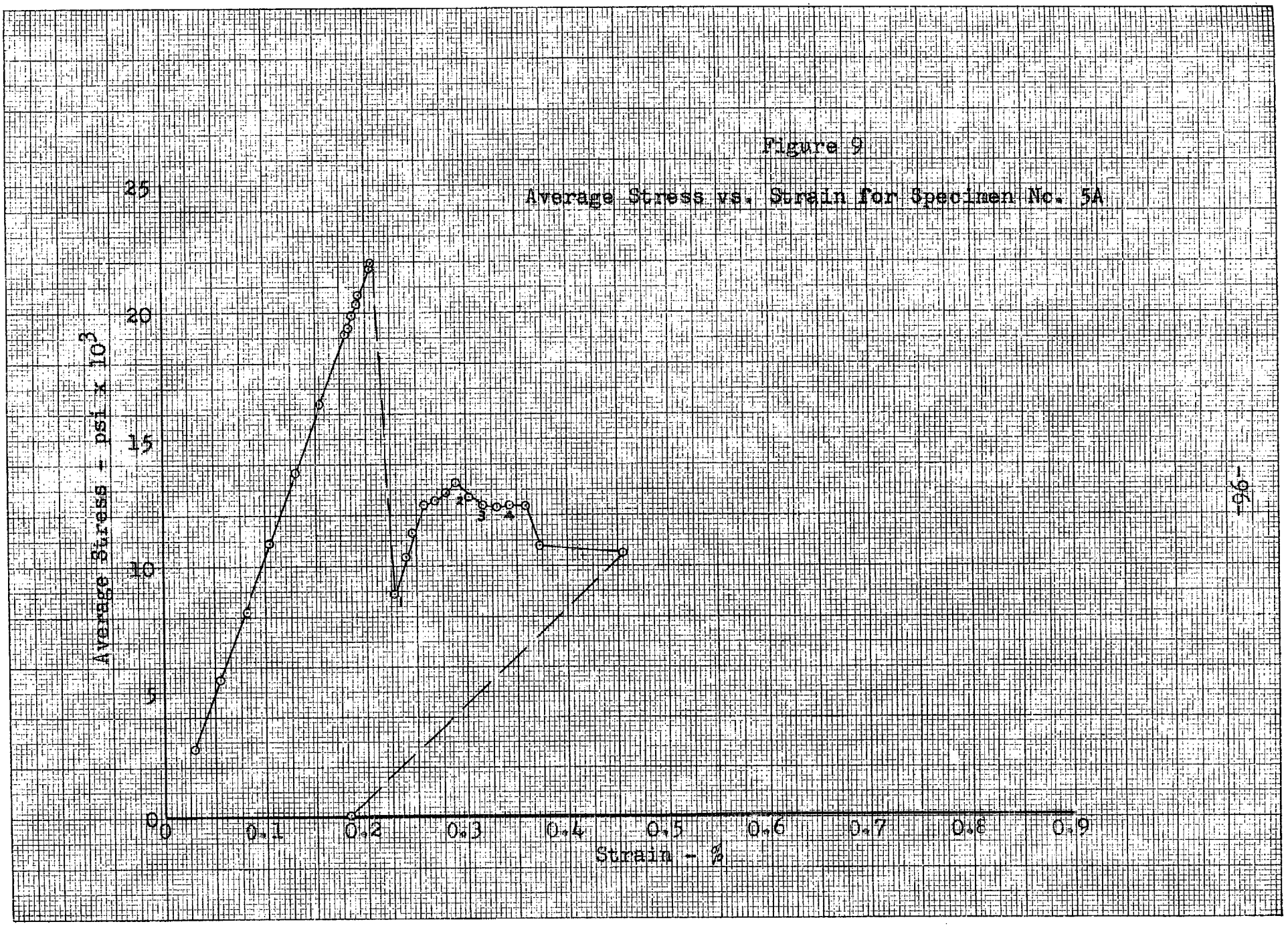

Figure 10

Average Stress vs. Strain for Specimen No. 5B

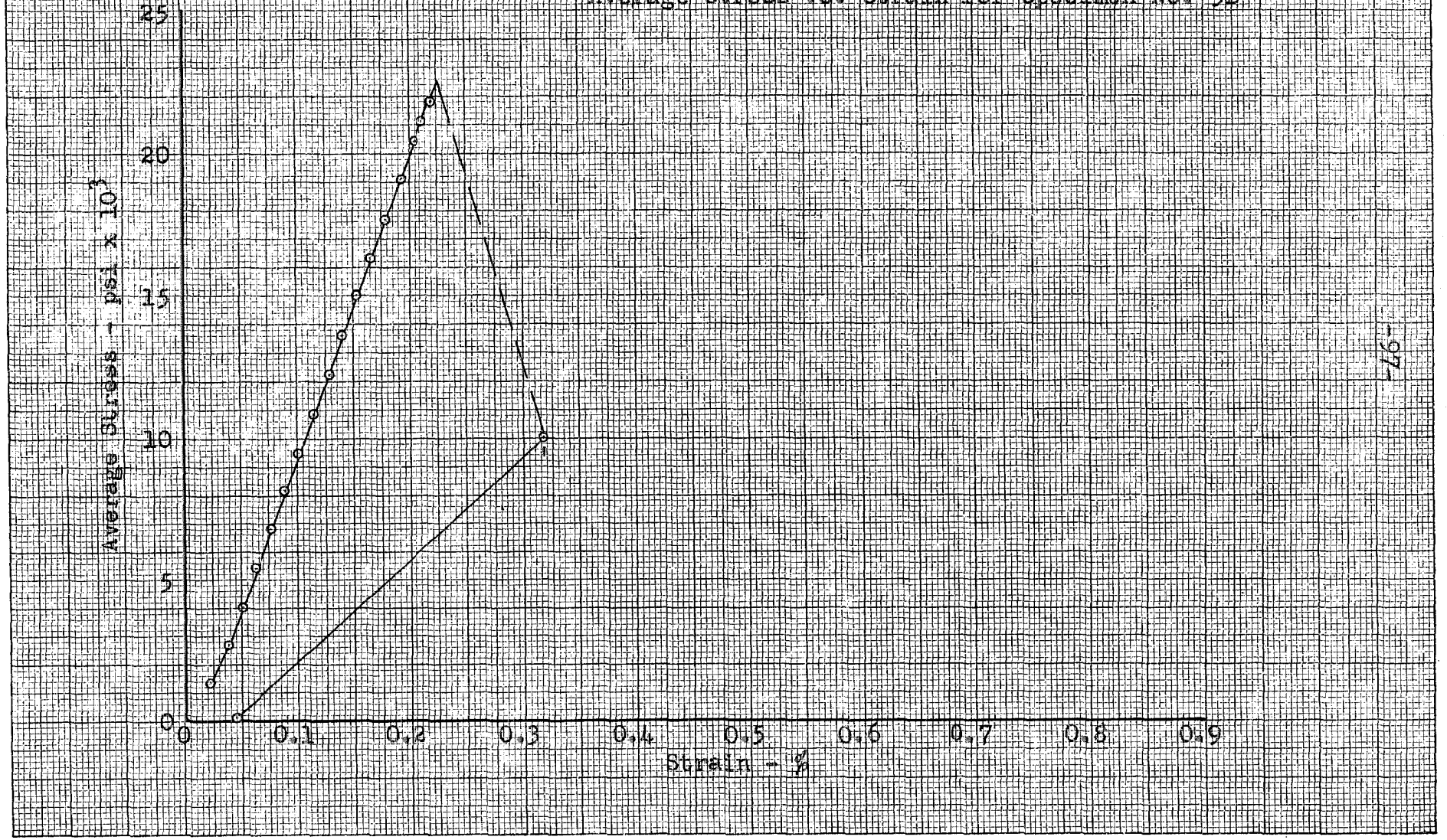

Average Stress vs. Strain For Specimen No. 6
Average Stress → psi x 10³
Strain → %
0
5
10
15
20
25
0.1
0.2
0.3
0.4
0.5
0.6
0.7
0.8
0.9

Figure 11

Figure 12

Average Stress vs. Strain for Specimen No. 7

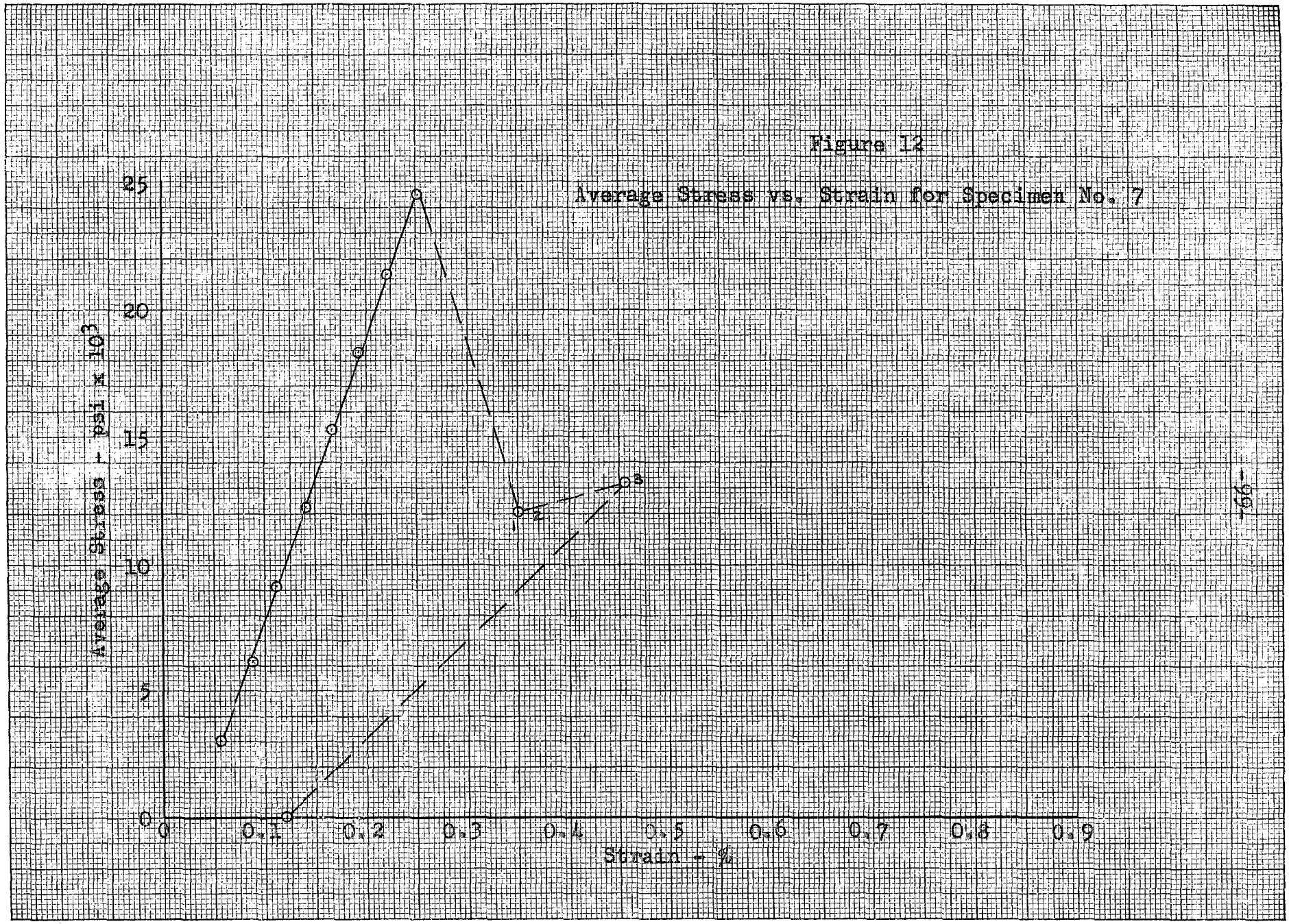

Figure 13

Average Stress vs. Strain for Specimen No. 8

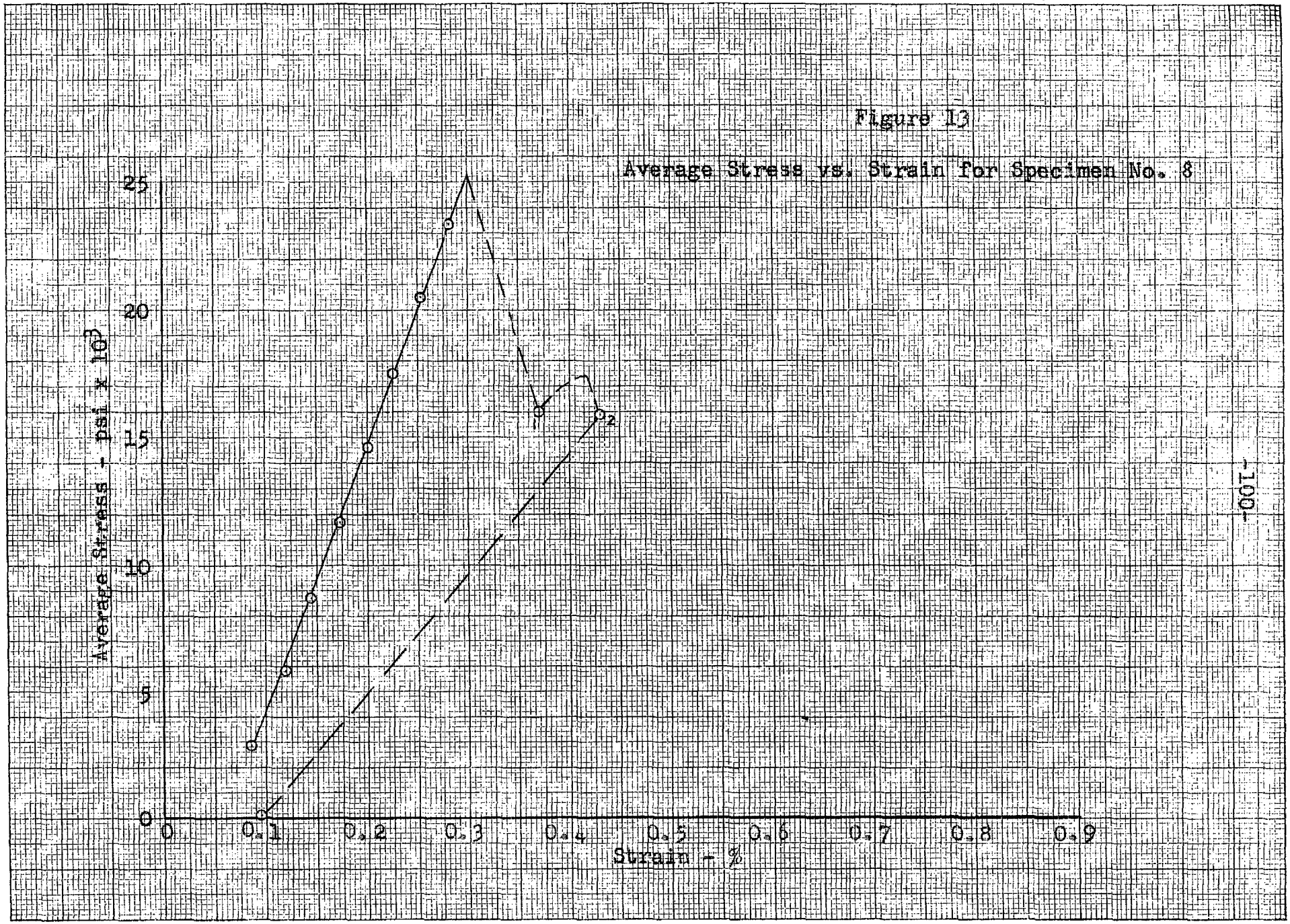

Figure 14

Average Stress vs. Strain for Specimen No. 9

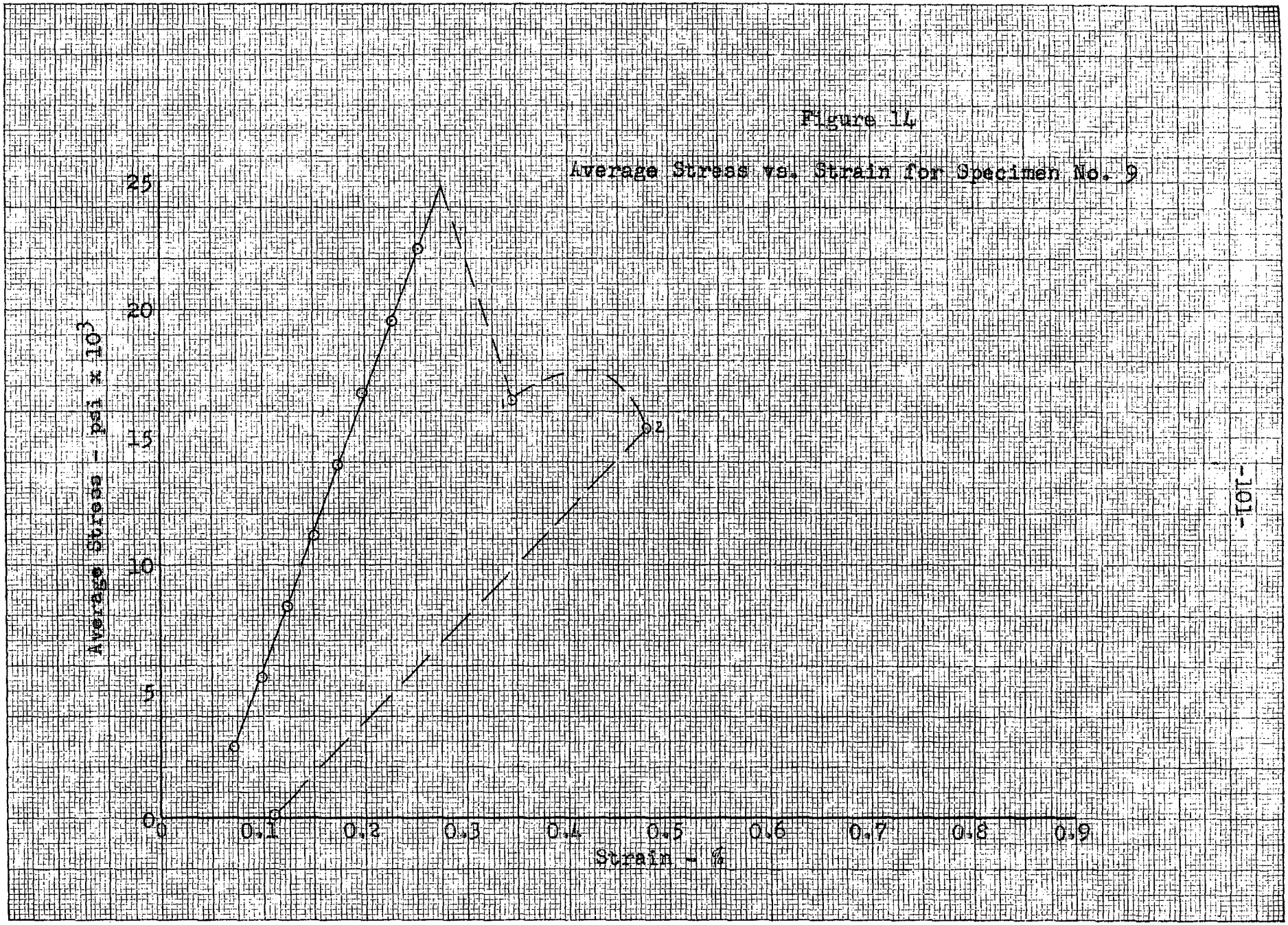

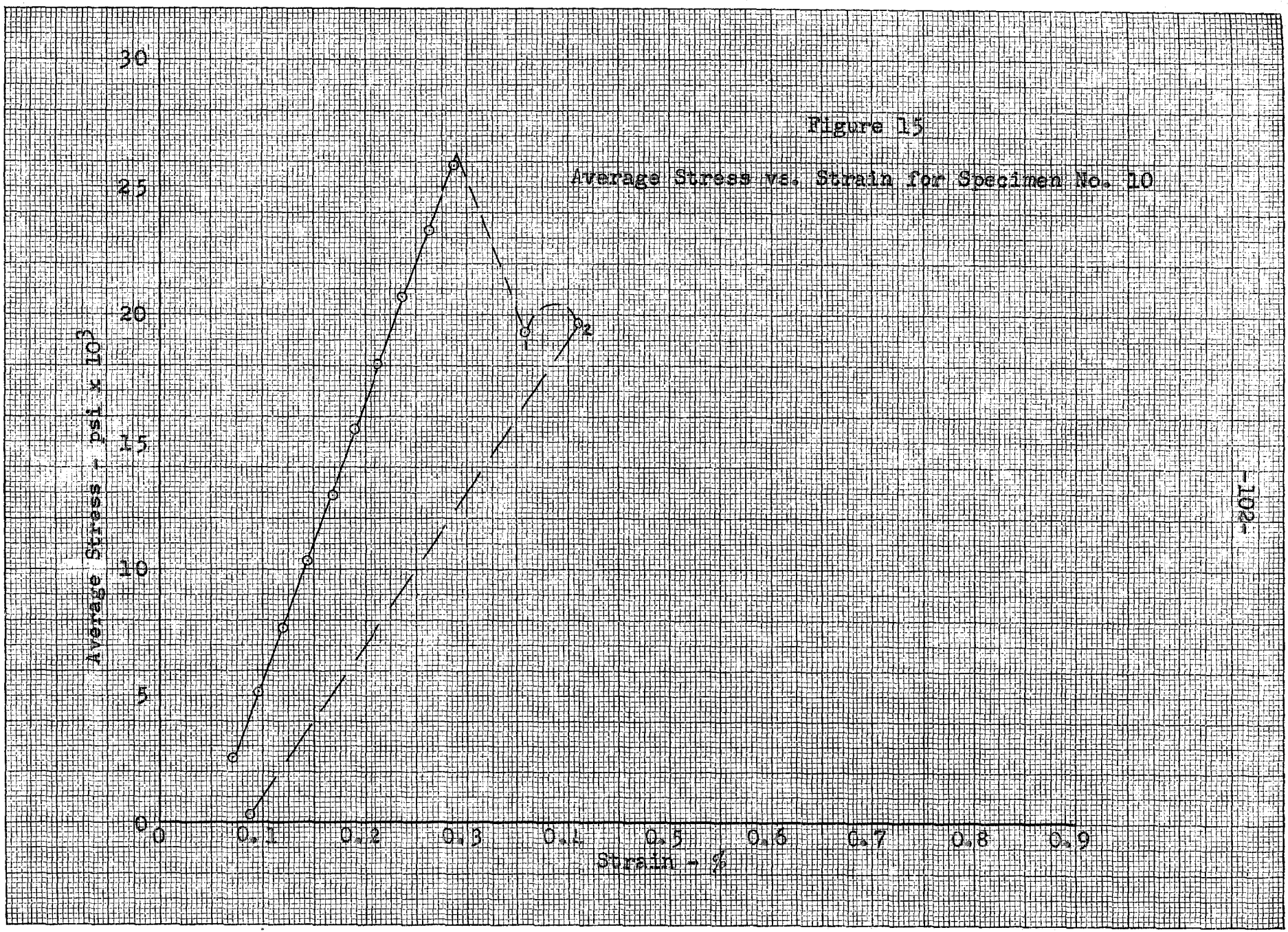

Figure 15

Average Stress vs. Strain for Specimen No. 10

Figure 16

Average Stress vs. Strain for Specimen No. 11

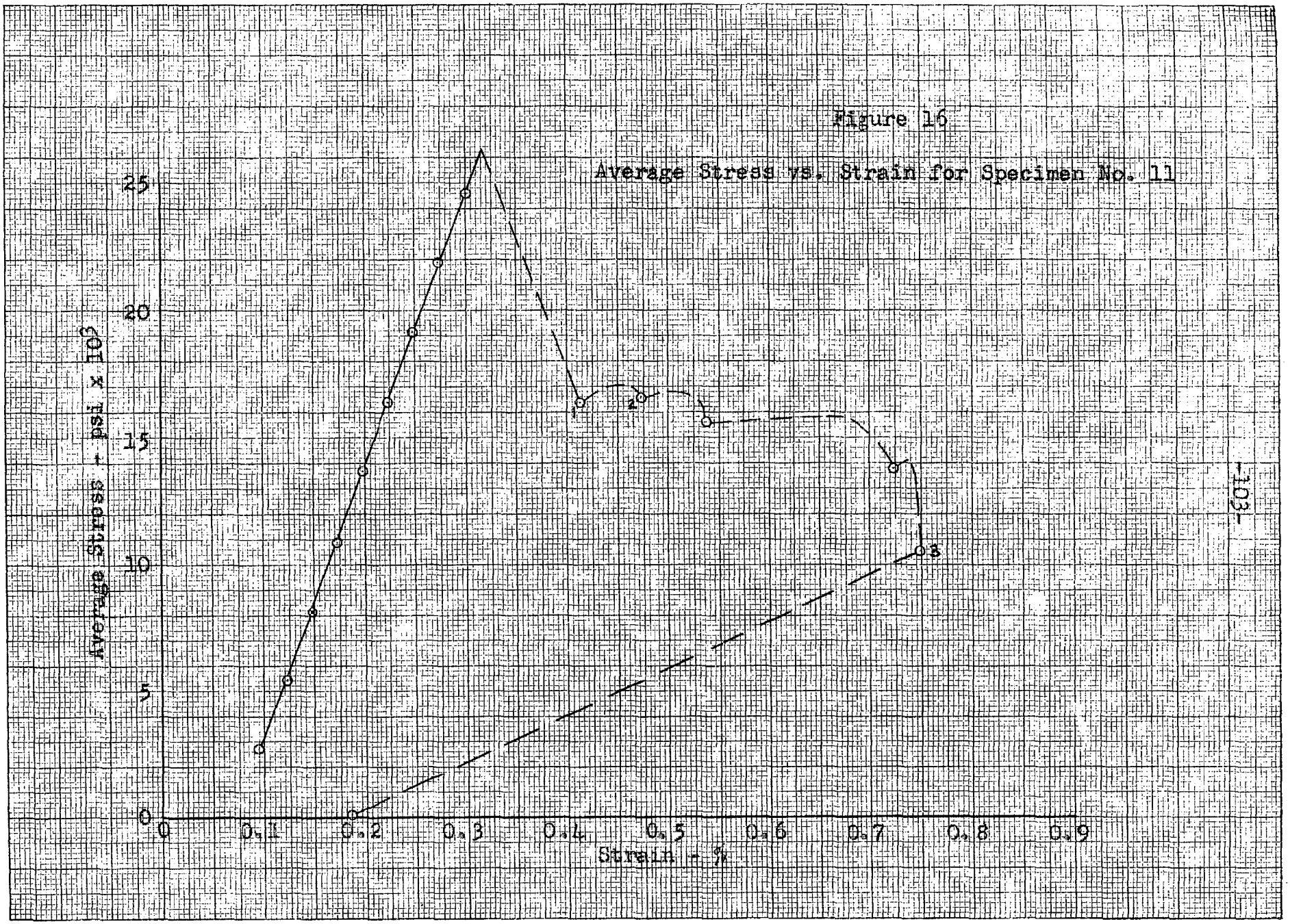

Figure 17

Average Stress vs. Strain for Specimen No. 12

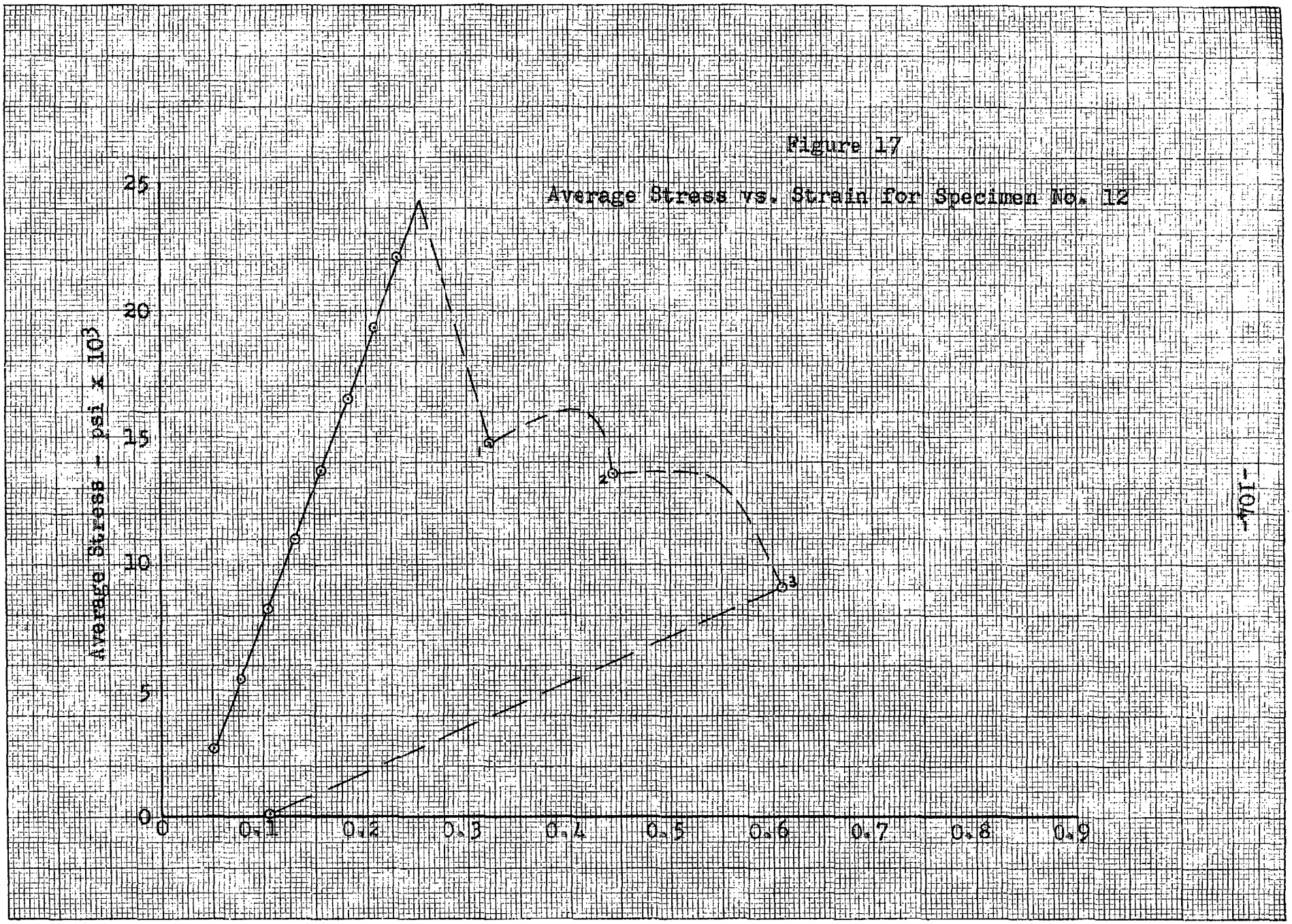

Figure 18

Average Stress vs. Strain for Specimen No. 13

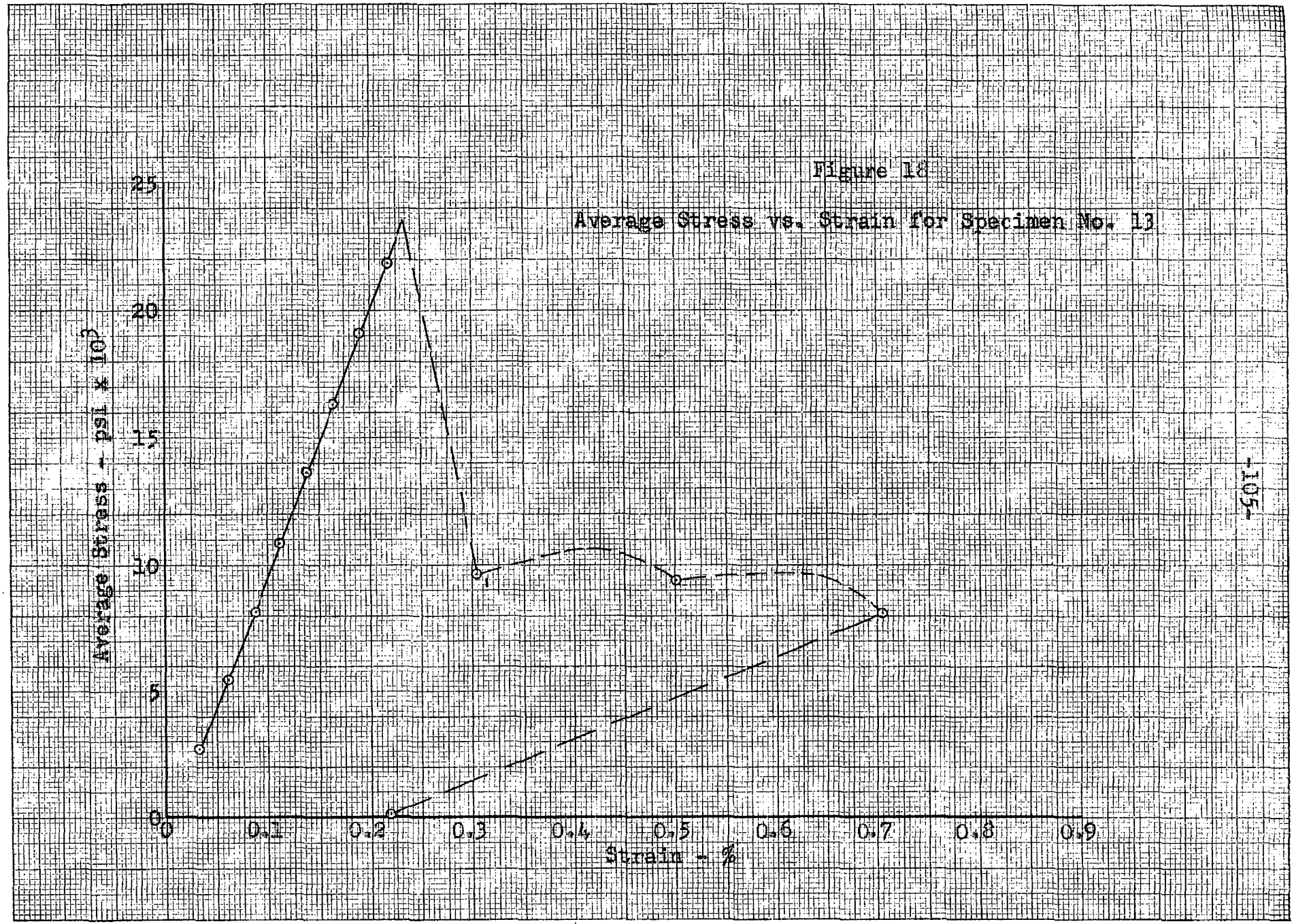

Figure 19

Average Stress vs. Strain for Specimen No. 14

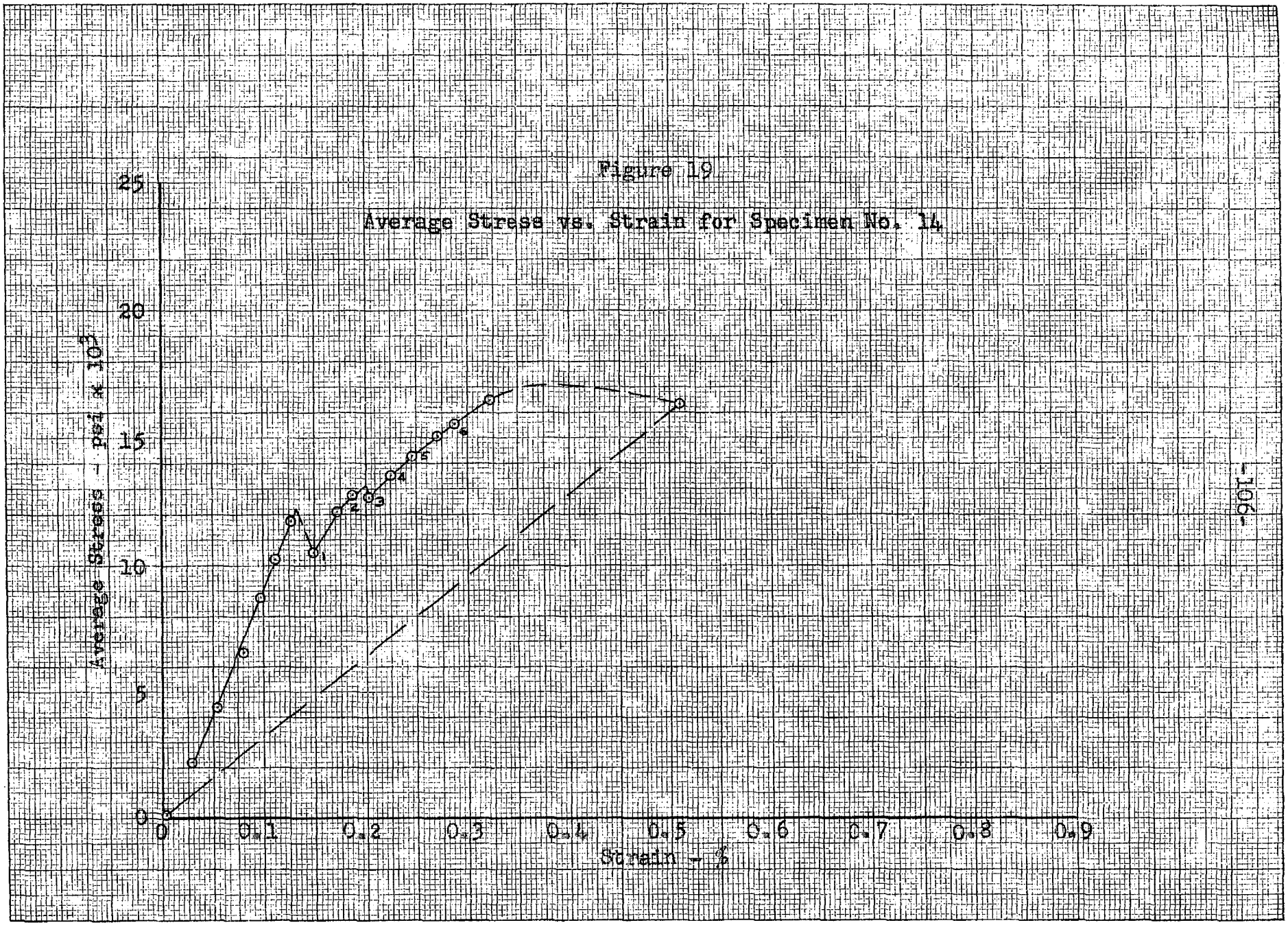

Figure 20
Average Stress vs. Strain for Specimen No. L5

Figure 21

Average Stress vs. Strain for Specimen No. 16

Figure 22

Average Stress vs. Strain for Specimen No. 17

Figure 23
Average Stress vs. Strain for Specimen No. 18

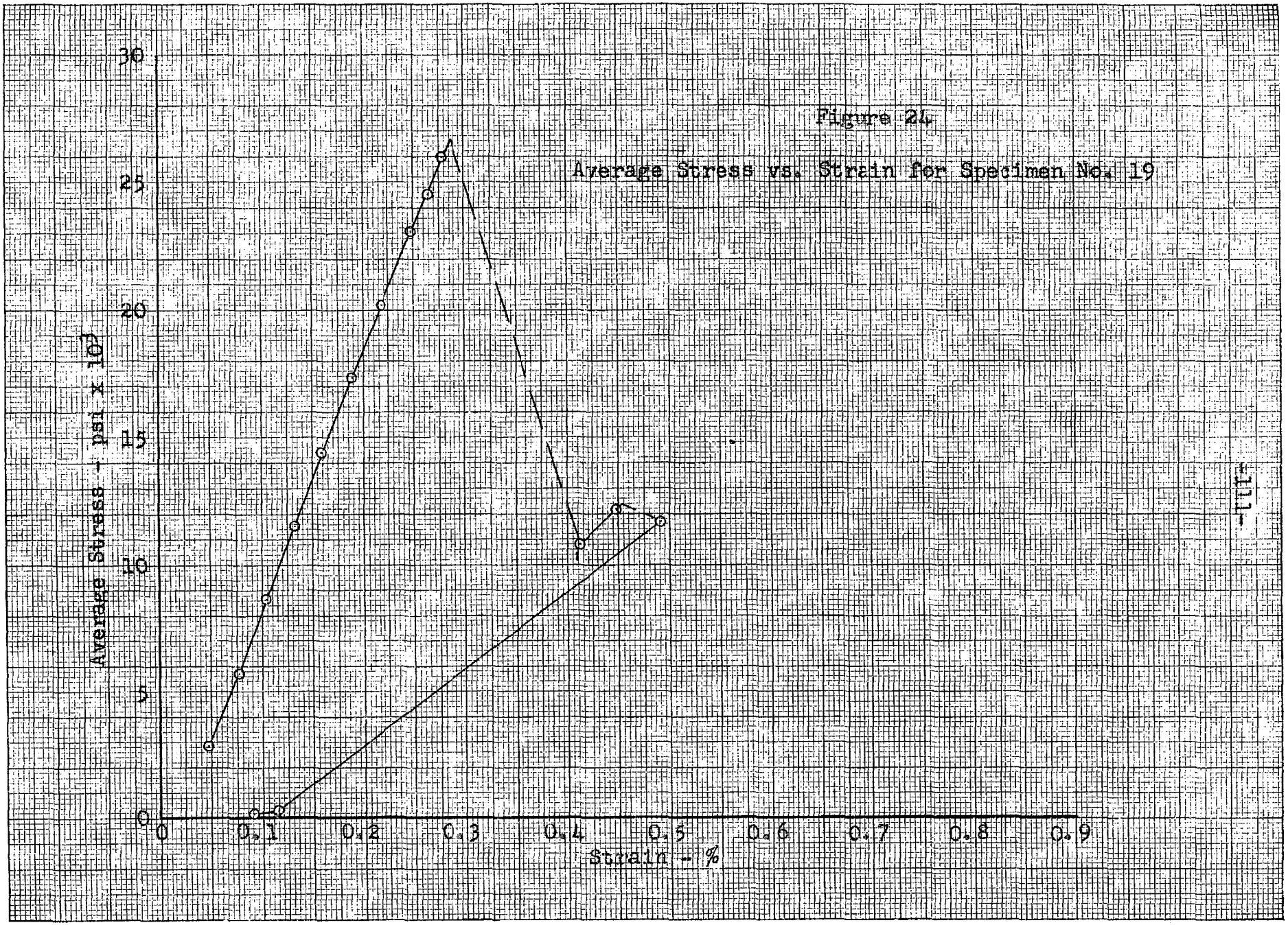

Figure 24

Average Stress vs. Strain for Specimen No. 19

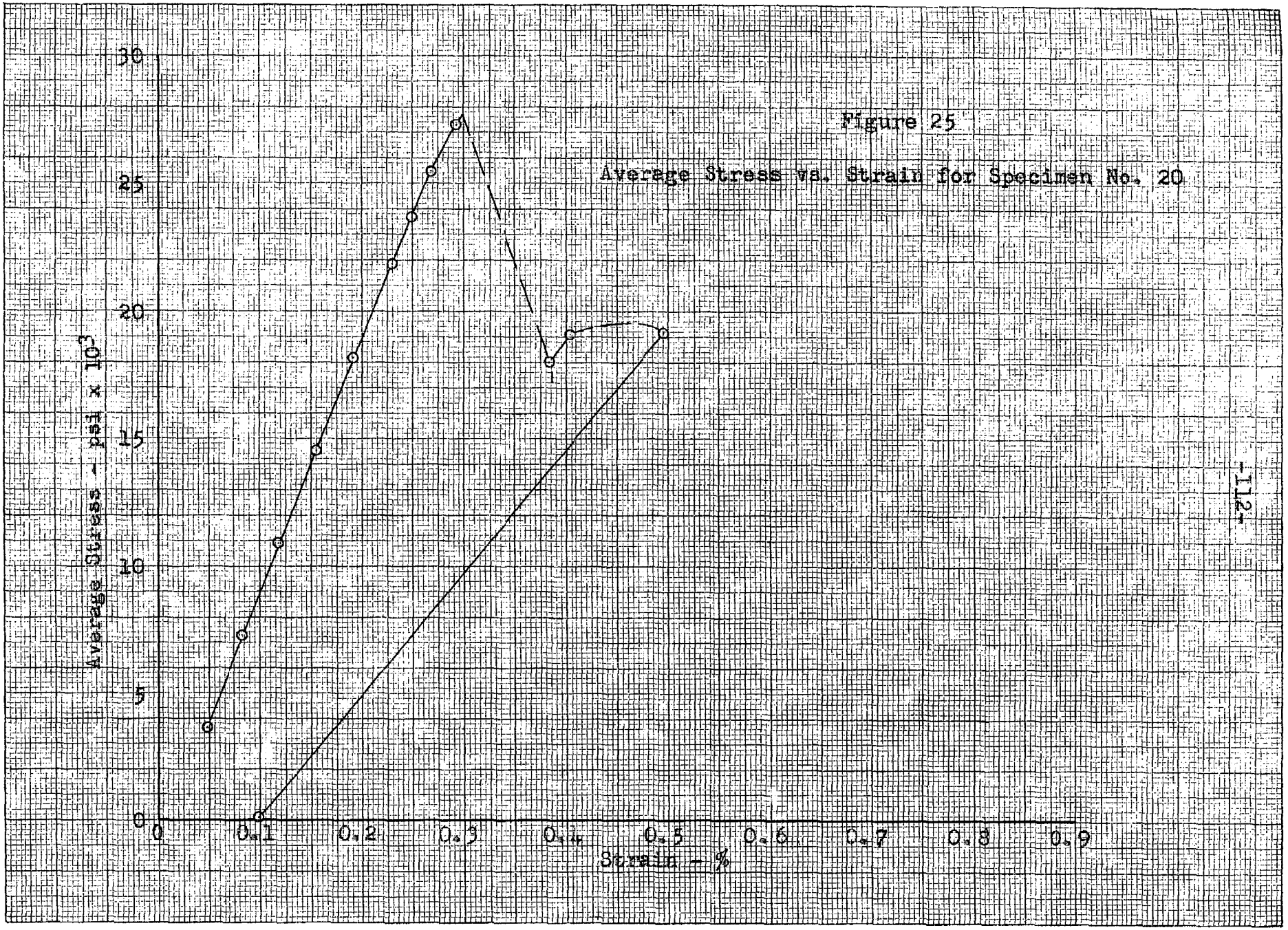
Figure 25
Average Stress vs. Strain for Specimen No. 20
Average Stress - σ_1 x psi
Strain - %
0
5
10
15
20
25
30
0.1
0.2
0.3
0.4
0.5
0.6
0.7
0.8
0.9

Figure 26

Average Stress vs. Strain for Specimen No. 21

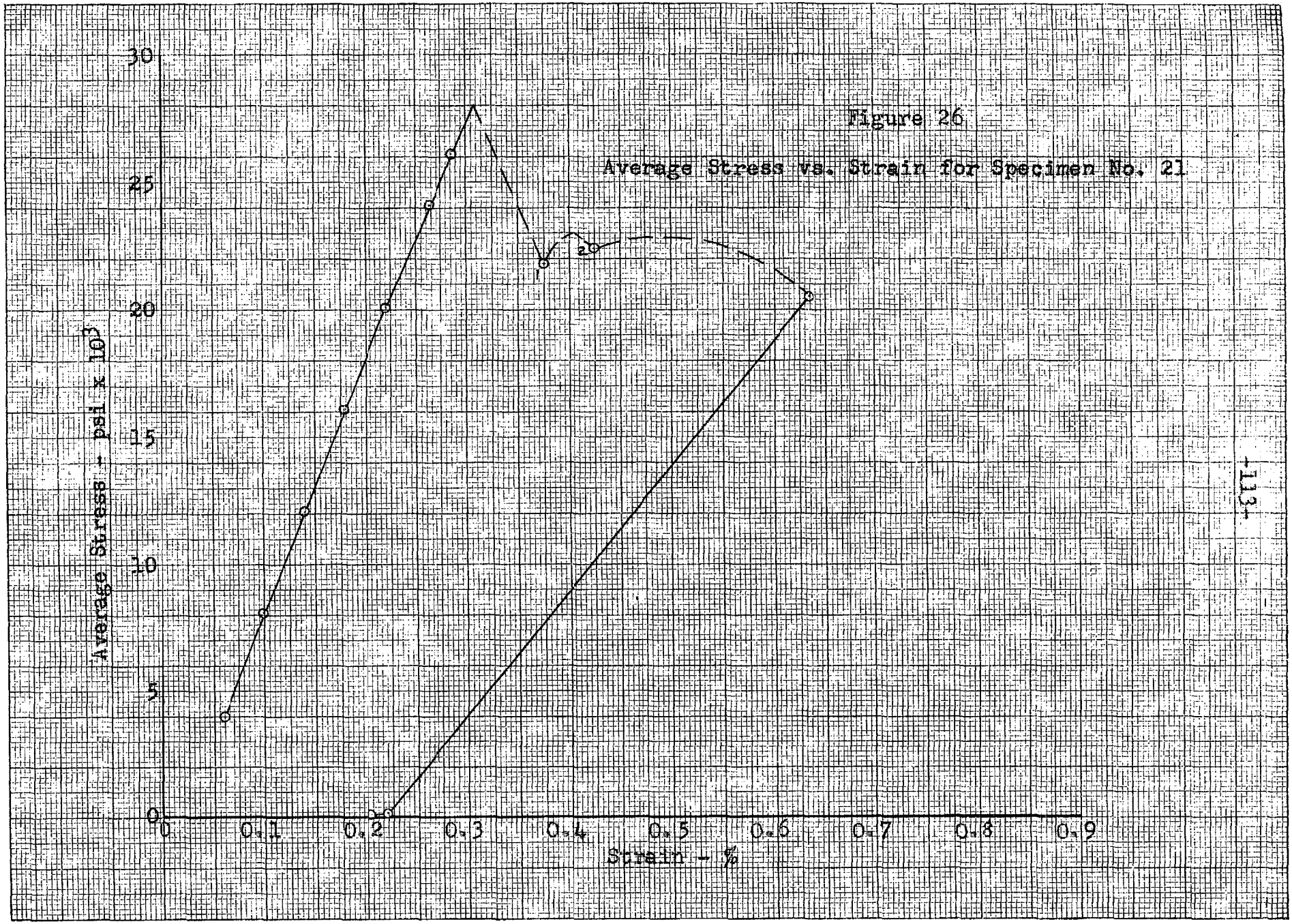

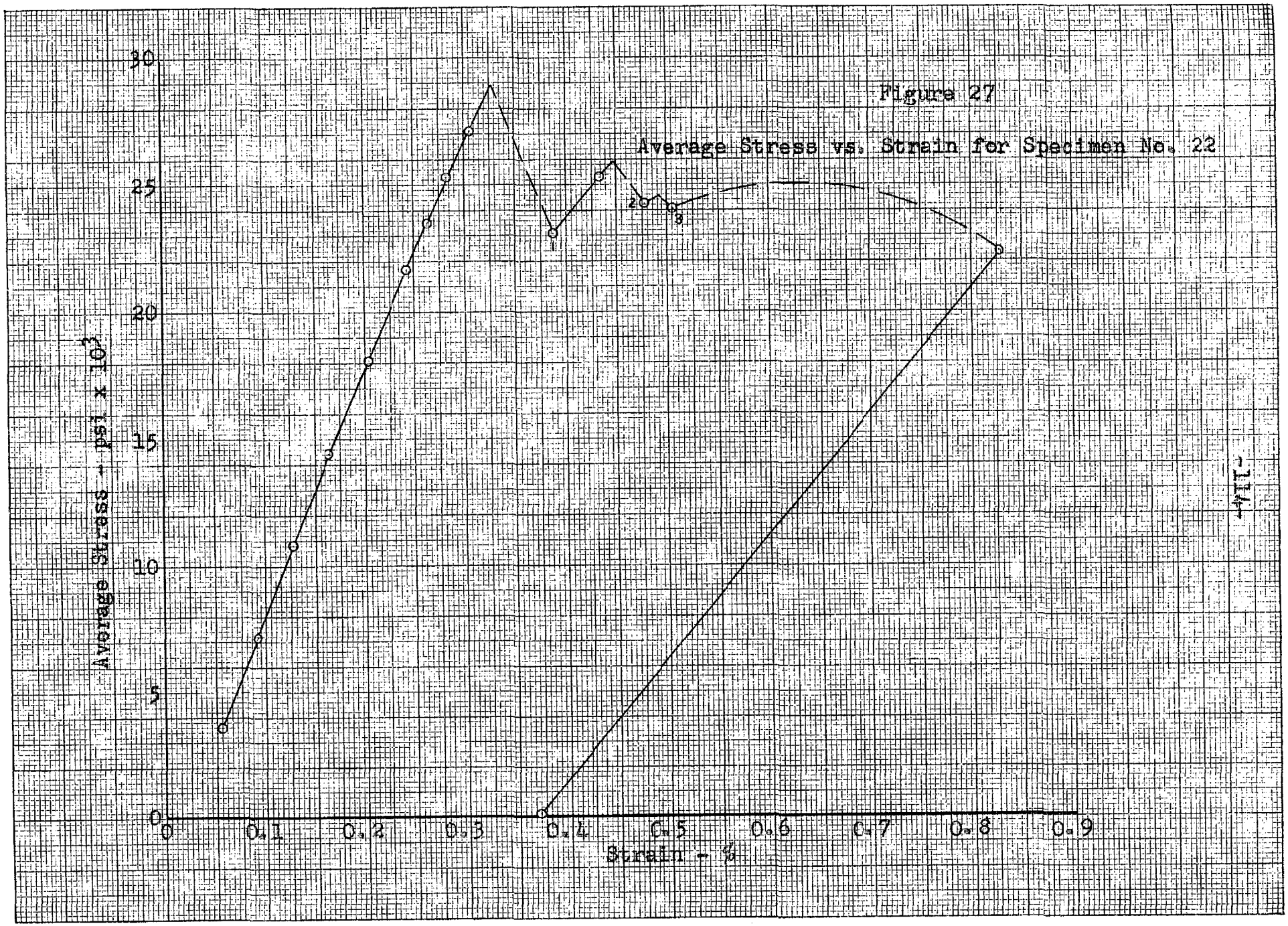
Figure 27
Average Stress vs. Strain for Specimen No. 22
Average Stress - psi x 10³
Strain - %
0
5
10
15
20
25
30
0
0.1
0.2
0.3
0.4
0.5
0.6
0.7
0.8
0.9
2
3

Figure 28

Circumferential Stress Distribution as a Function of Average Stress for Specimen No. I

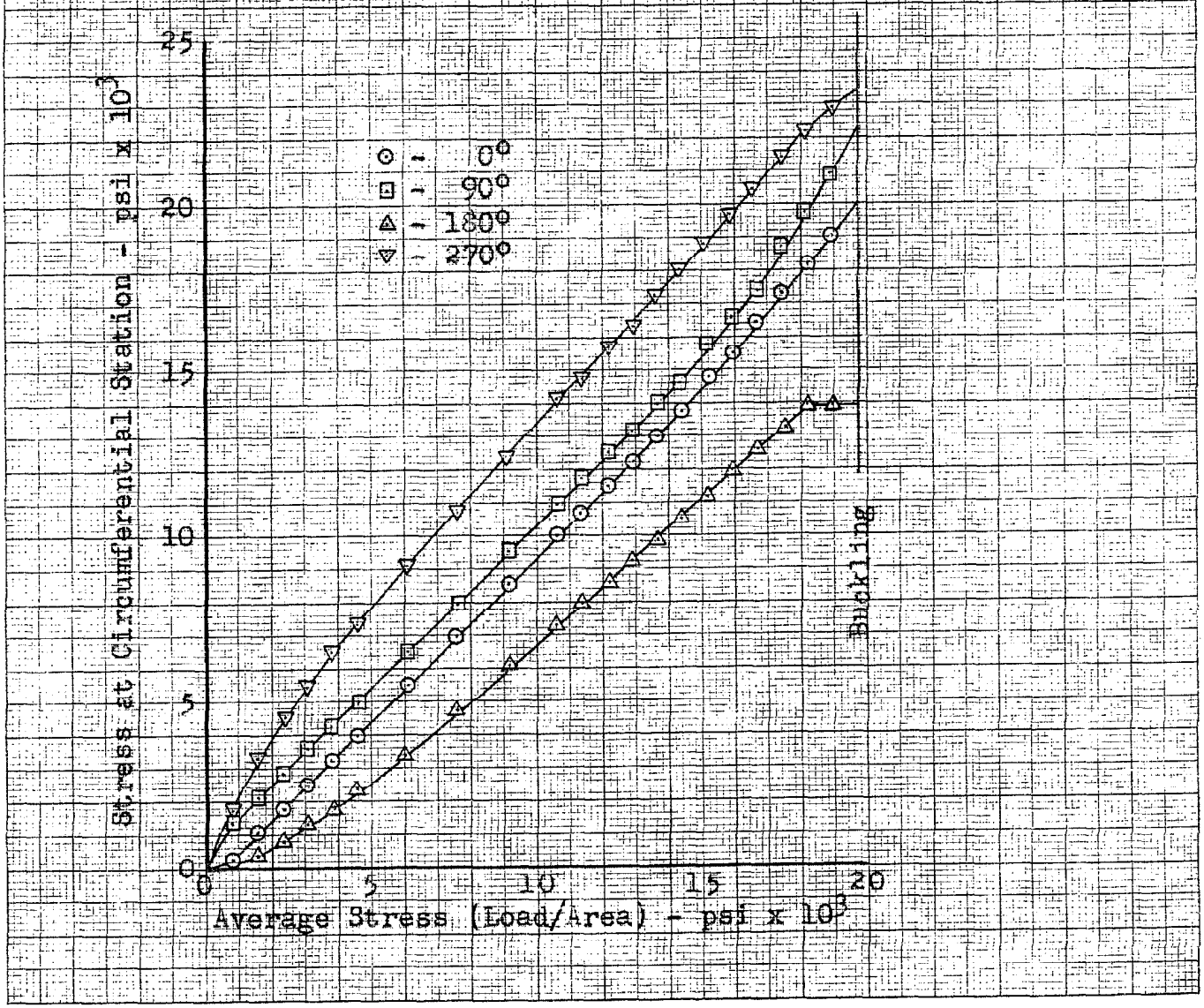

Figure 29

Circumferential Stress Distribution as a Function of Average Stress for Specimen No. 1A

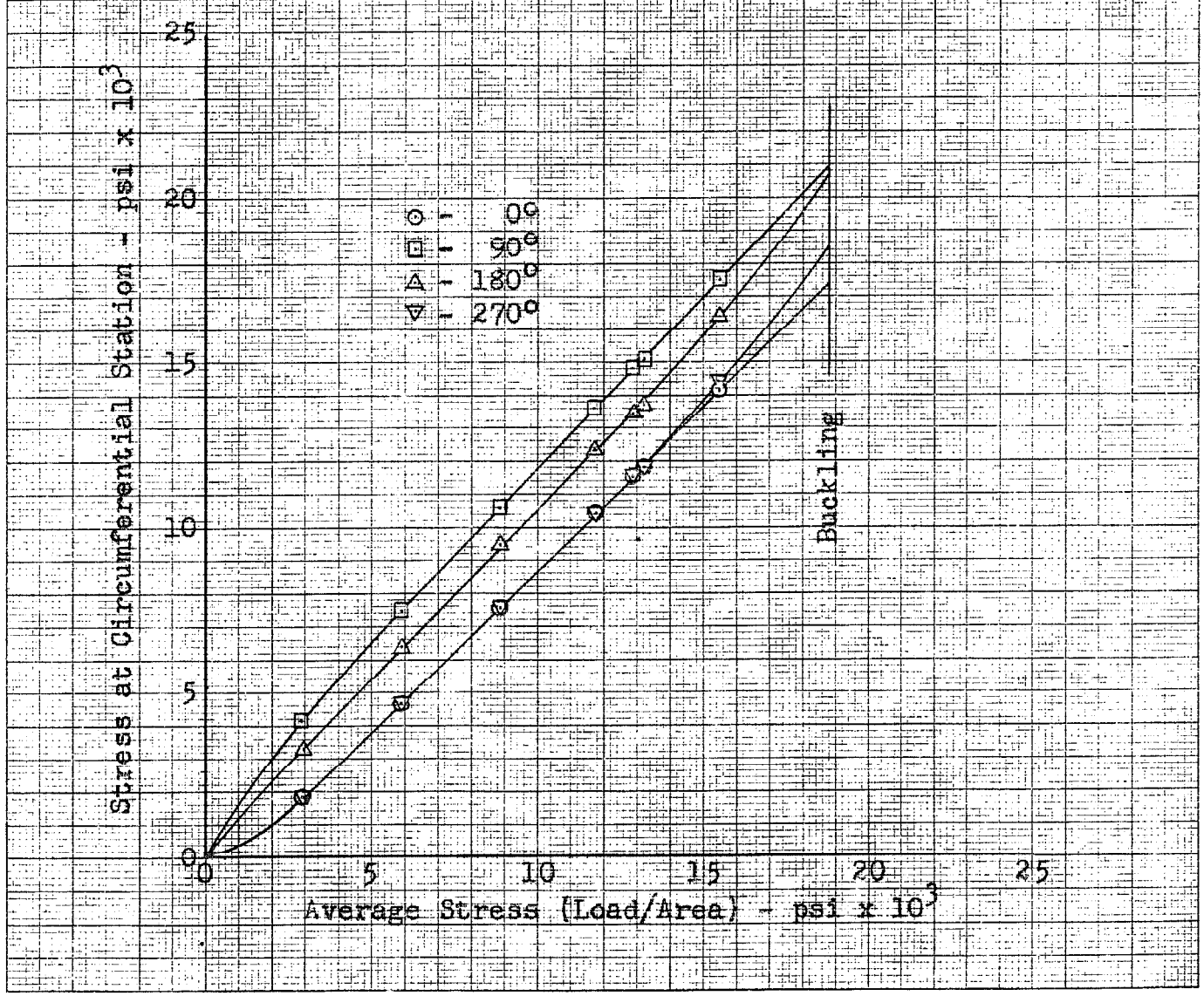

Figure 30

Circumferential Stress Distribution as a Function of Average Stress for Specimen No. 2

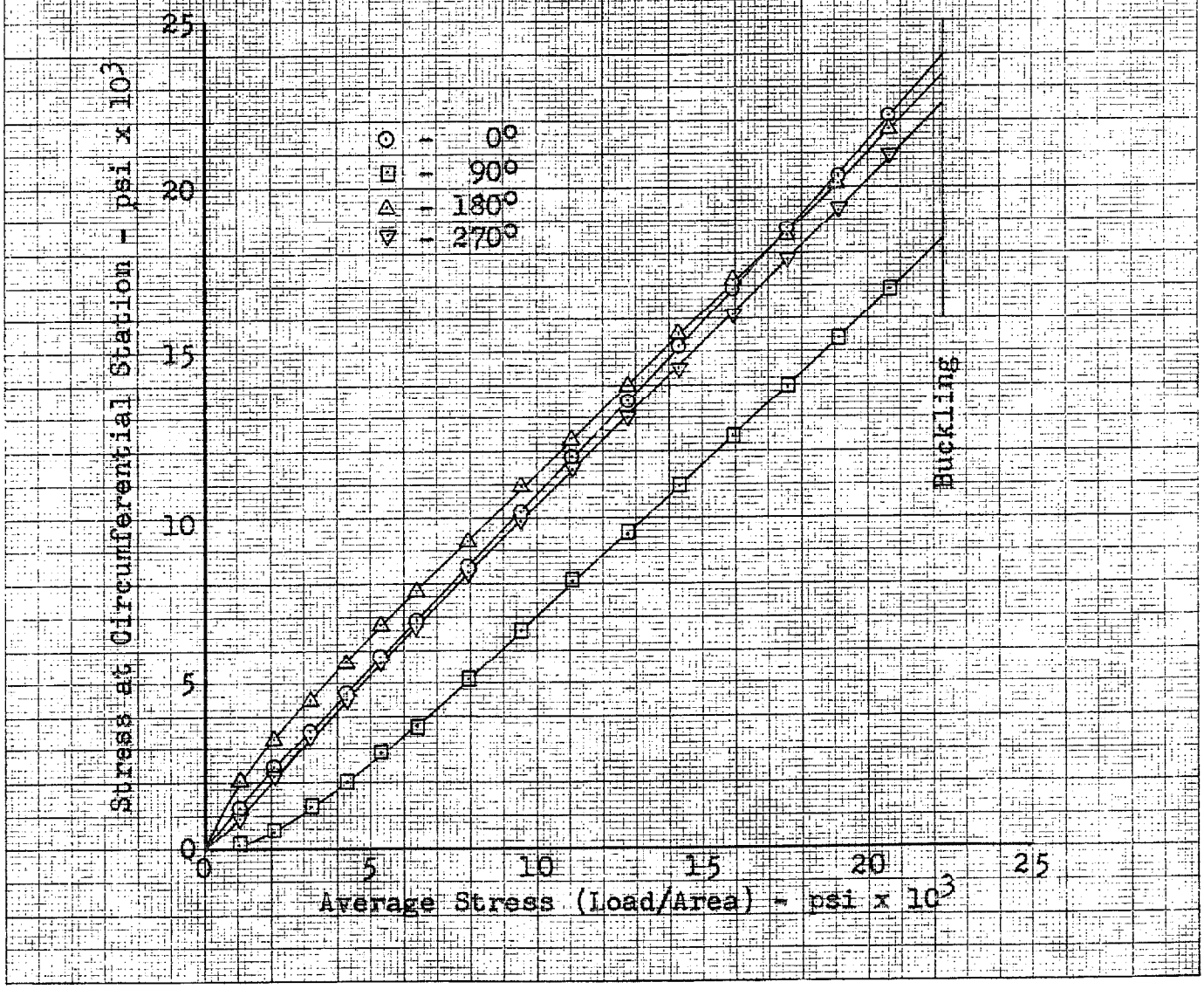

Figure 31

Circumferential Stress Distribution as a Function of Average Stress for Specimen No. 3

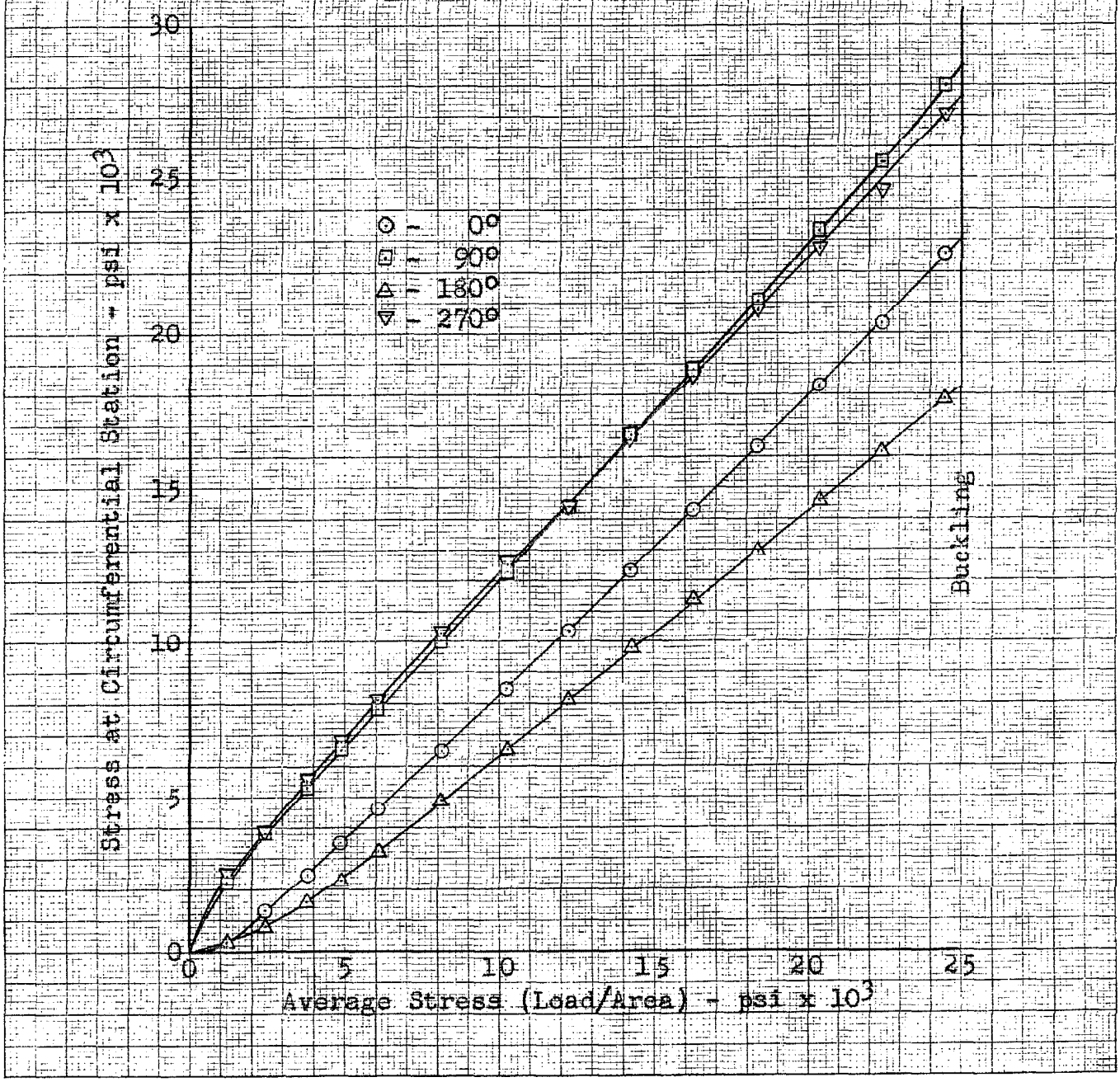

Figure 32

Circumferential Stress Distribution as a Function of Average Stress for Specimen No. 4

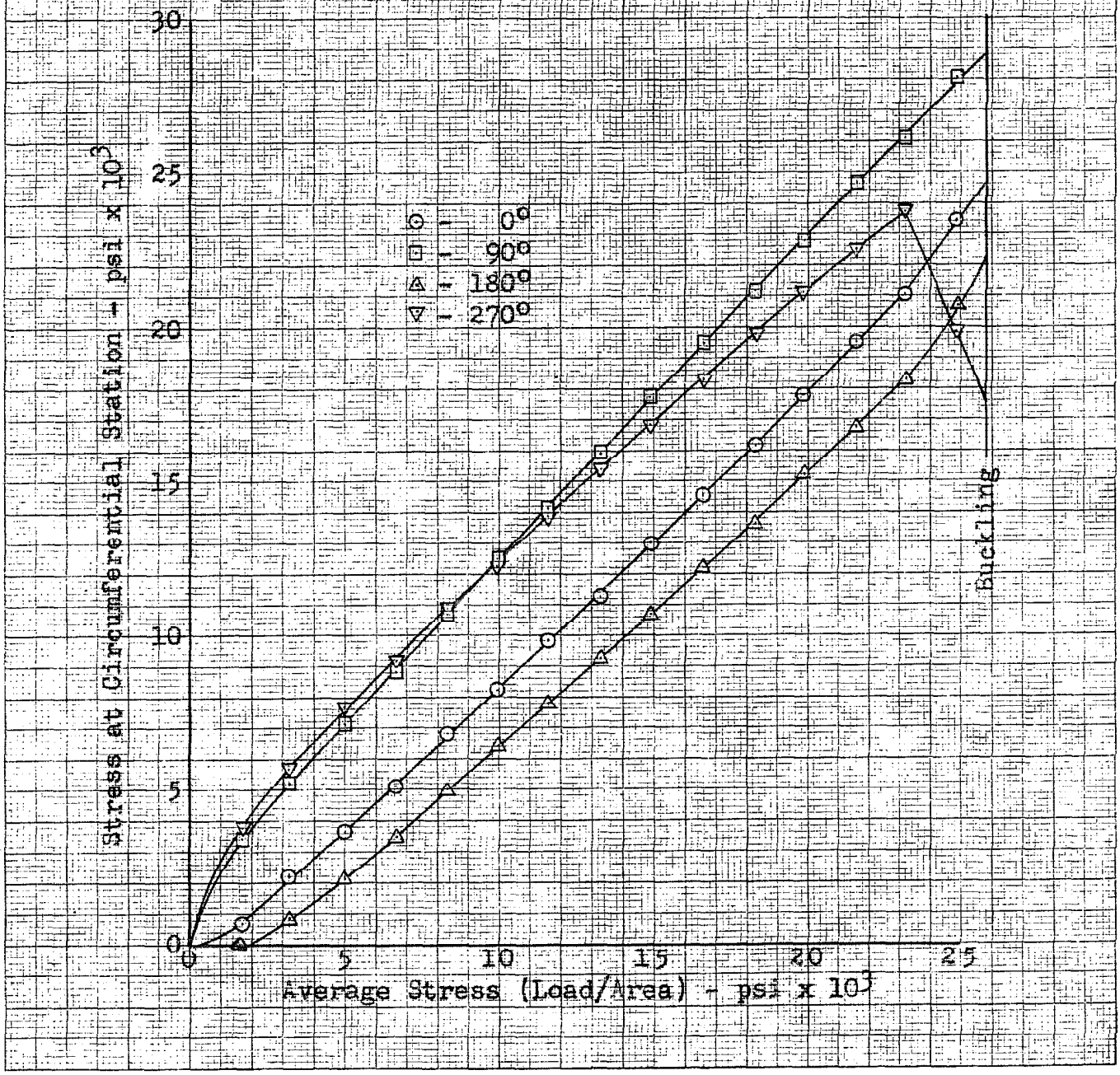

Figure 33

Circumferential Stress Distribution as a Function of Average Stress for Specimen No. 5

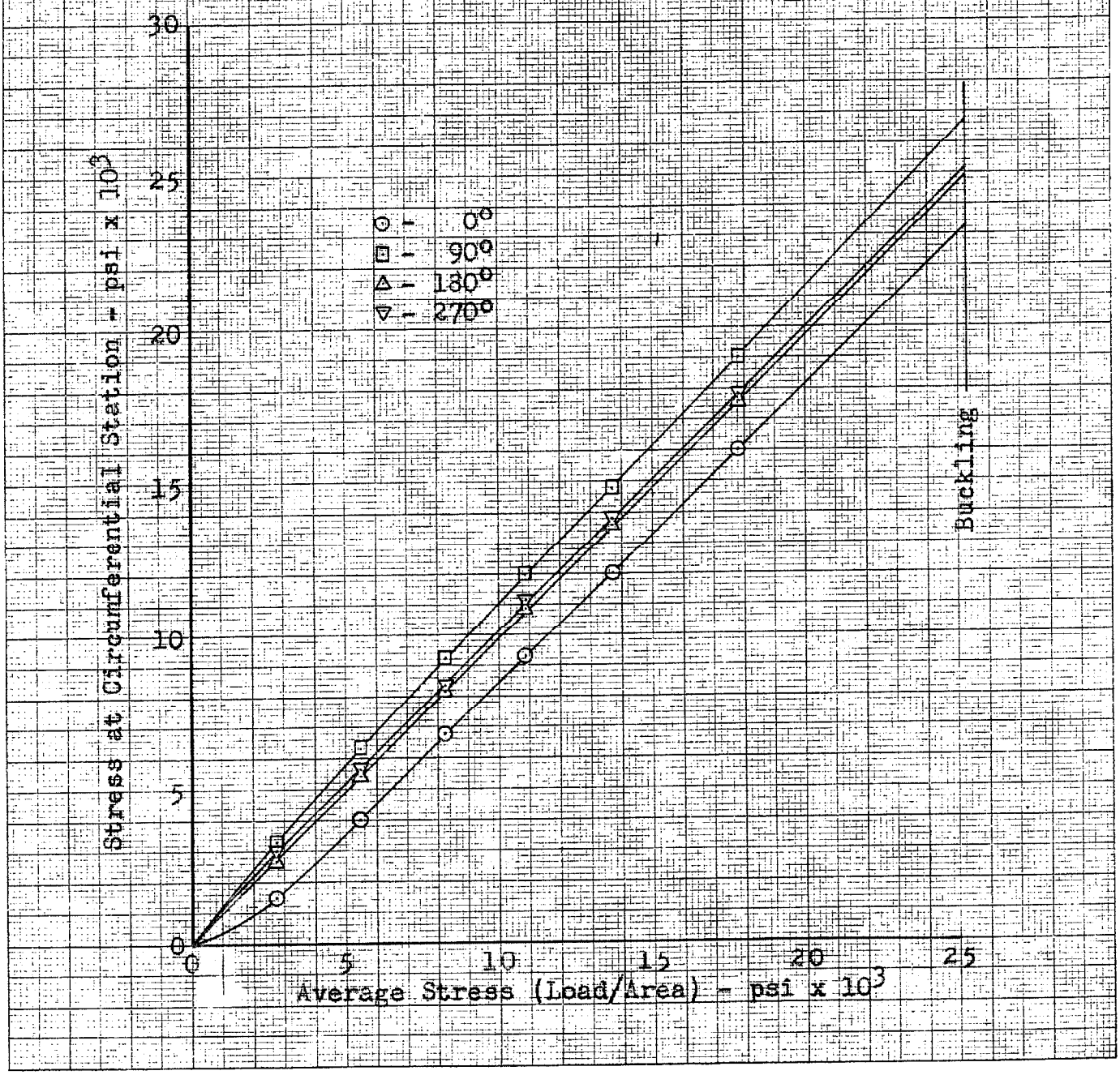

Figure 34

Circumferential Stress Distribution as a Function of Average Stress for Specimen No. 5A

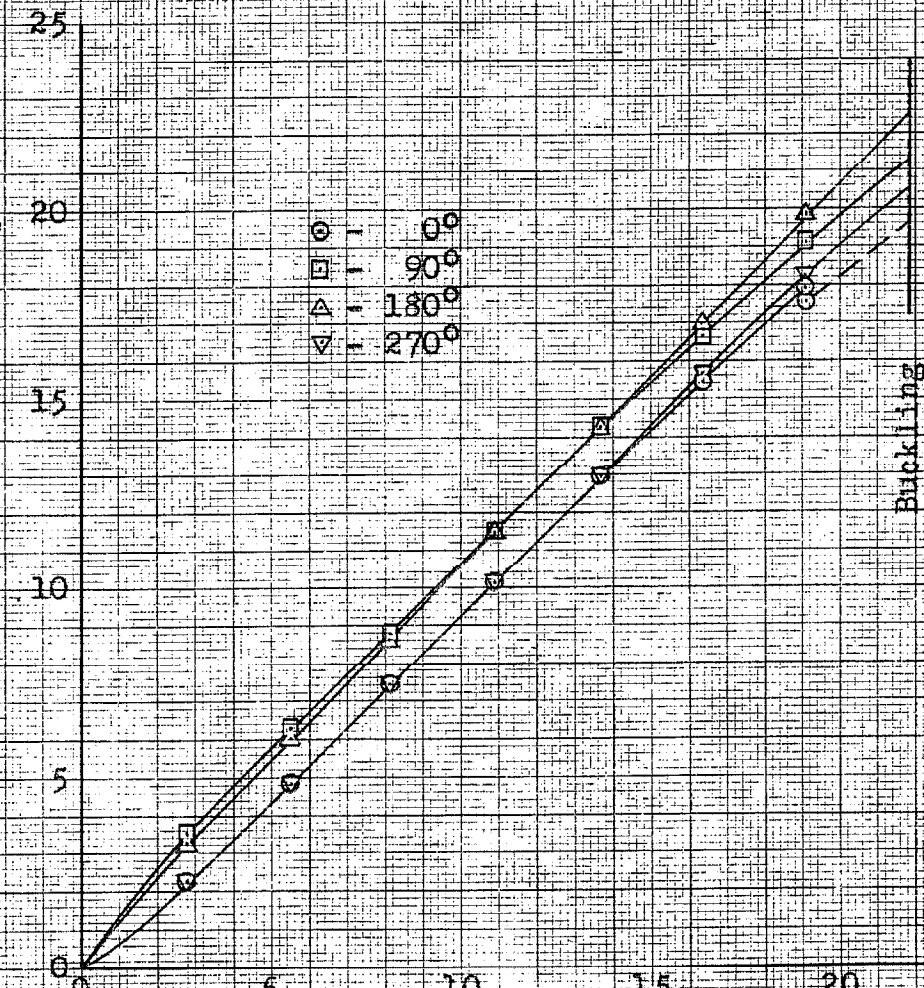

Figure 35

Circumferential Stress Distribution as a Function of Average Stress for Specimen No. 6

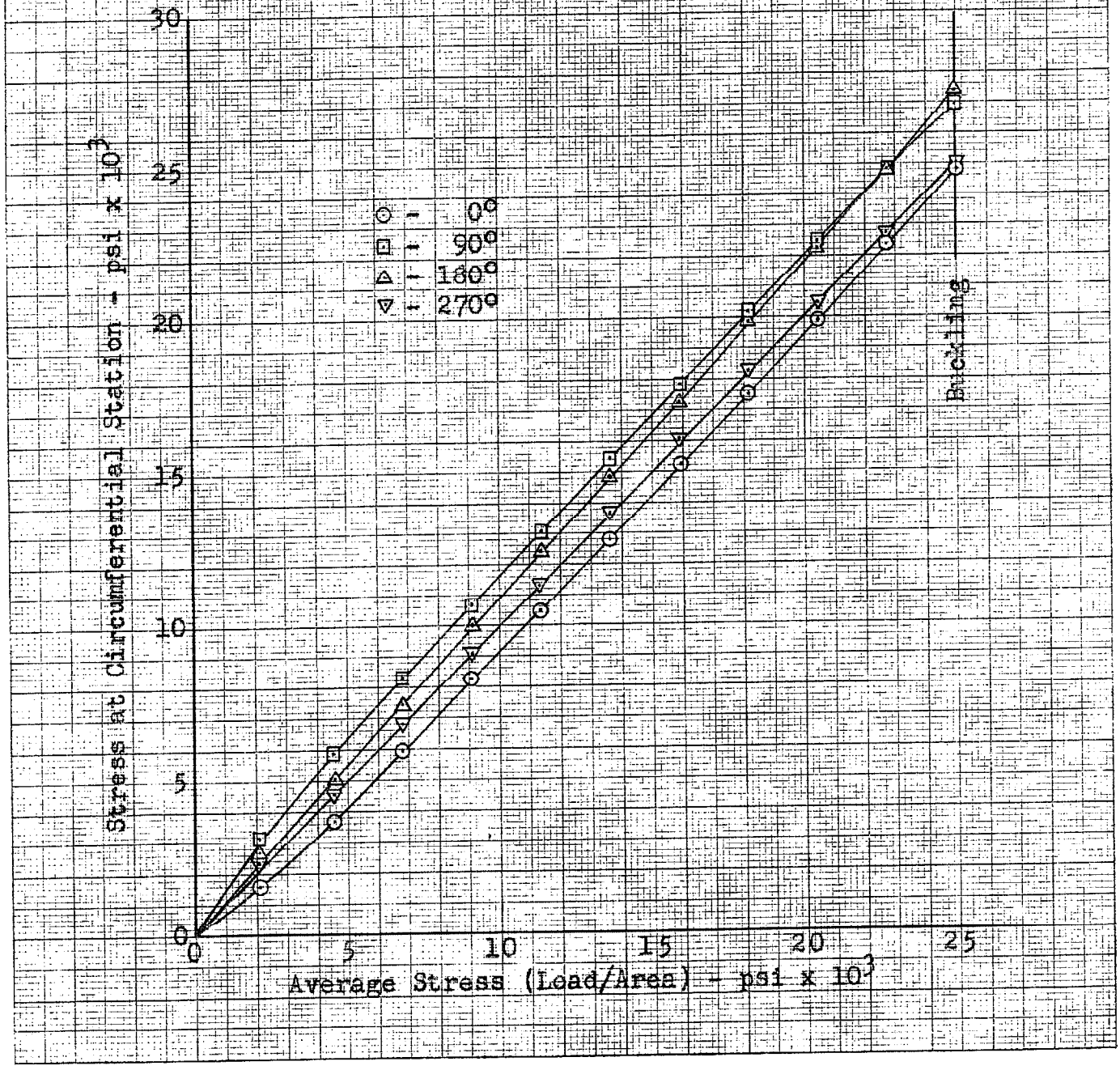

Figure 36

Circumferential Stress Distribution as a Function of Average Stress for Specimen No. 7

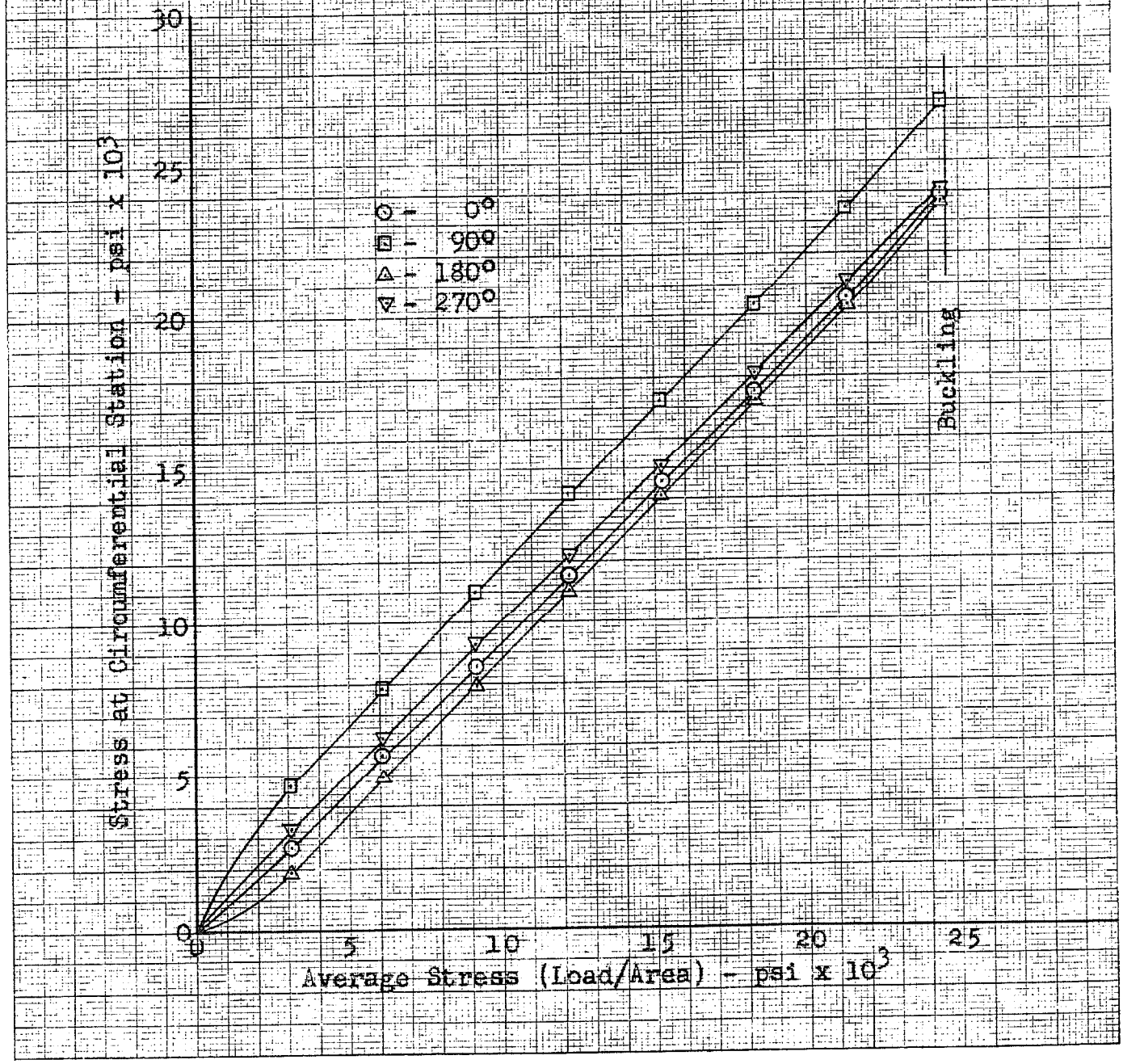

Figure 37

Circumferential Stress Distribution as a Function of Average Stress for Specimen No. 8

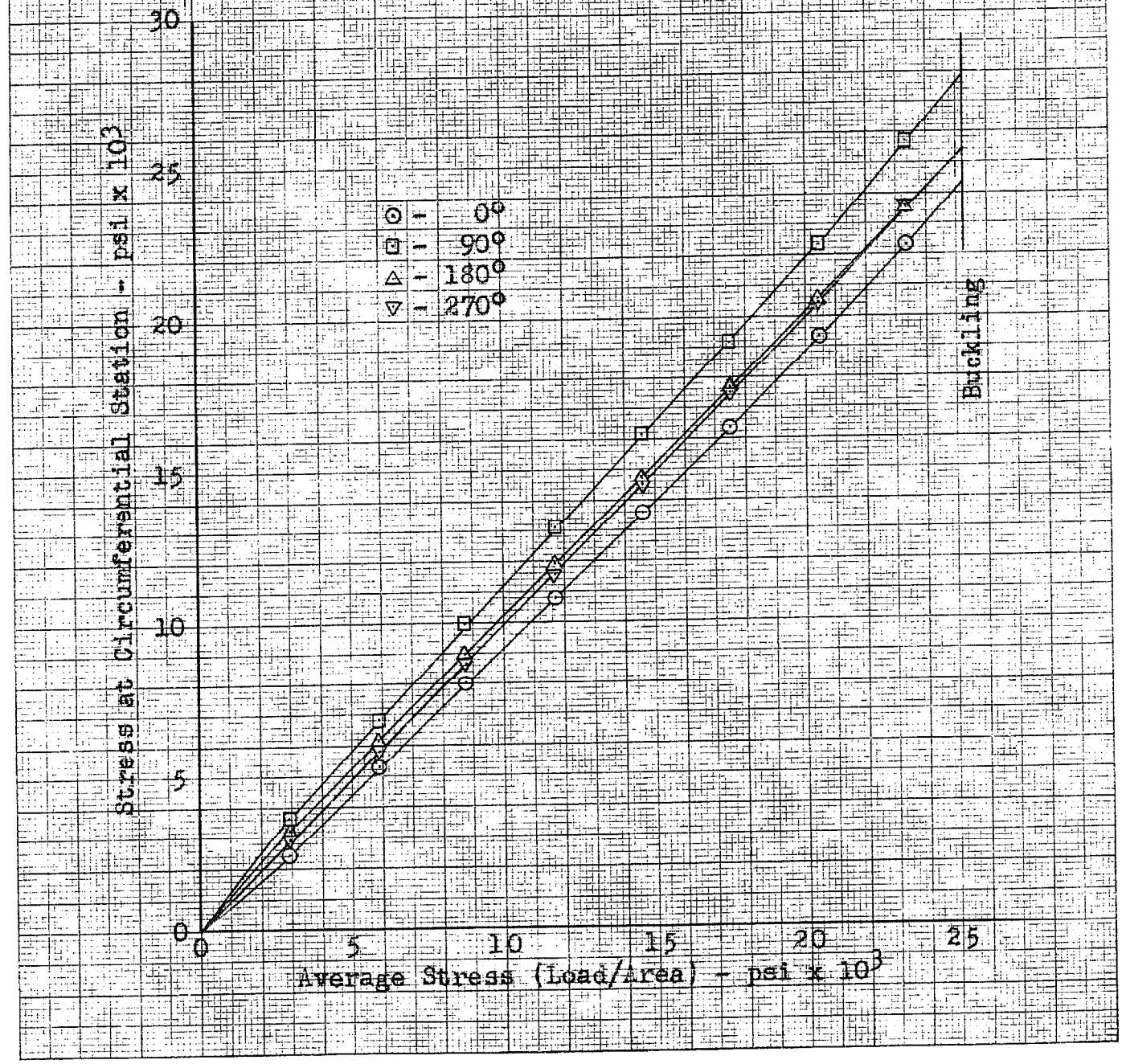

Figure 38

Circumferential Stress Distribution as a Function of Average Stress for Specimen No. 9

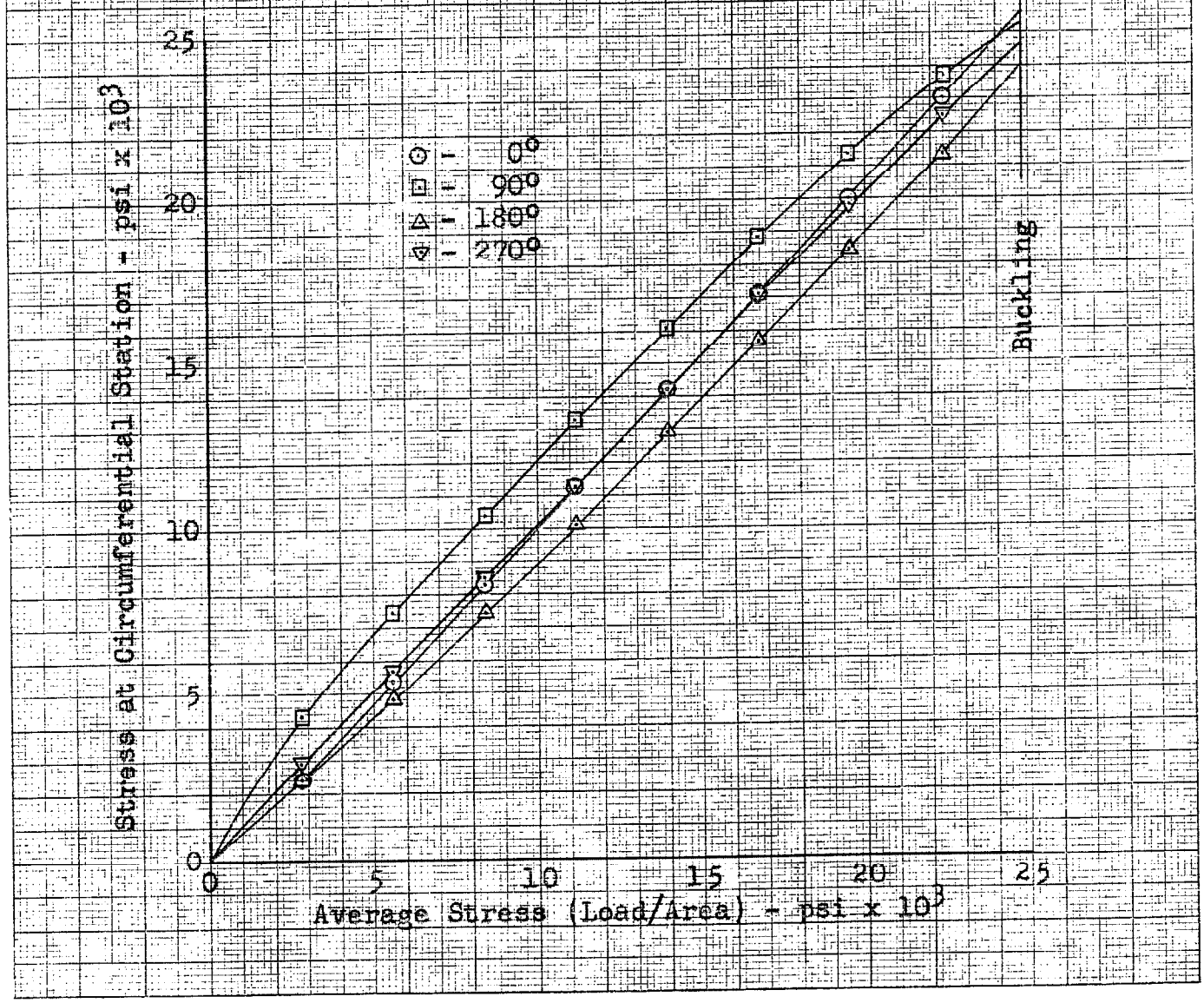

Figure 39

Circumferential Stress Distribution as a Function of Average Stress for Specimen No. 10

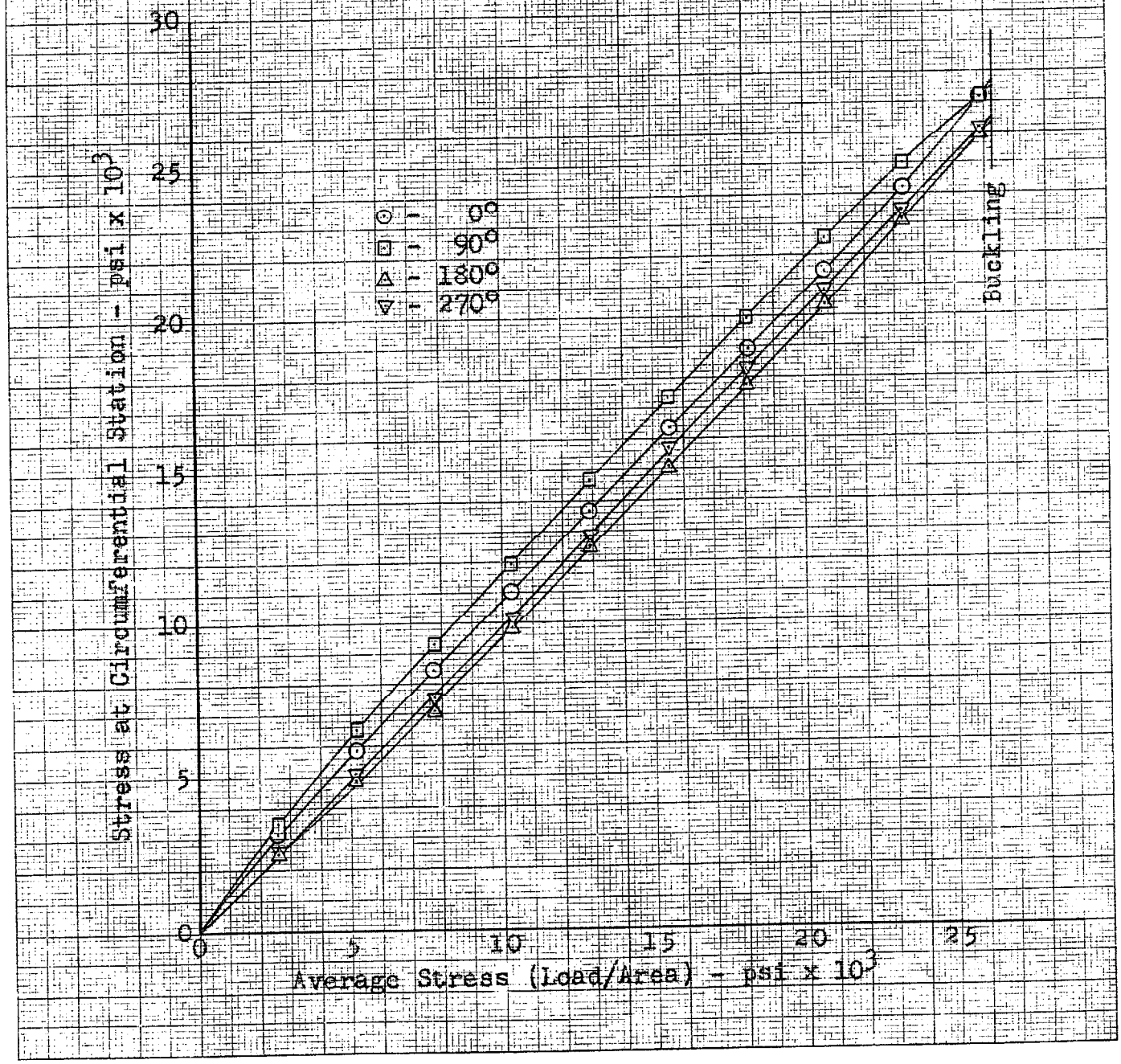

Figure 40

Circumferential Stress Distribution as a Function of Average Stress for Specimen No. 11

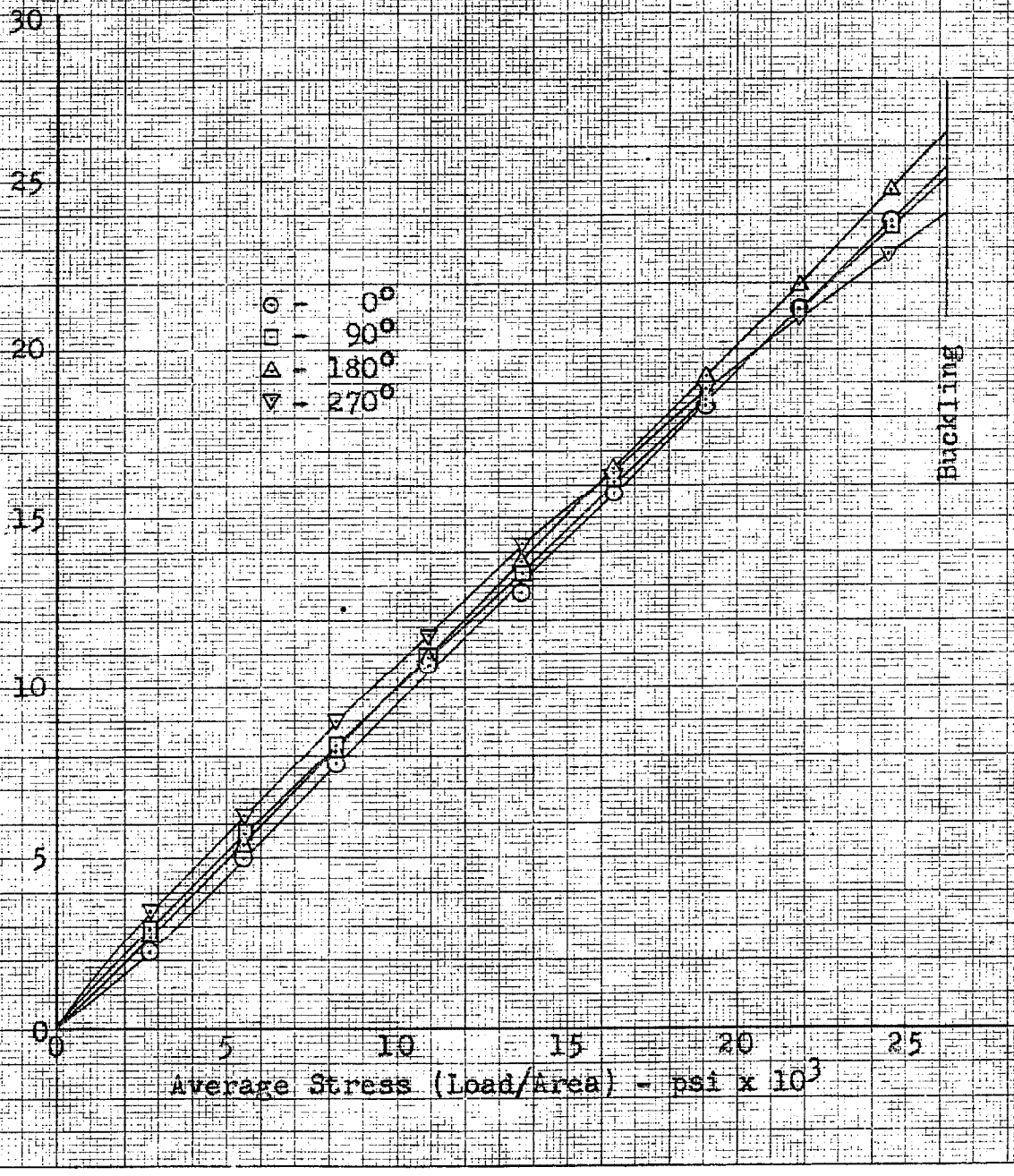

Figure 41

Circumferential Stress Distribution as a Function of Average Stress for Specimen No. 12

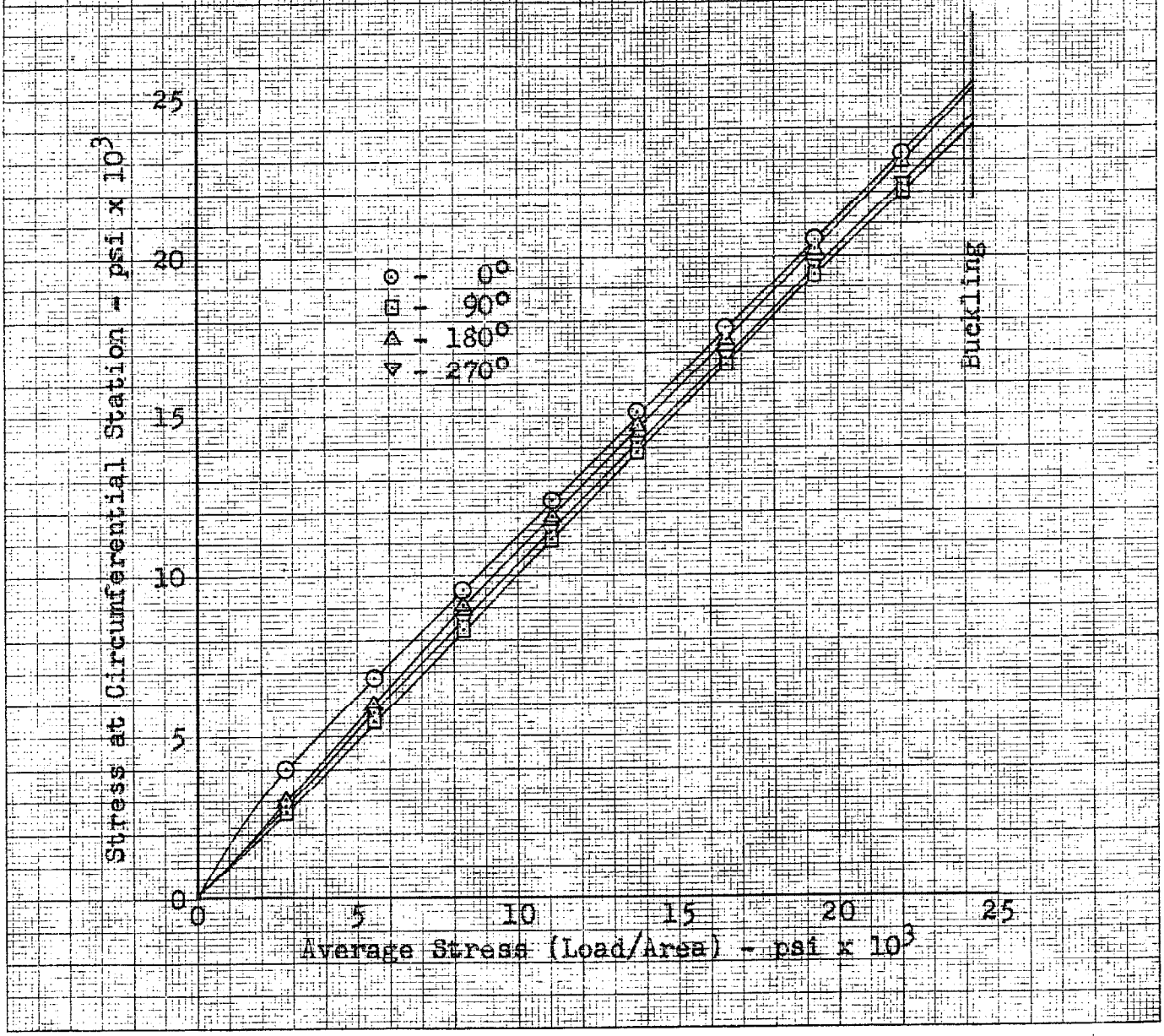

Figure 42

Circumferential Stress Distribution as a Function of Average Stress for Specimen No. 13

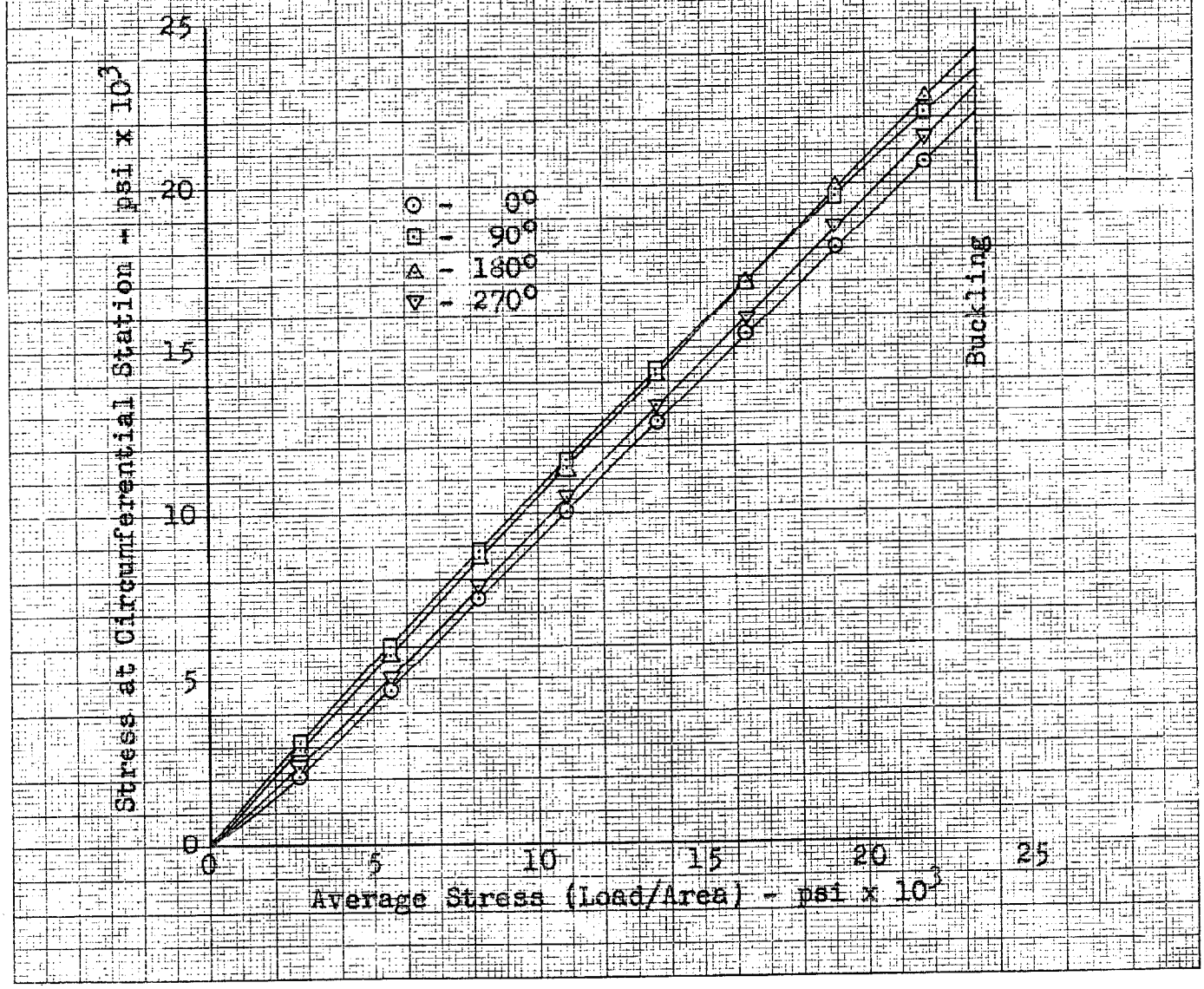

Figure 43

Circumferential Stress Distribution as a Function of Average Stress for Specimen No. 14

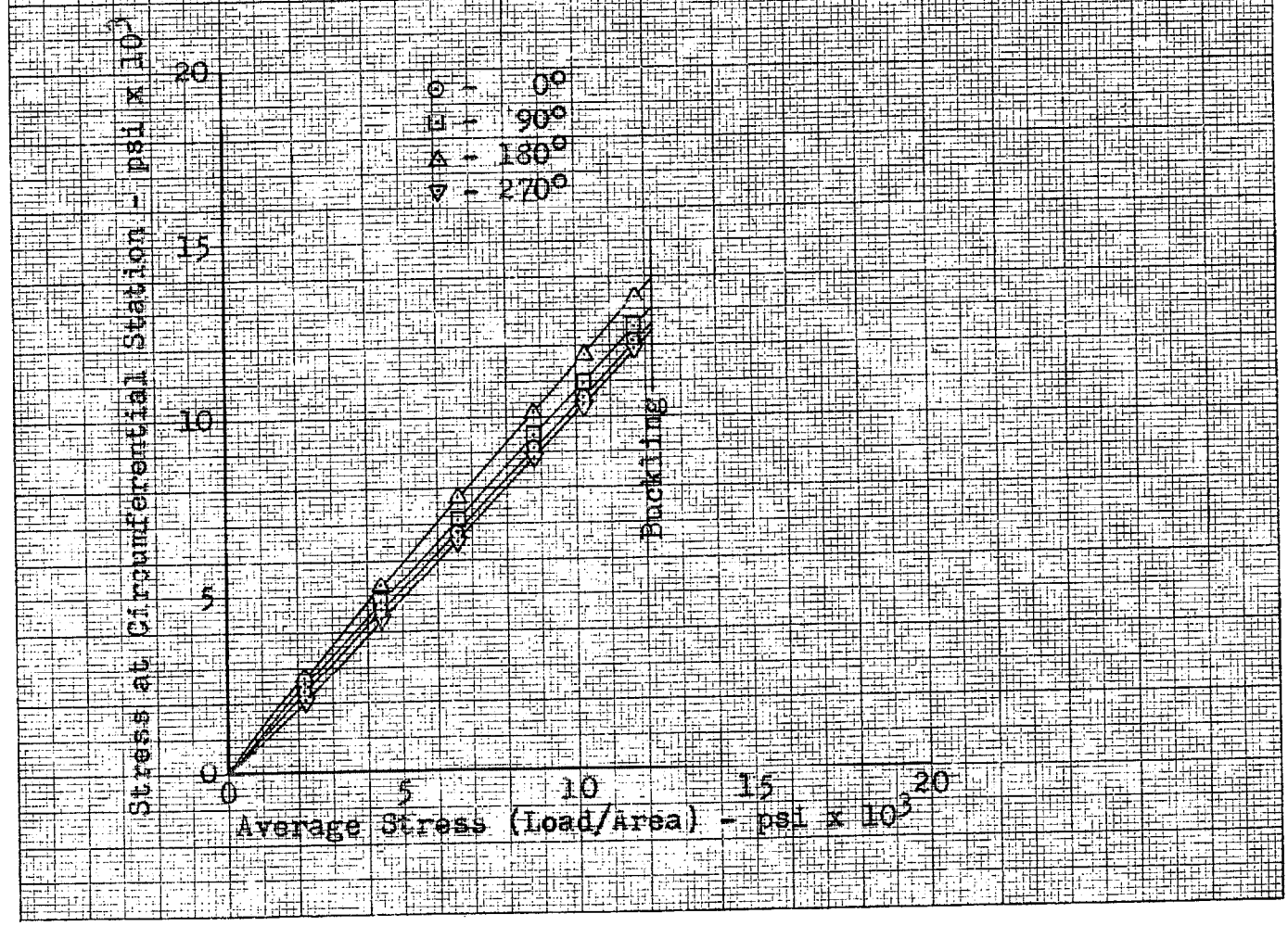

Figure 44

Circumferential Stress Distribution as a Function of Average Stress for Specimen No. 15

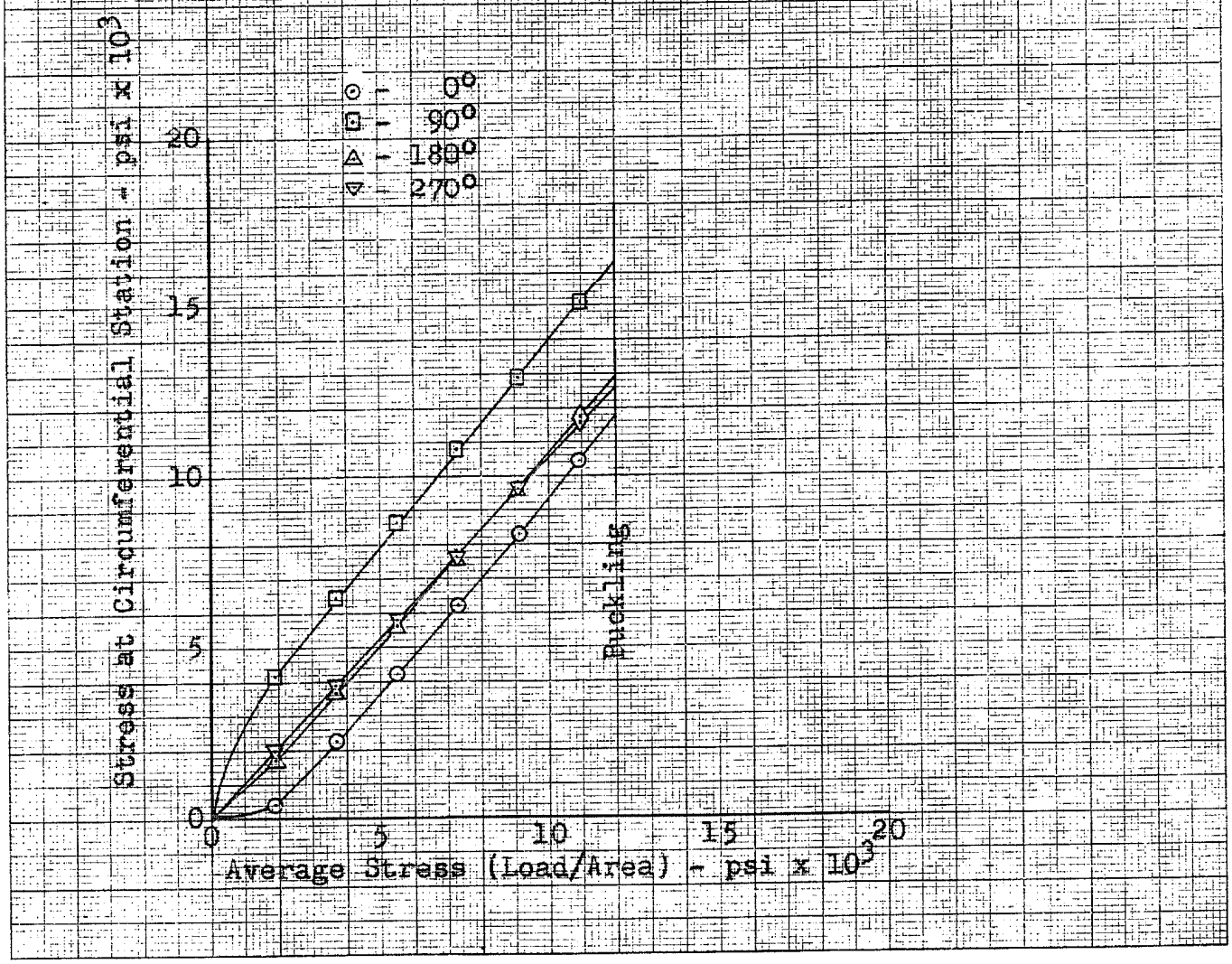

Figure 45

Circumferential Stress Distribution as a Function of Average Stress for Specimen No. 16

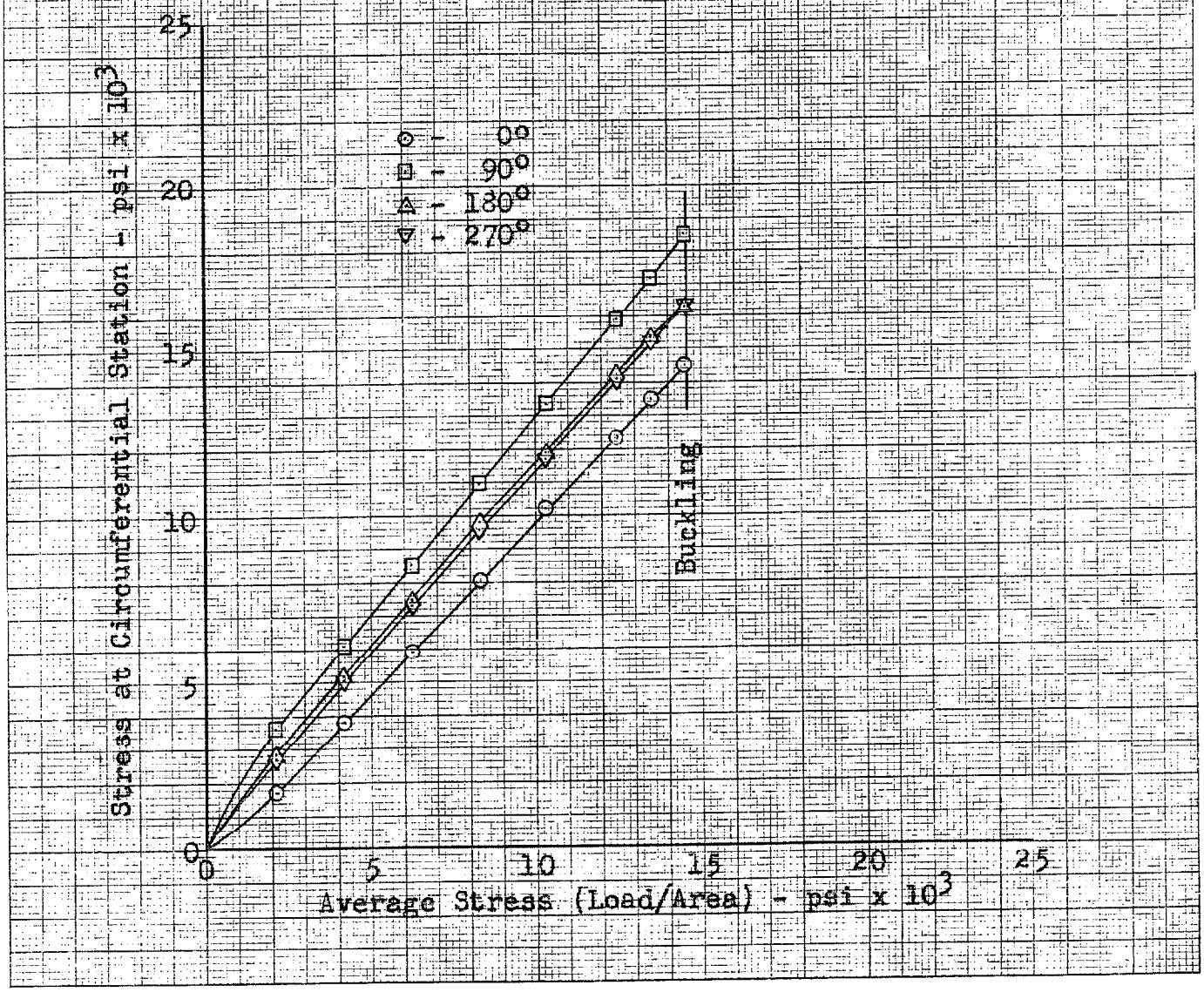

Figure 46

Circumferential Stress Distribution as a Function of Average Stress for Specimen No. 17

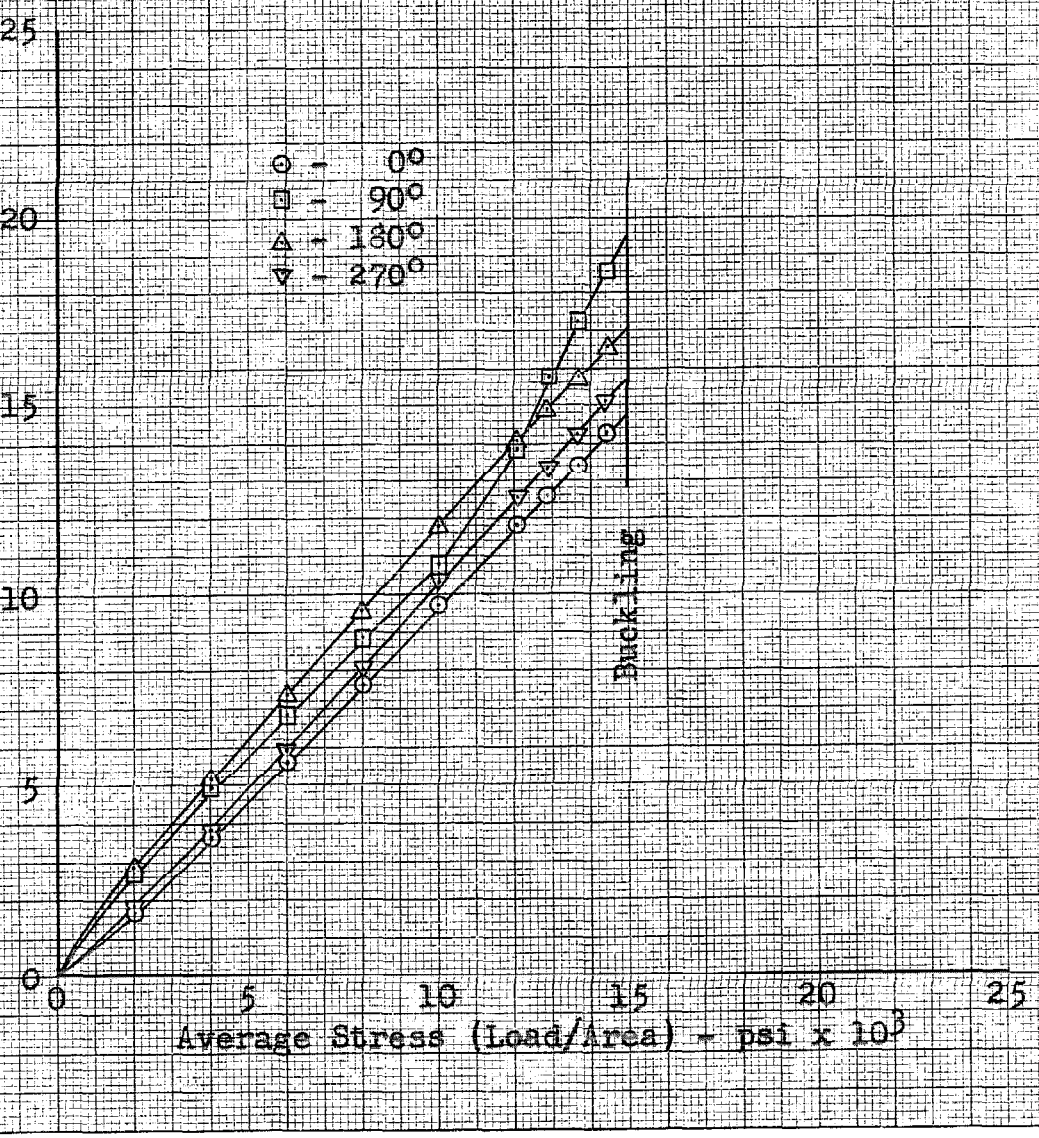

Figure 47

Circumferential Stress Distribution as a Function of Average Stress for Specimen No. 19

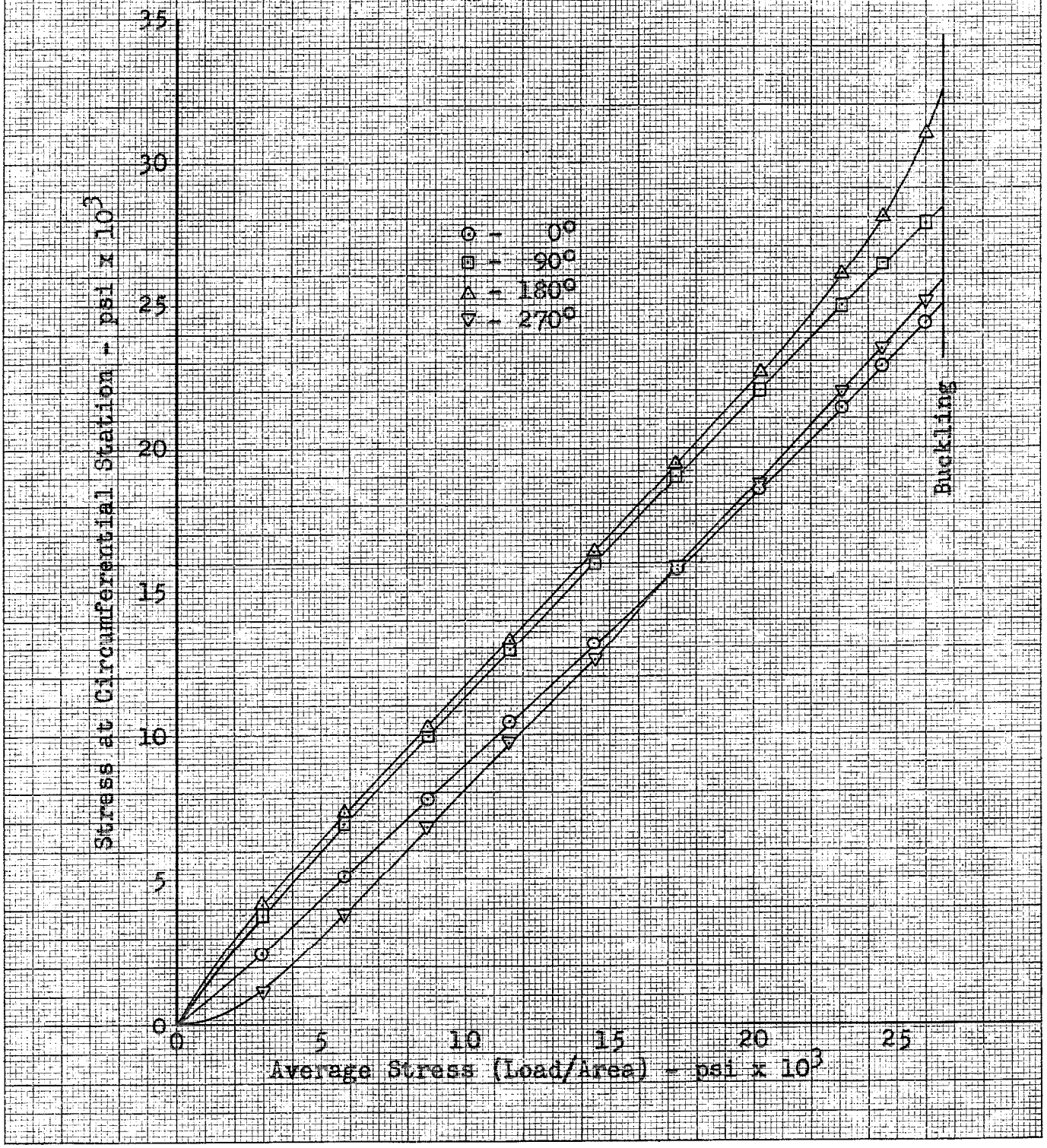

Figure 48

Circumferential Stress Distribution as a Function of Average Stress for Specimen No. 20

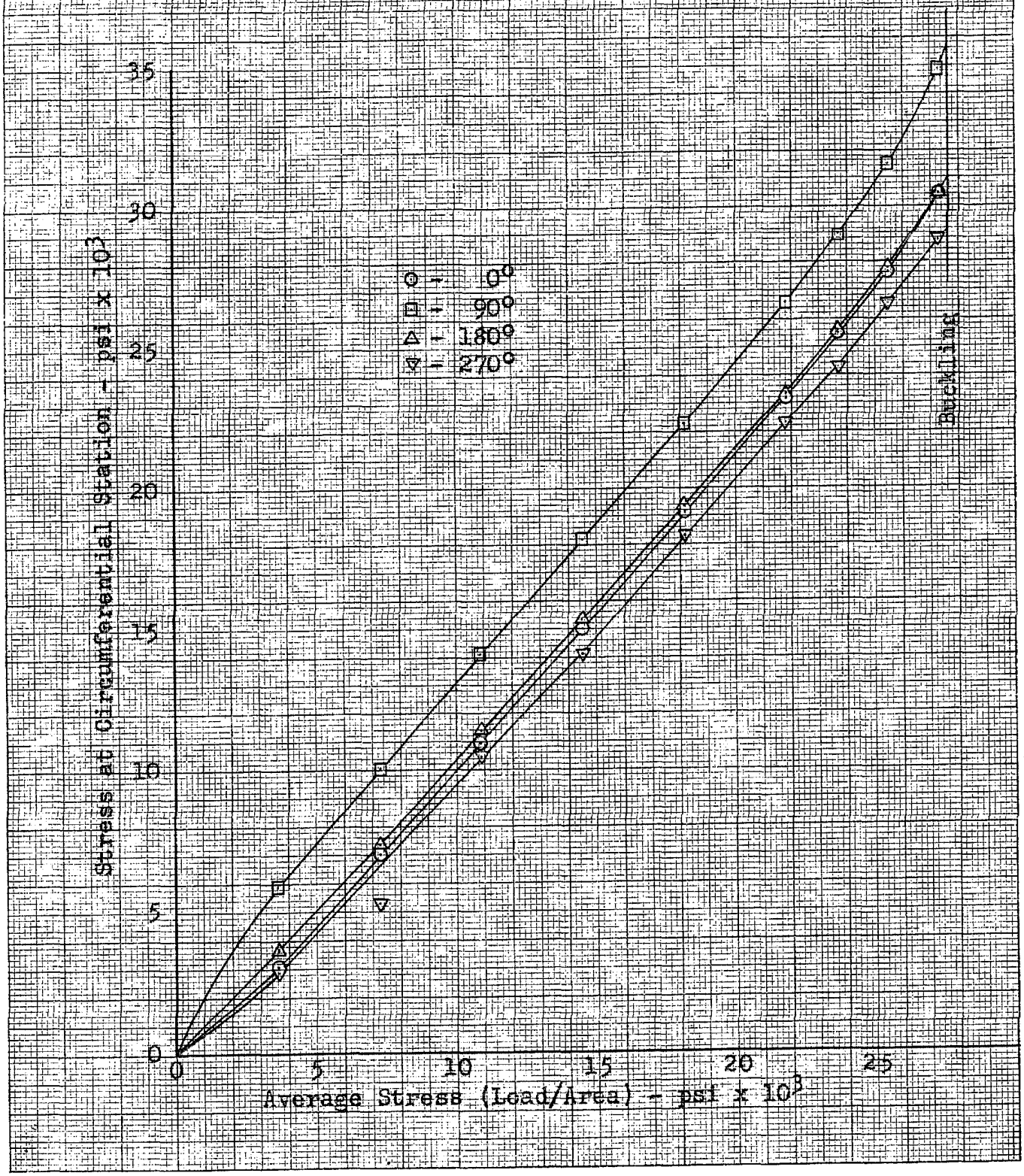

Figure 49

Circumferential Stress Distribution as a Function of Average Stress for Specimen No. 21

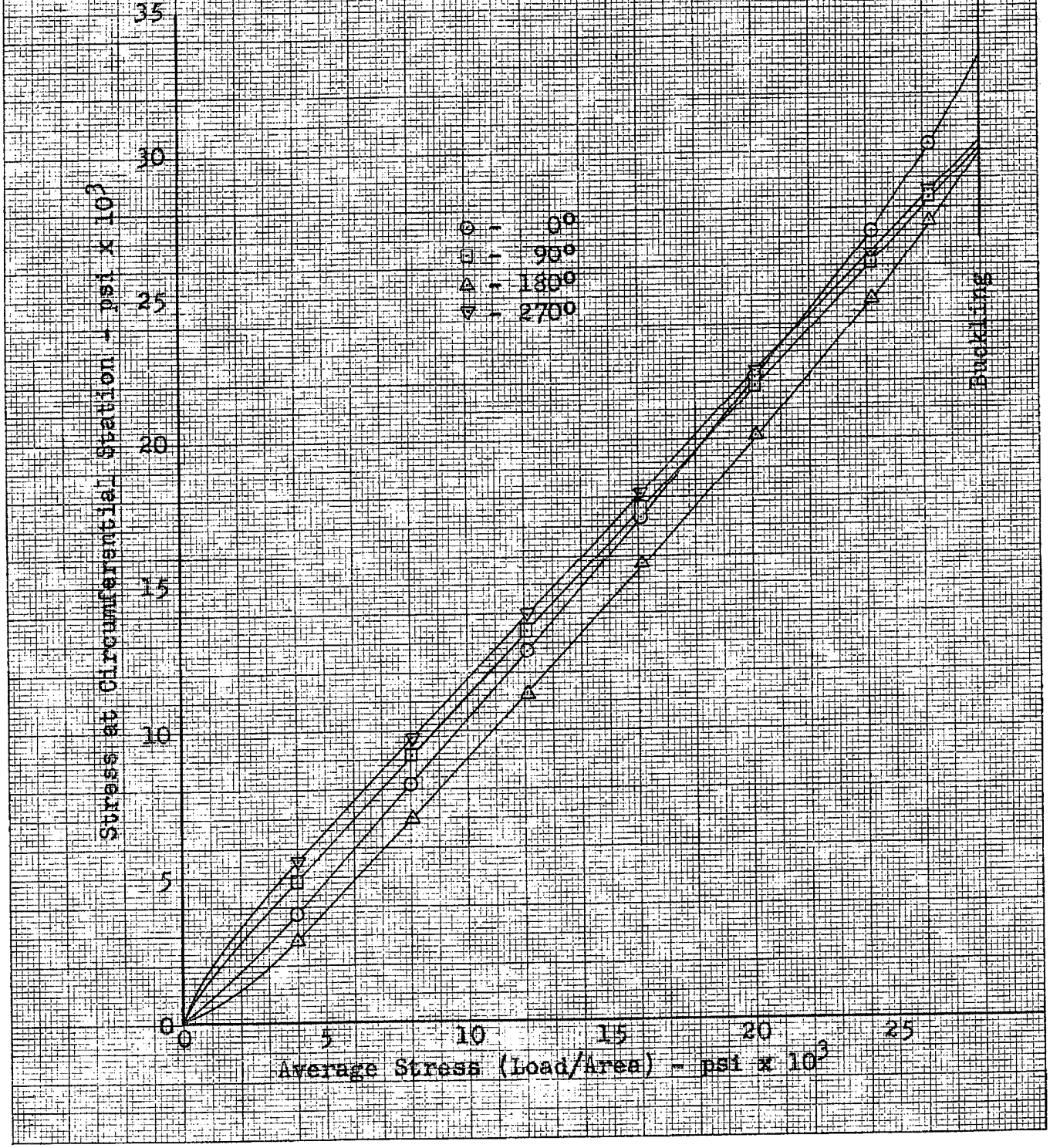

Figure 50

Circumferential Stress Distribution as a Function of Average Stress for Specimen No. 72

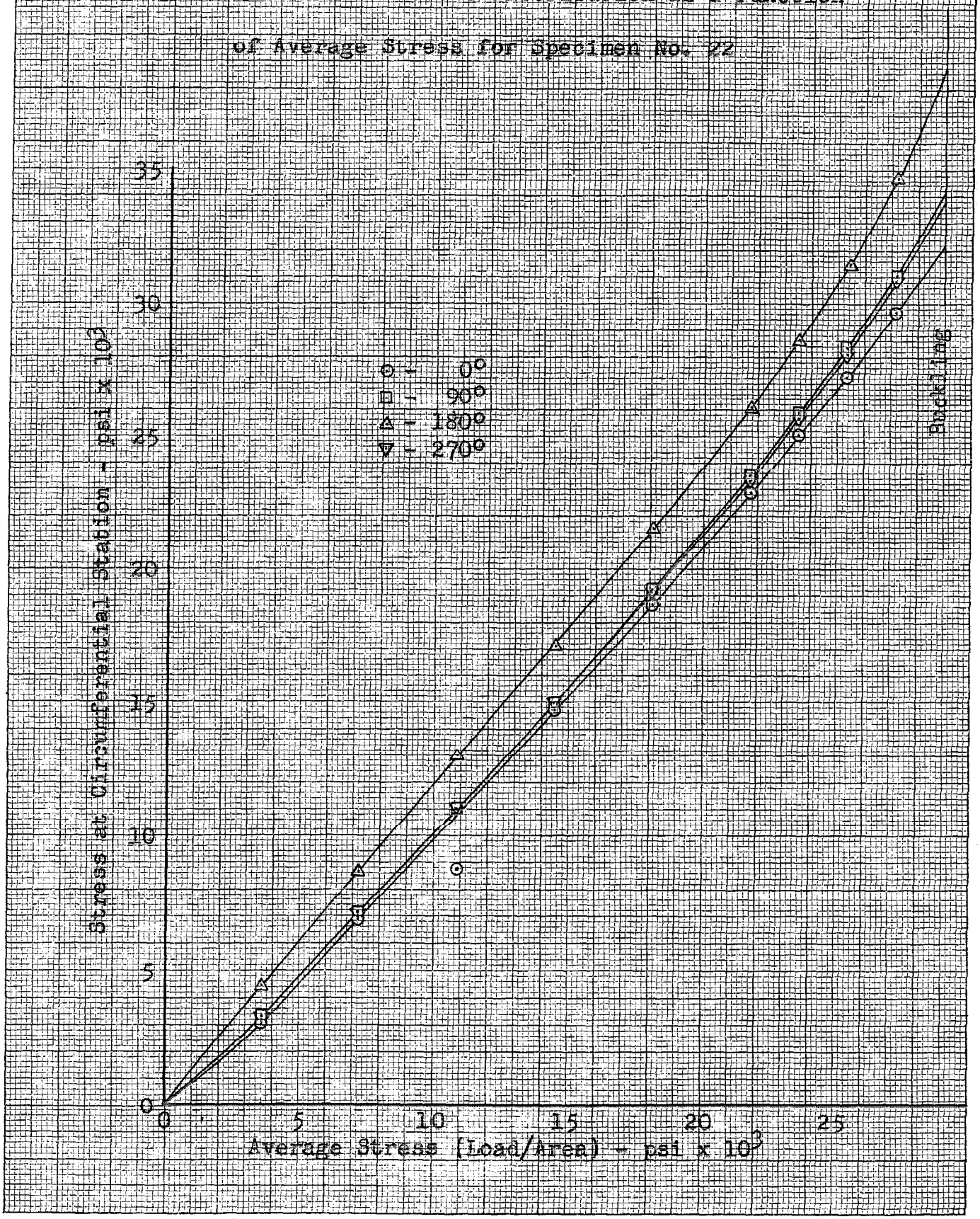

Note: The numbers within the buckles on Figures 51 through 75 refer to the Buckle State. (the order in which the buckles appeared)

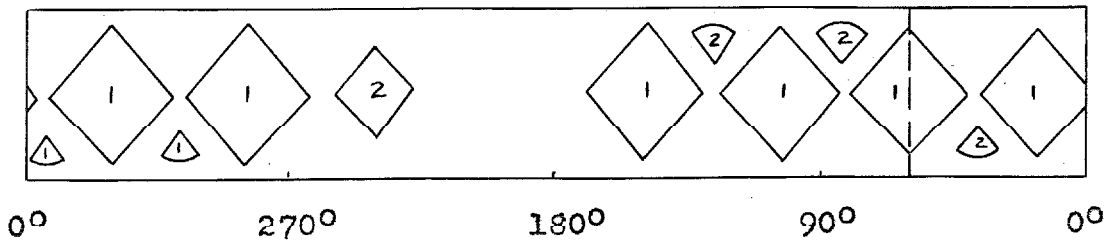

Figure 51

Buckle Pattern of Specimen No. 1

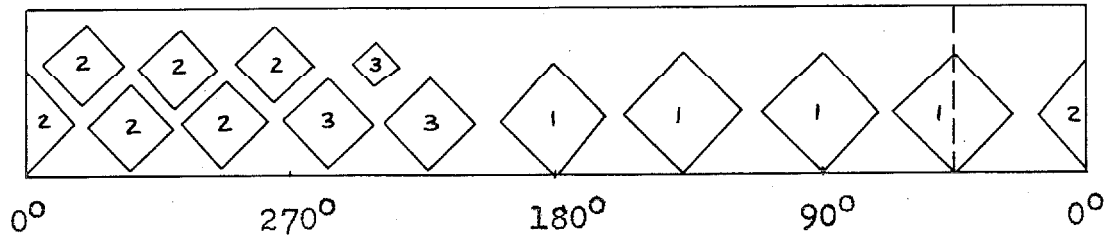

Figure 52

Buckle Pattern of Specimen No. 1A

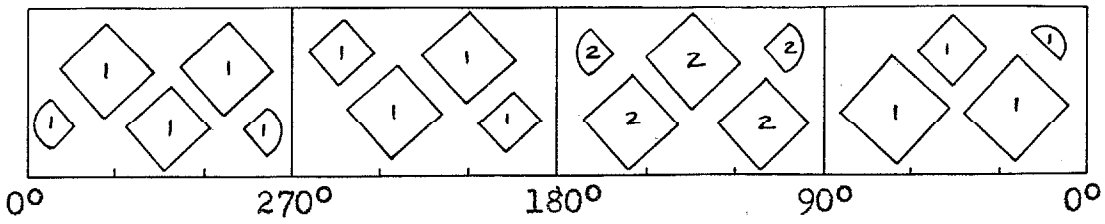

Figure 53

Buckle Pattern of Specimen No. 2

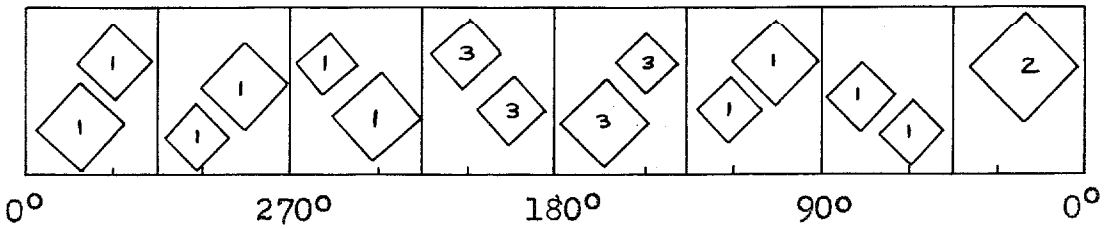

Figure 54

Buckle Pattern of Specimen No. 3

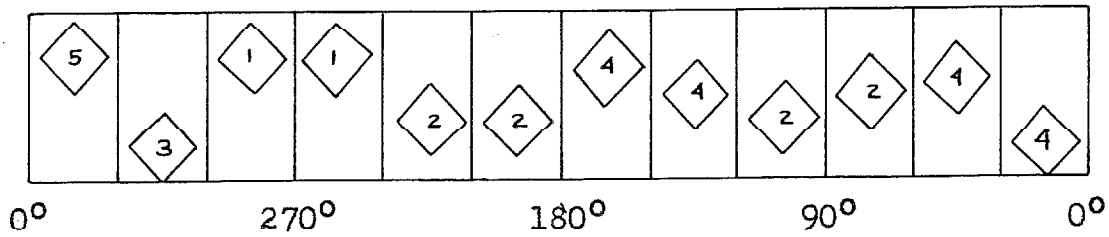

Figure 55

Buckle Pattern of Specimen No. 4

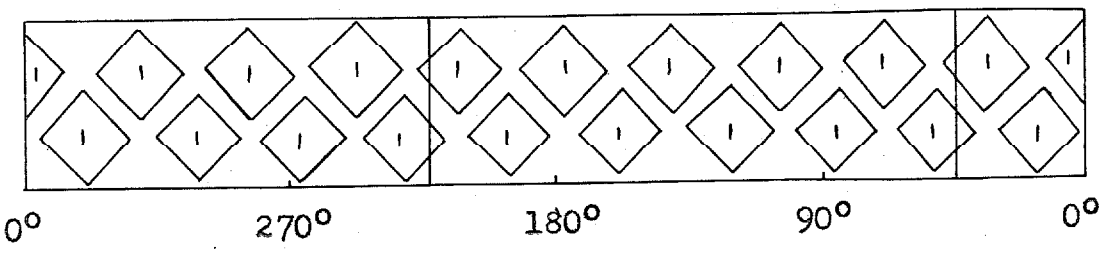

Figure 56

Buckle Pattern of Specimen No. 5

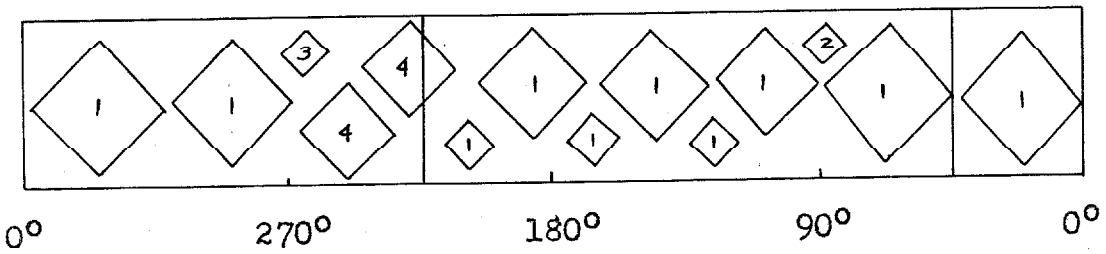

Figure 57

Buckle Pattern of Specimen No. 5A

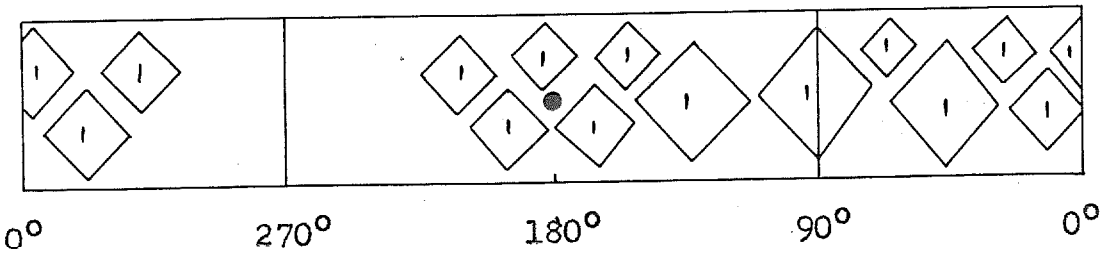

Figure 58

Buckle Pattern of Specimen No. 5B

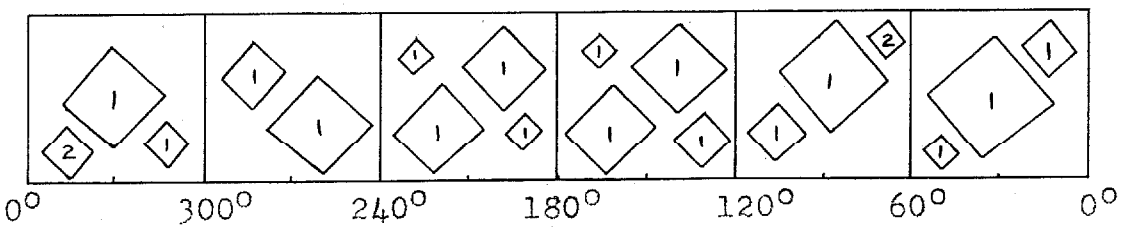

Figure 59

Buckle Pattern of Specimen No. 6

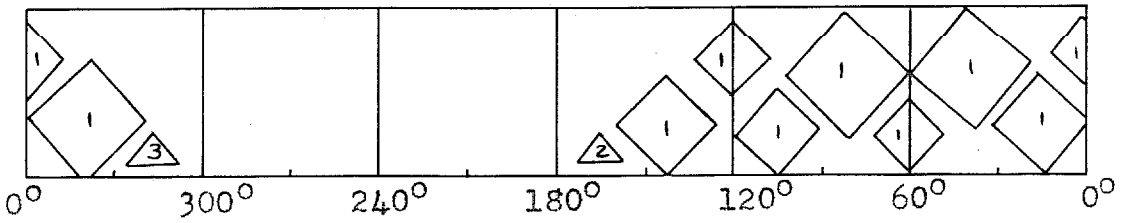

Figure 60

Buckle Pattern of Specimen No. 7

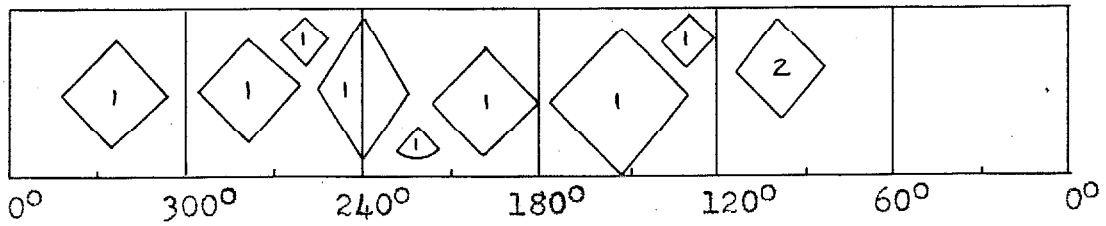

Figure 61

Buckle Pattern of Specimen No. 8

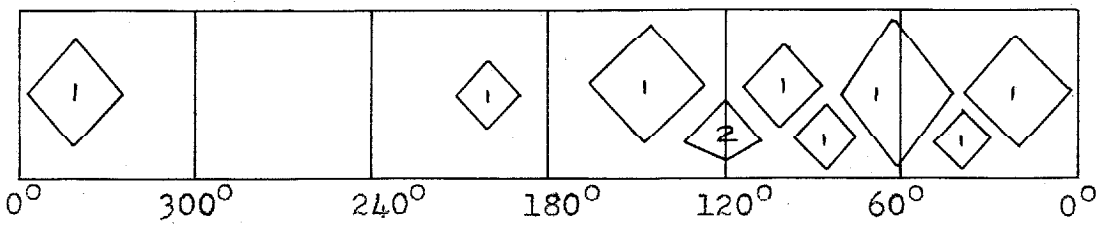

Figure 62

Buckle Pattern of Specimen No. 9

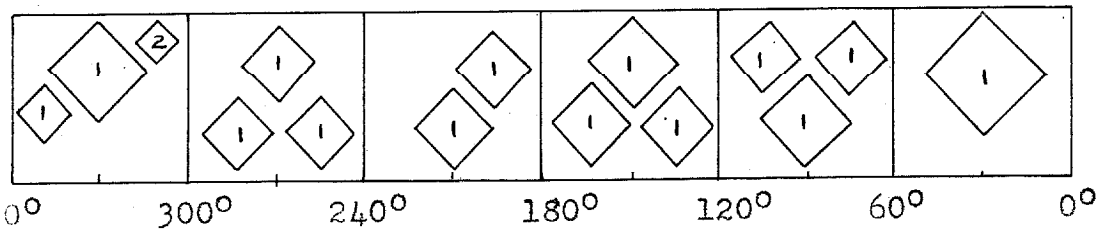

Figure 63

Buckle Pattern of Specimen No. 10

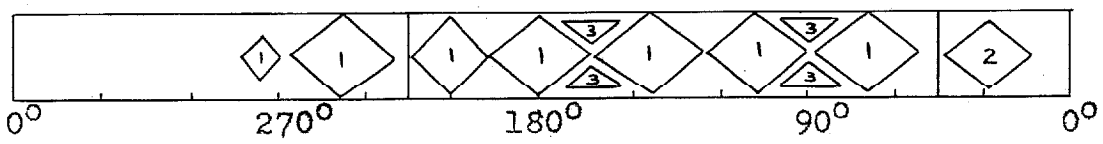

Figure 64

Buckle Pattern of Specimen No. 11

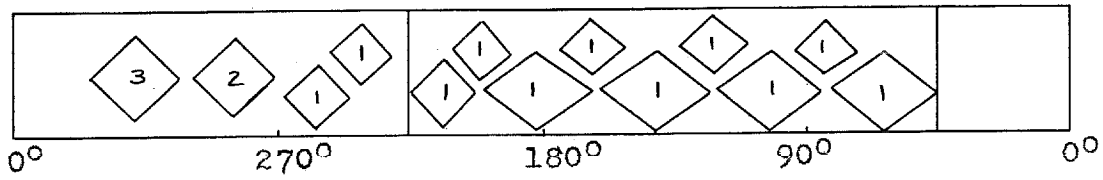

Figure 65

Buckle Pattern of Specimen No. 12

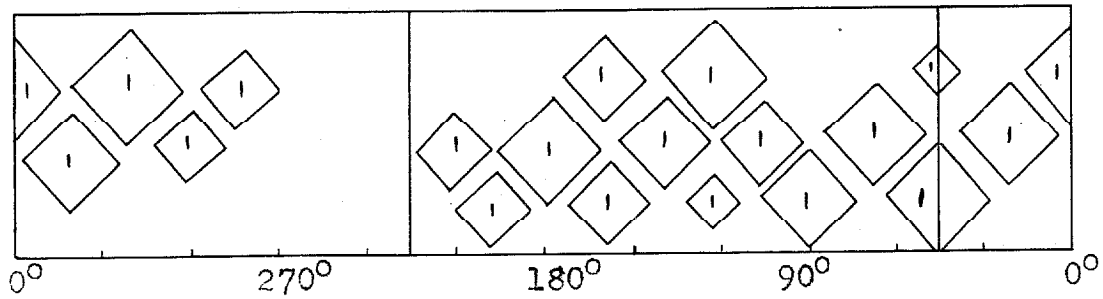

Figure 66

Buckle Pattern of Specimen No. 13

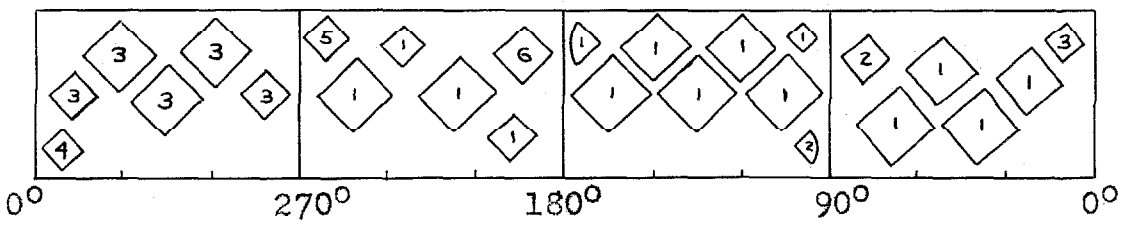

Figure 67

Buckle Pattern of Specimen No. 14

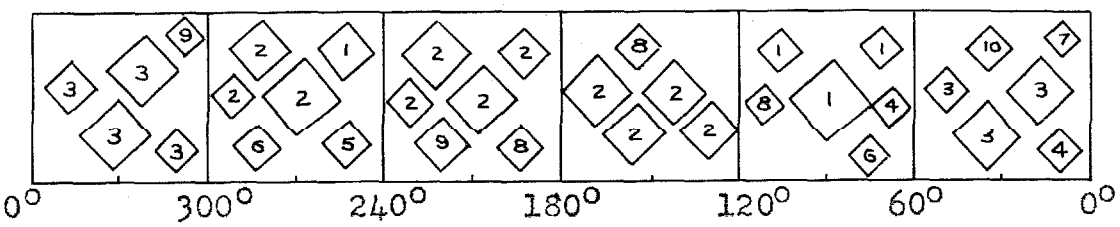

Figure 68

Buckle Pattern of Specimen No. 15

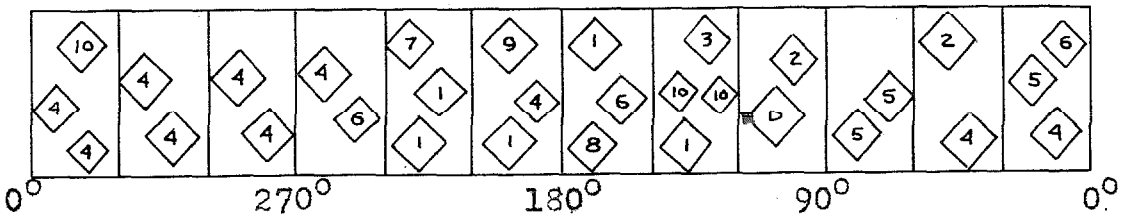

Figure 69

Buckle Pattern of Specimen No. 17

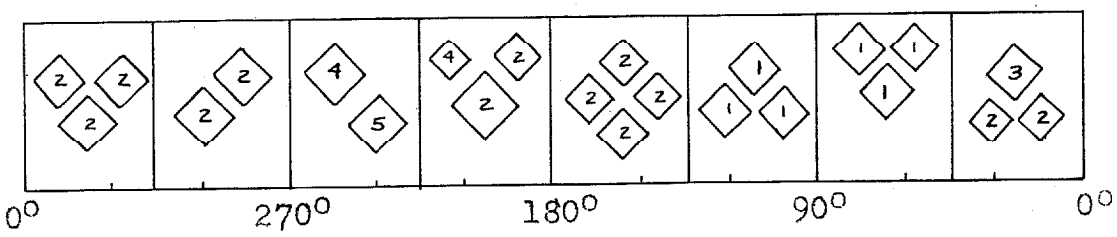

Figure 70

Buckle Pattern of Specimen No. 16

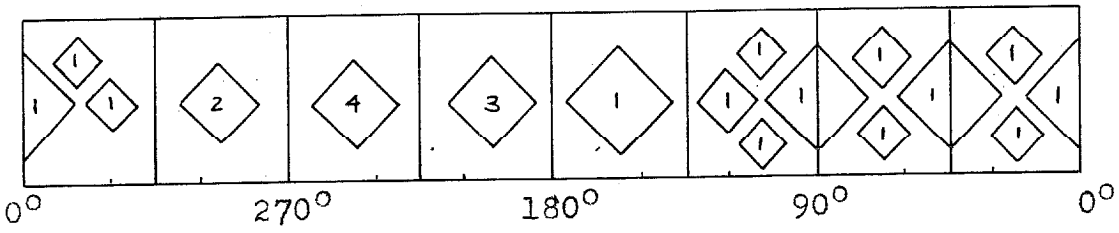

Figure 71

Buckle Pattern of Specimen No. 18

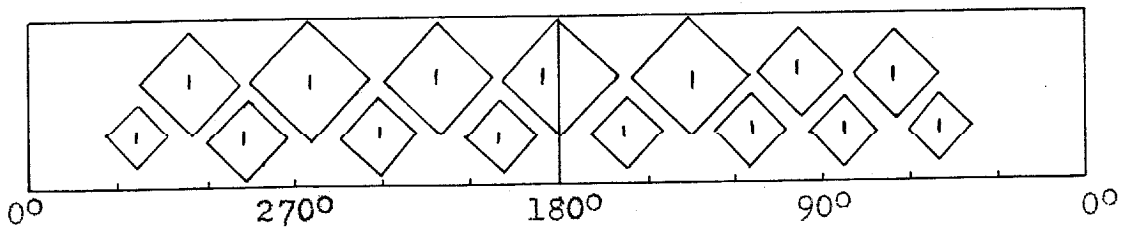

Figure 72

Buckle Pattern of Specimen No. 19

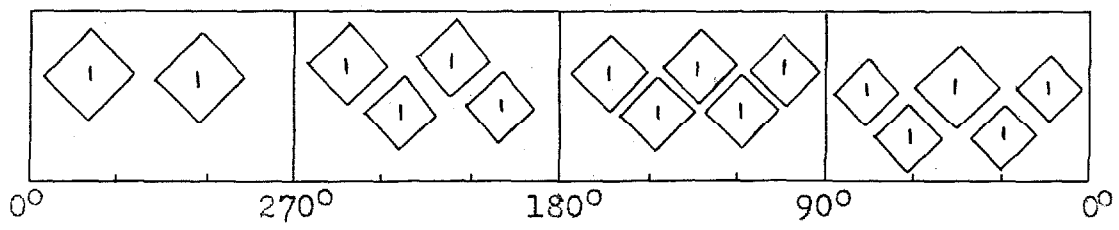

Figure 73

Buckle Pattern of Specimen No. 20

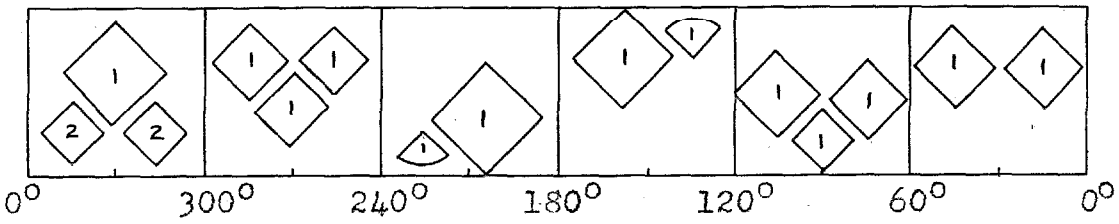

Figure 74

Buckle Pattern of Specimen No. 21

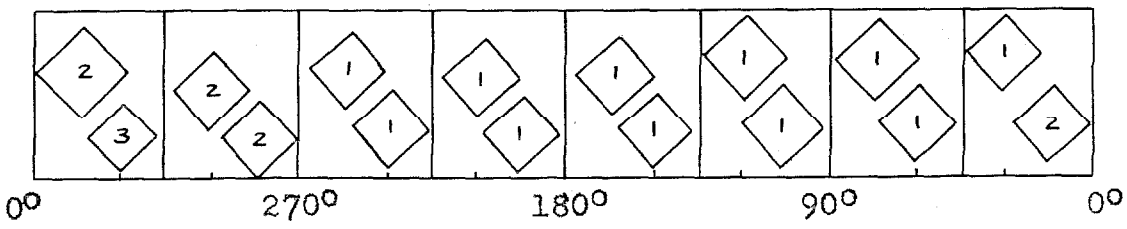

Figure 75

Buckle Pattern of Specimen No. 22

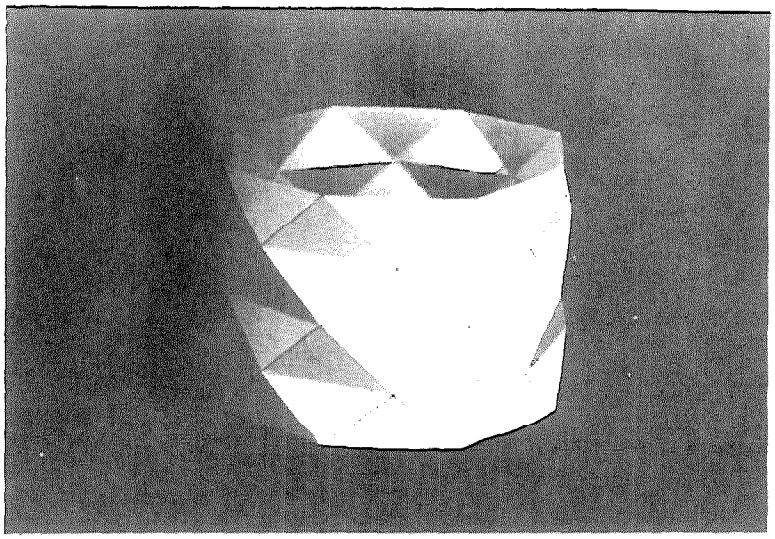

Figure 76

Developable Concave Polyhedron with Octagonal Section

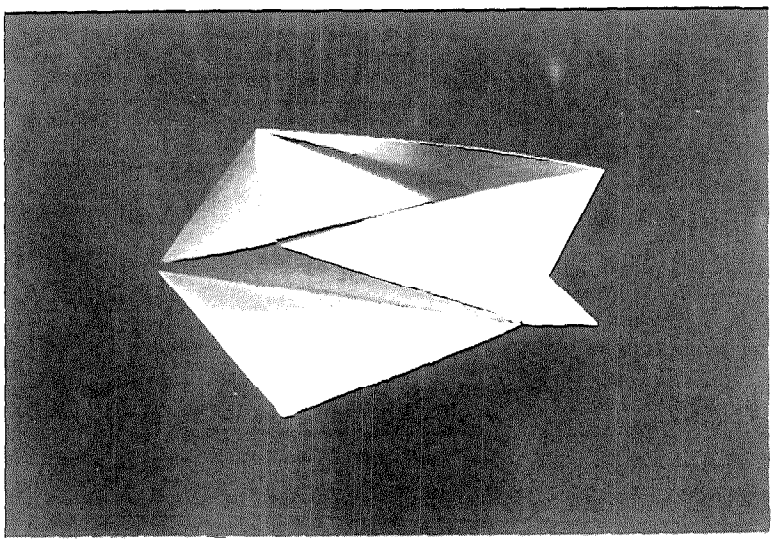

Figure 77

Developable Concave Polyhedron with Triangular Section

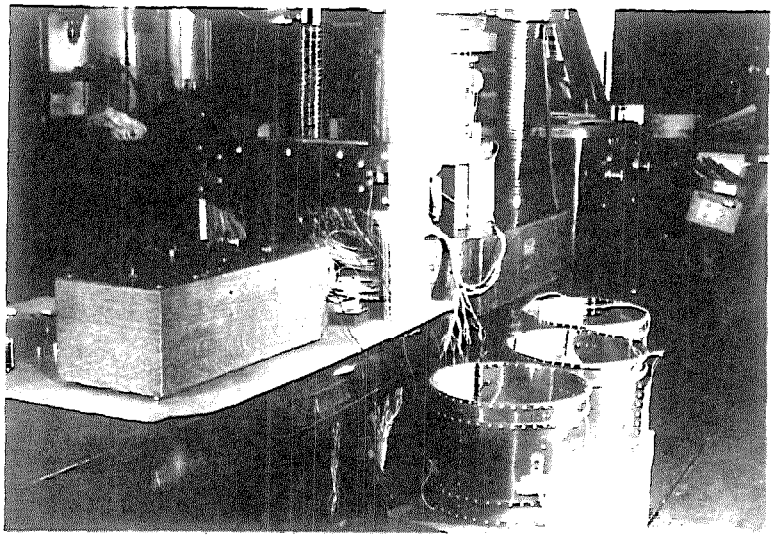

Figure 78

Experimental Test Equipment

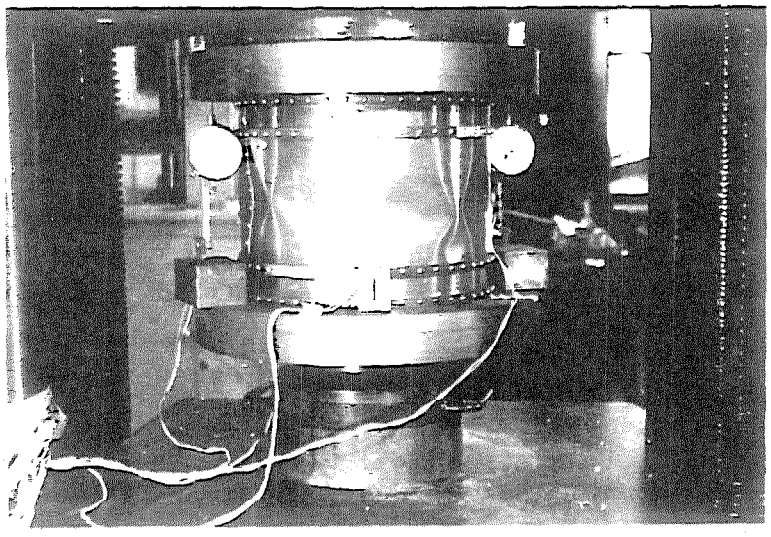

Figure 79

Specimen No. 1 at Buckle State 1

(note Buckle State on Figure 3)

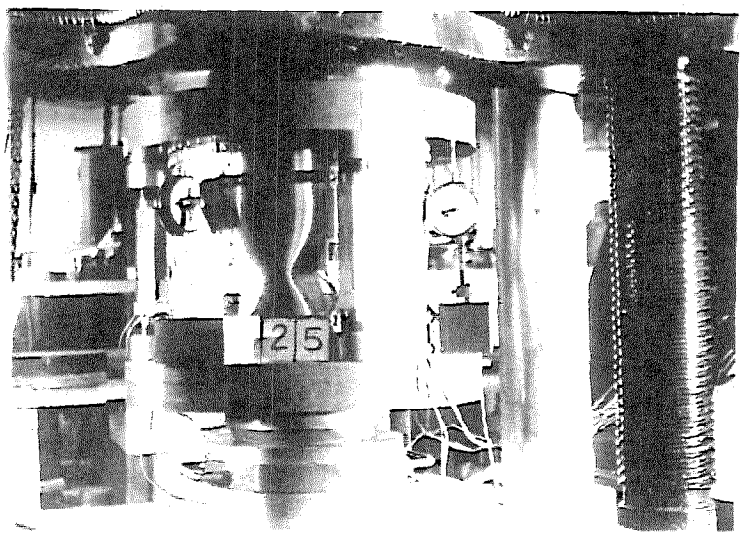

Figure 80

Specimen No. 1A at Buckle State 3

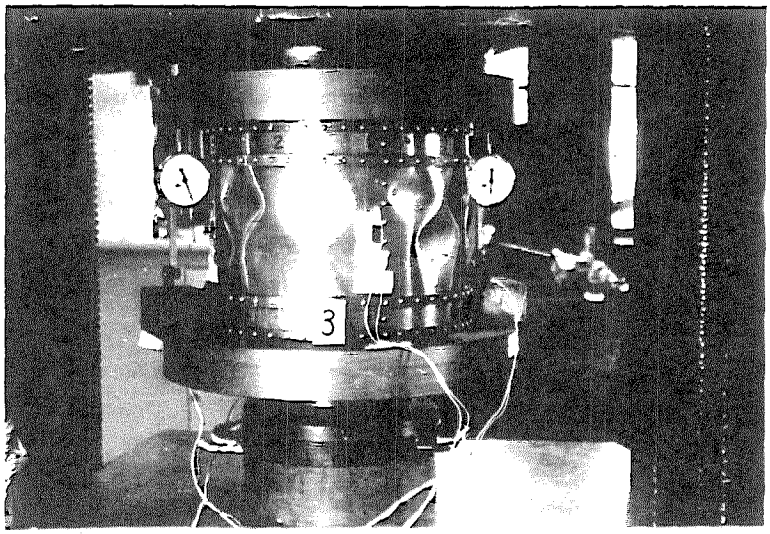

Figure 81

Specimen No. 2 at Buckle State 1

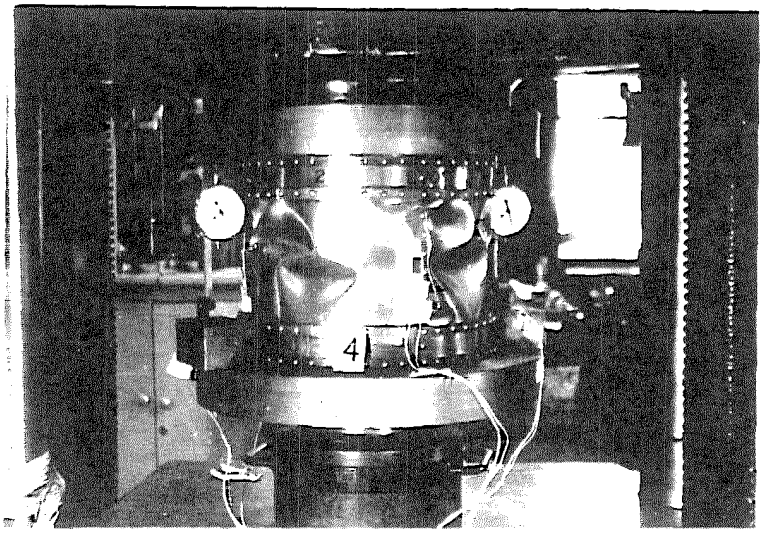

Figure 82

Specimen No. 2 at Buckle State 2

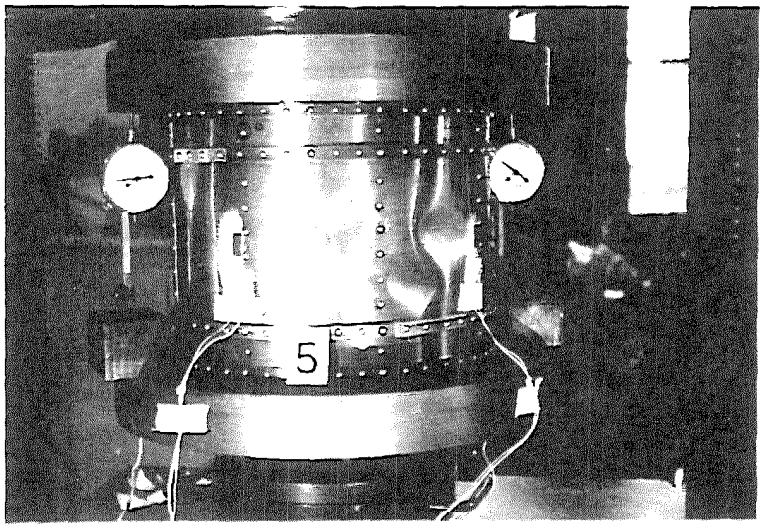

Figure 83

Specimen No. 3 at Buckle State 1

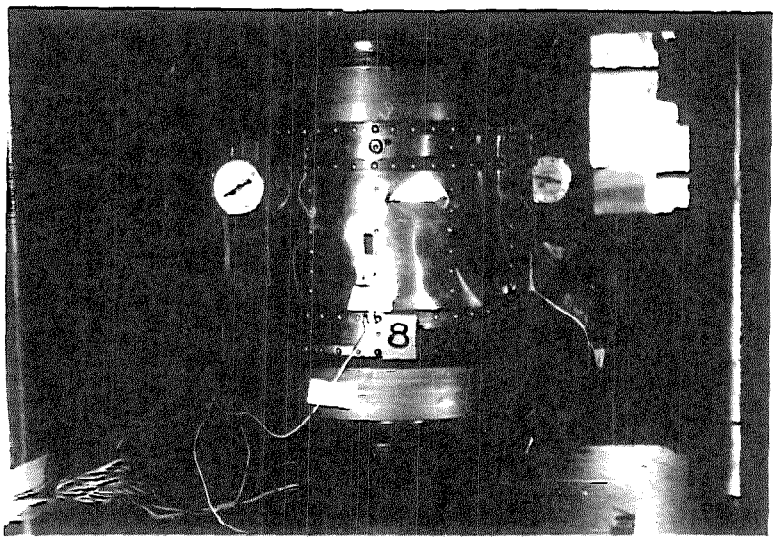

Figure 84

Specimen No. 4 at Buckle State 5

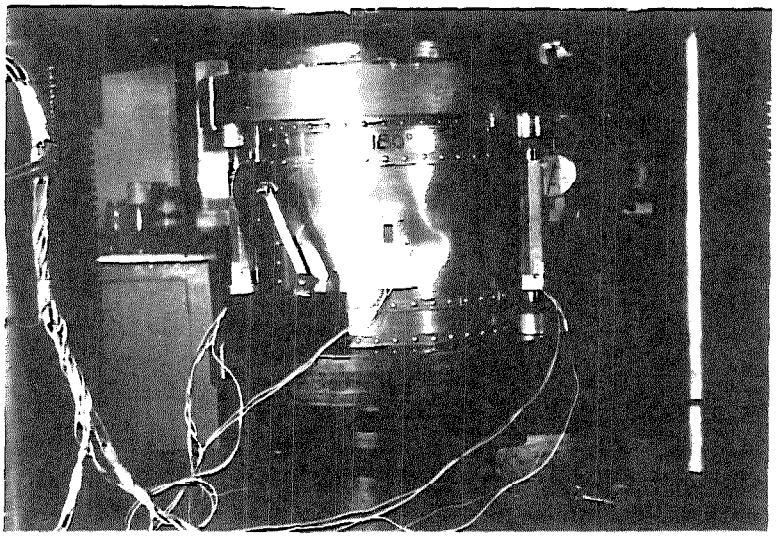

Figure 85

Specimen No. 5 at Buckle State 1

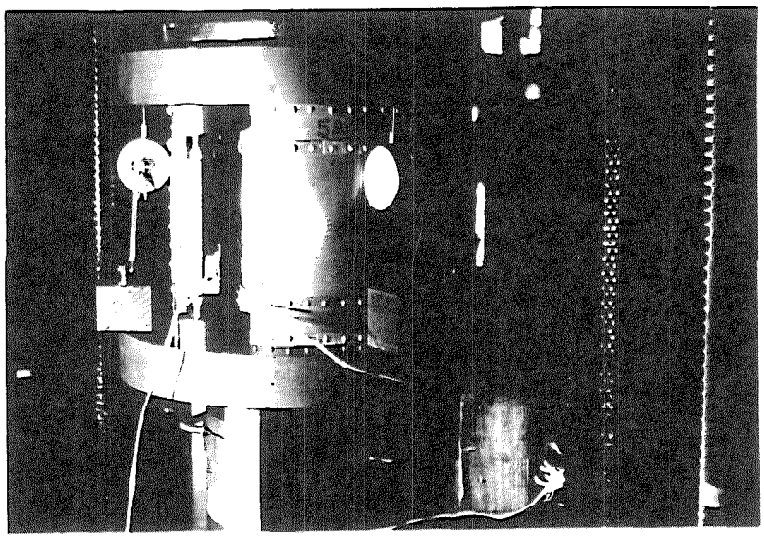

Figure 86

Specimen No. 5A at Buckle State 1

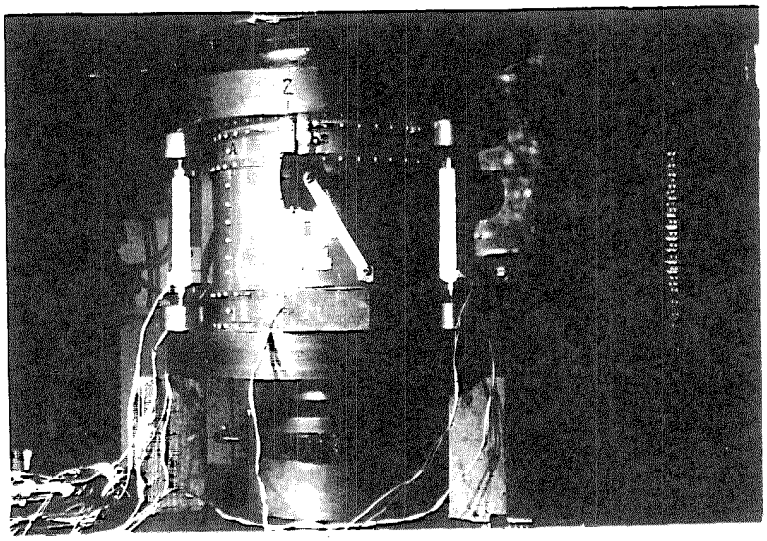

Figure 87

Specimen No. 5A at Buckle State 1

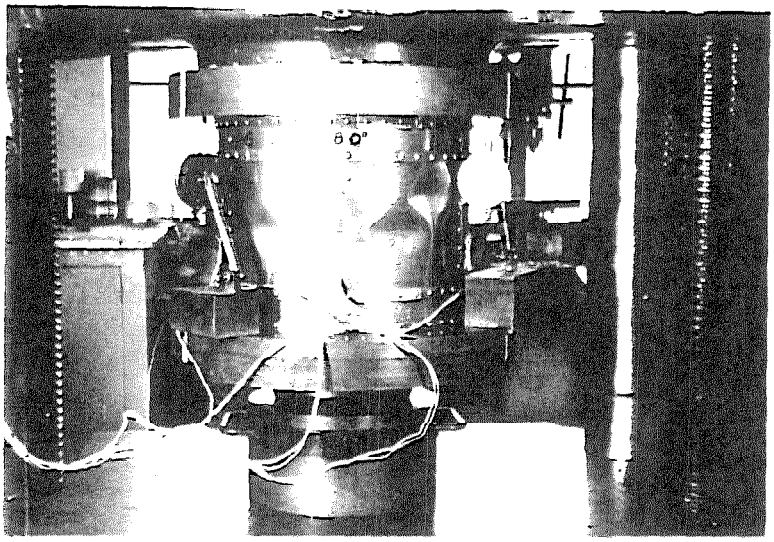

Figure 88

Specimen No. 6 at Buckle State 1

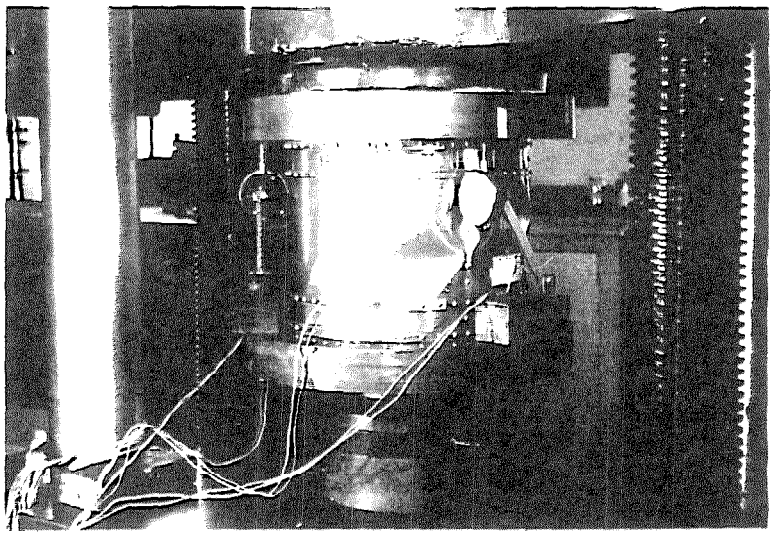

Figure 89

Specimen No. 7 at Buckle State 1

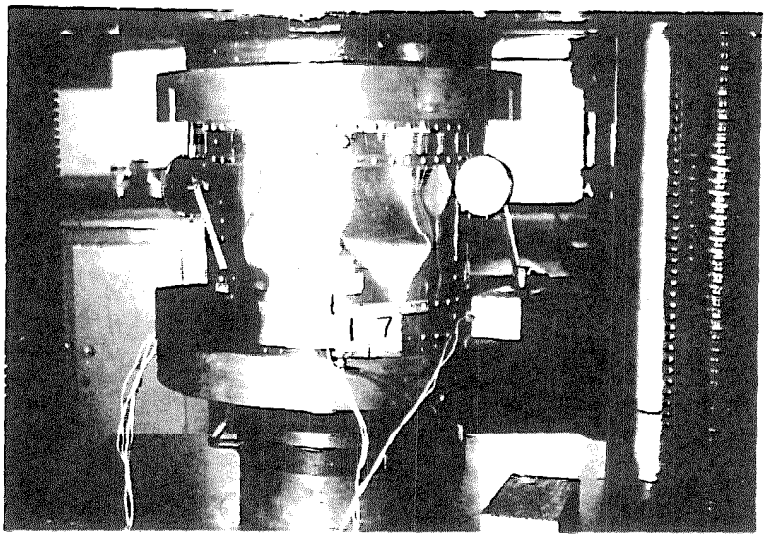

Figure 90

Specimen No. 8 at Buckle State 1

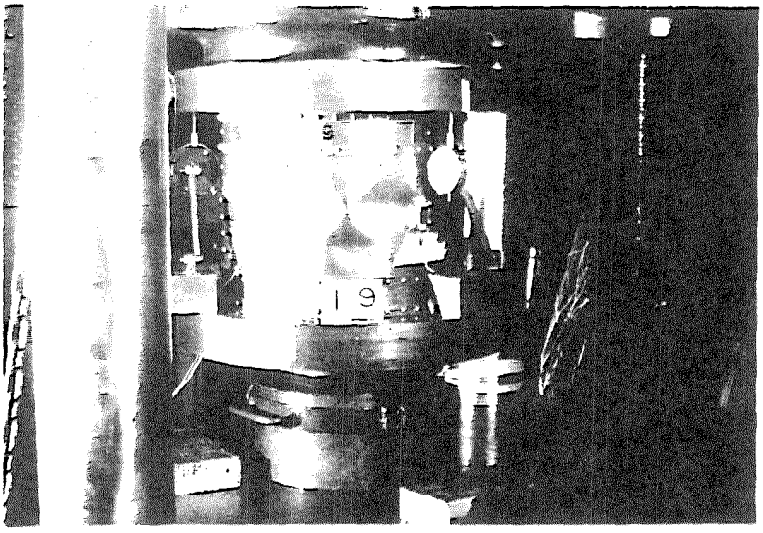

Figure 91

Specimen No. 9 at Buckle State 1

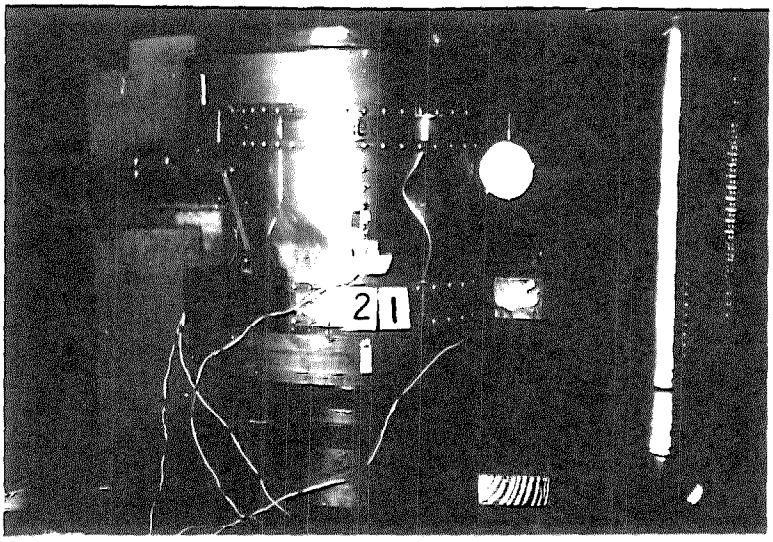

Figure 92

Specimen No. 10 at Buckle State 1

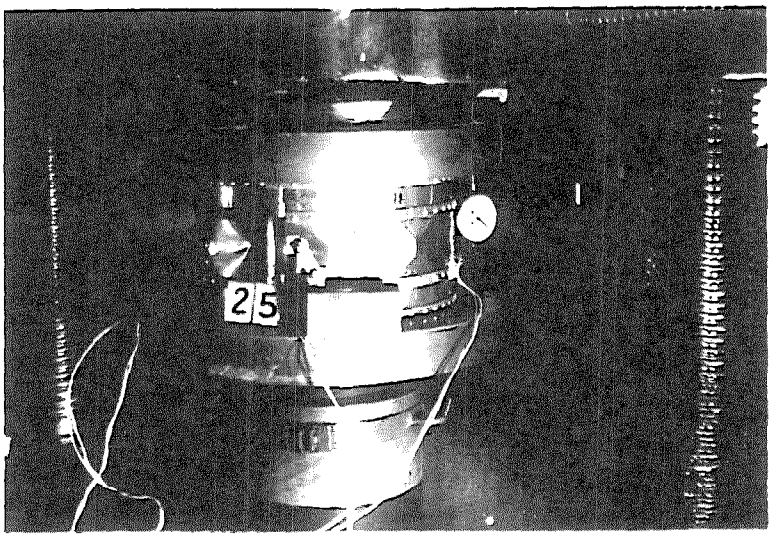

Figure 93

Specimen No. 11 at Buckle State 1

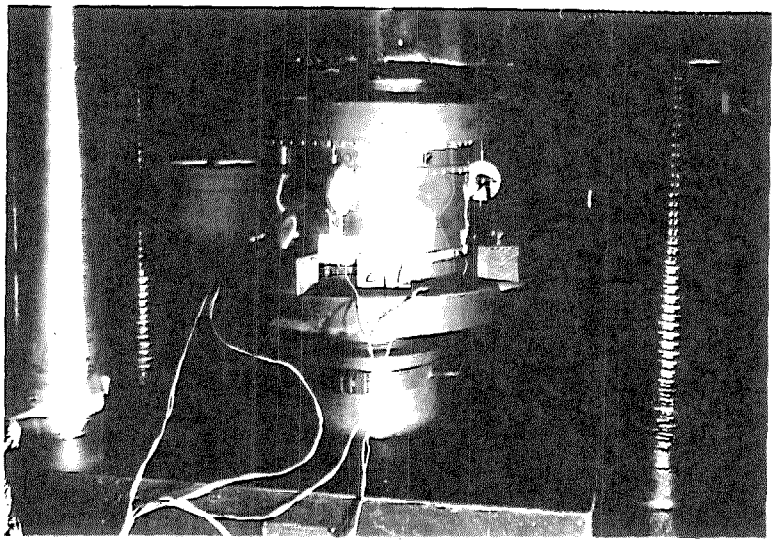

Figure 94

Specimen No. 12 at Buckle State 1

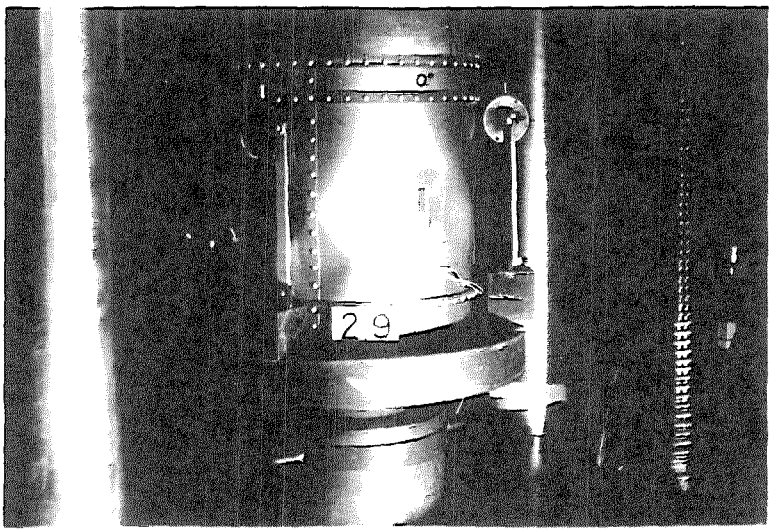

Figure 95

Specimen No. 13 at Buckle State 1

(compare with Figure 76)

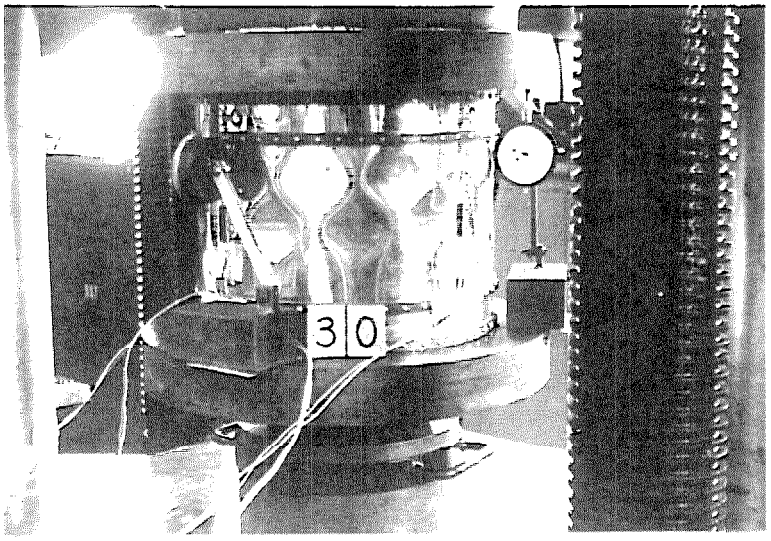

Figure 96

Specimen No. 14 at Buckle State 1

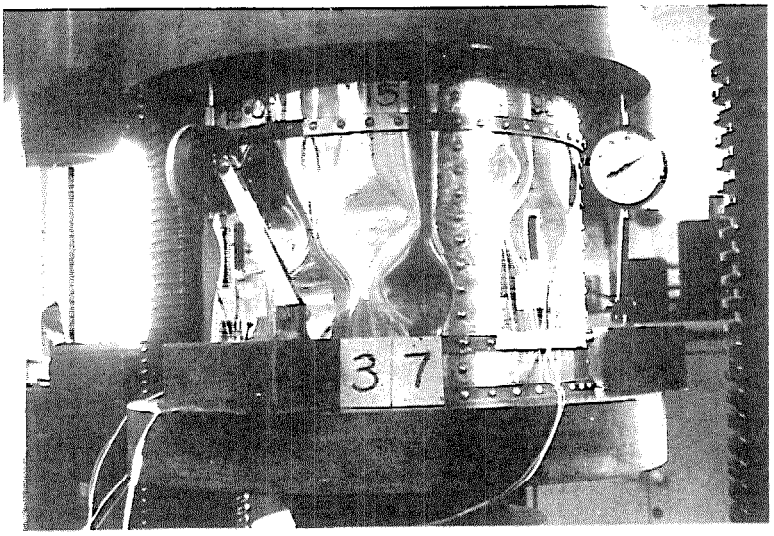

Figure 97

Specimen No. 15 at Buckle State 2

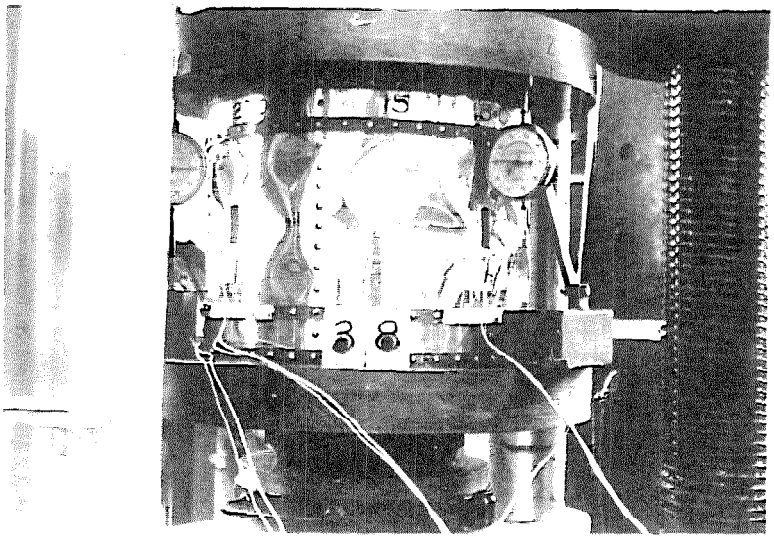

Figure 98

Specimen No. 15 at Buckle State 5

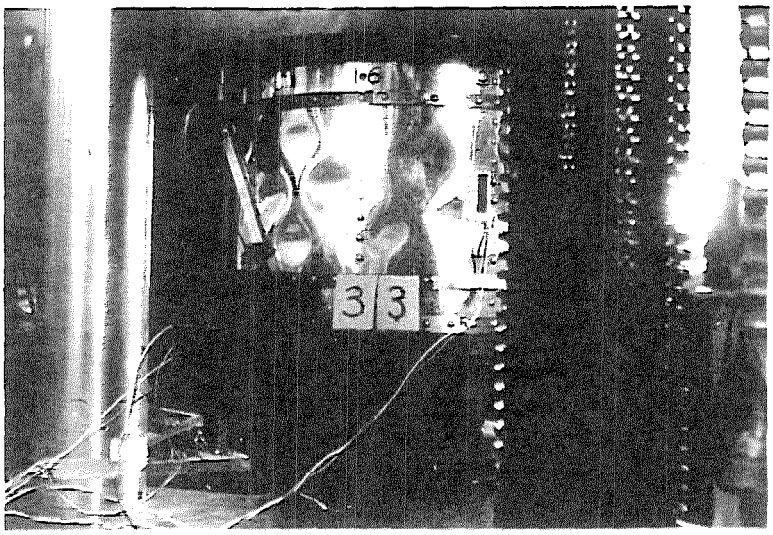

Figure 99

Specimen No. 16 at Buckle State 2

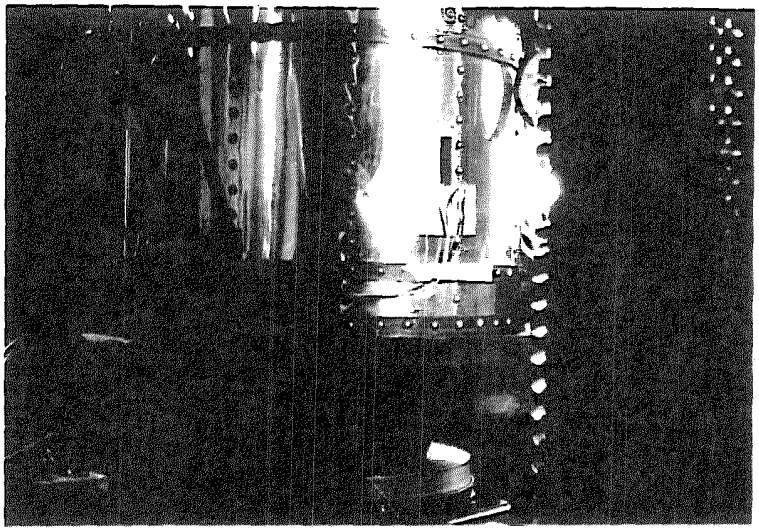

Figure 100

Buckle in Specimen No. 17

Resulting From Rivet Gun Dent Near Stiffener

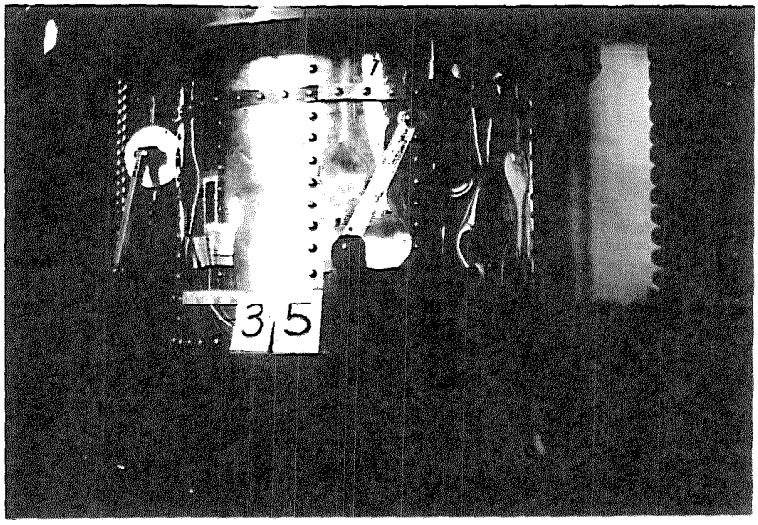

Figure 101

Specimen No. 17 at Buckle State 5

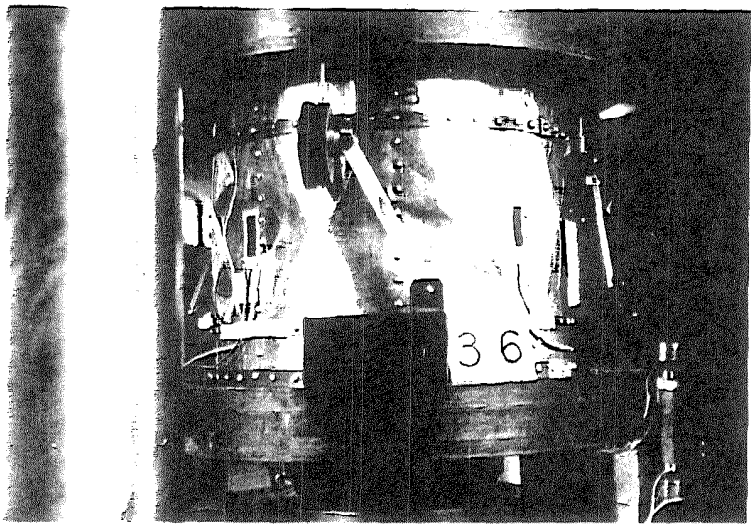

Figure 102

Specimen No. 18 at Buckle State 1

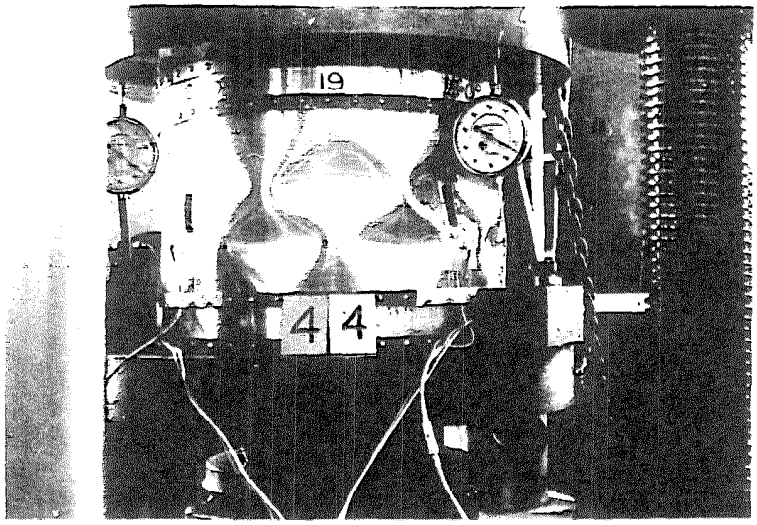

Figure 103

Specimen No. 19 at Buckle State 1

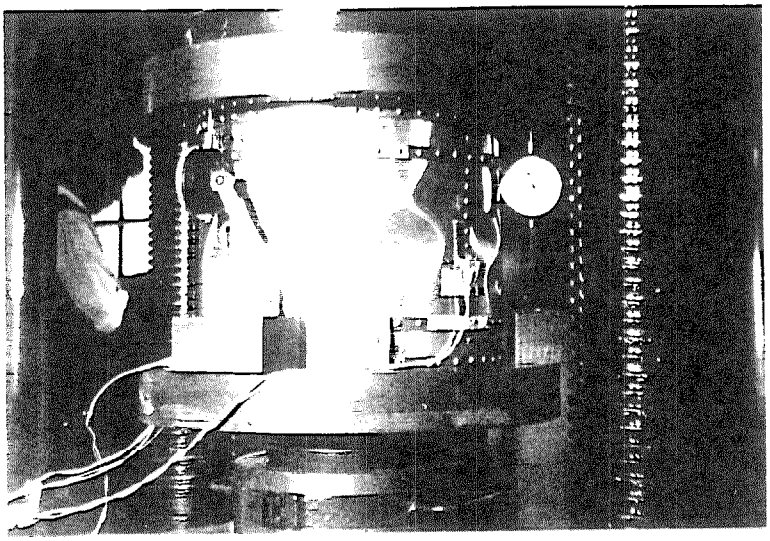

Figure 104

Specimen No. 20 at Buckle State 1

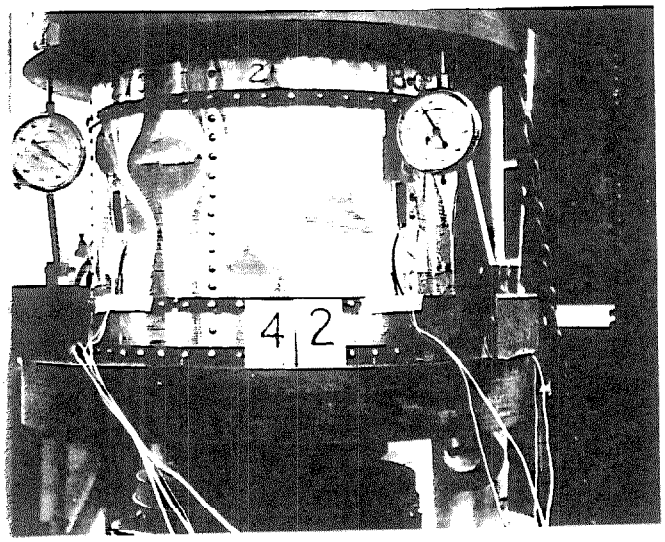

Figure 105

Specimen No. 21 at Buckle State 1

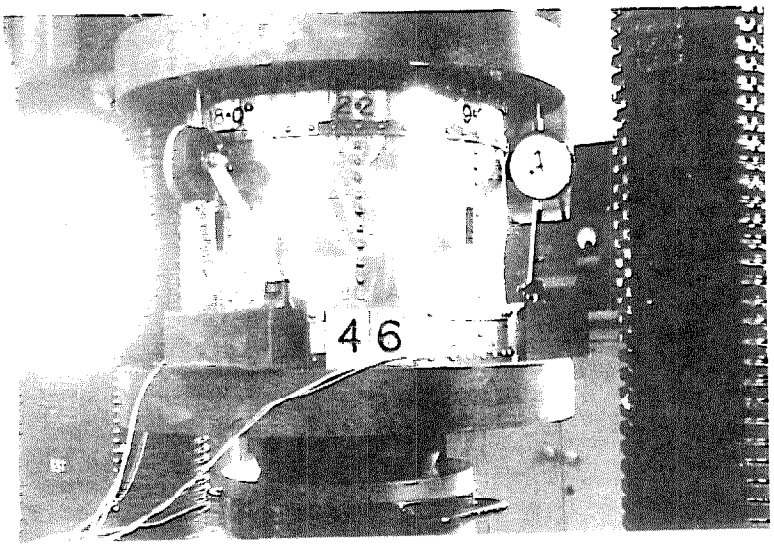

Figure 106

Specimen No. 22 at Buckle State 1

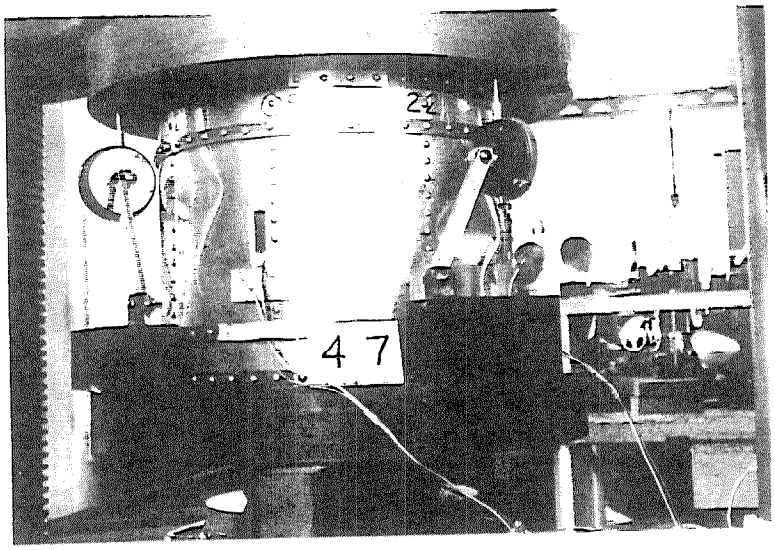

Figure 107

Specimen No. 22 at Buckle State 2

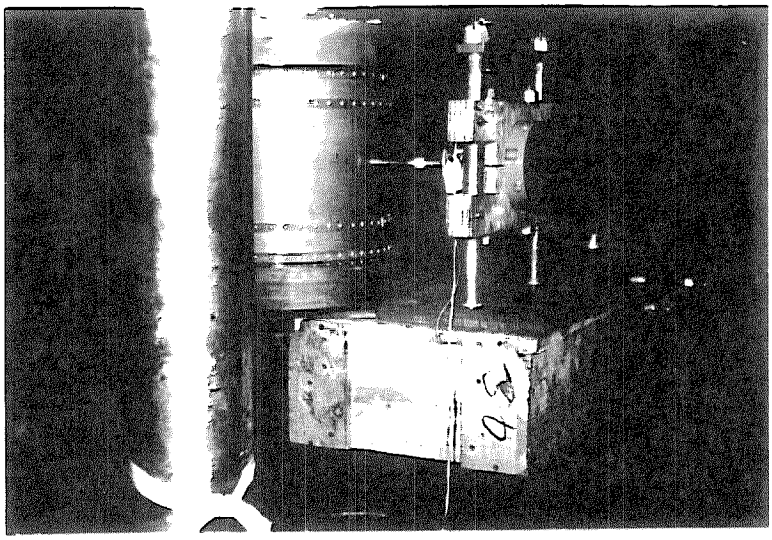

Figure 108

Vibrator Attached to Specimen No. 5b

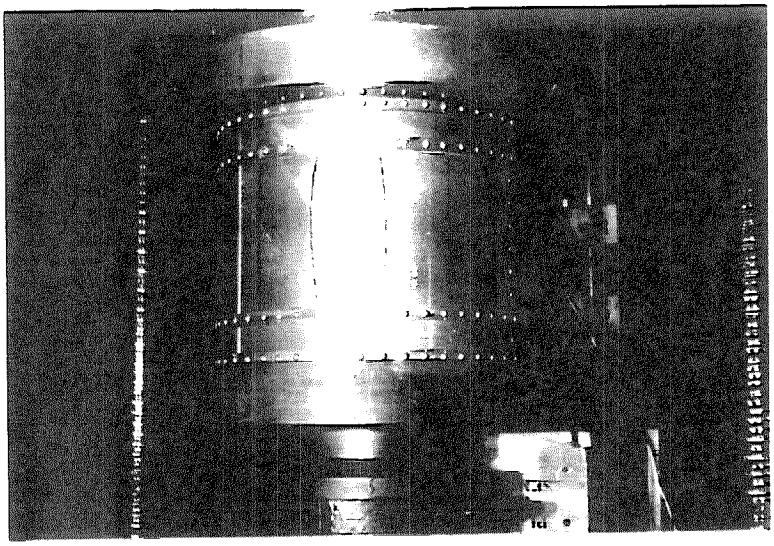

Figure 109

Vibration Node Lines on Specimen No. 5b

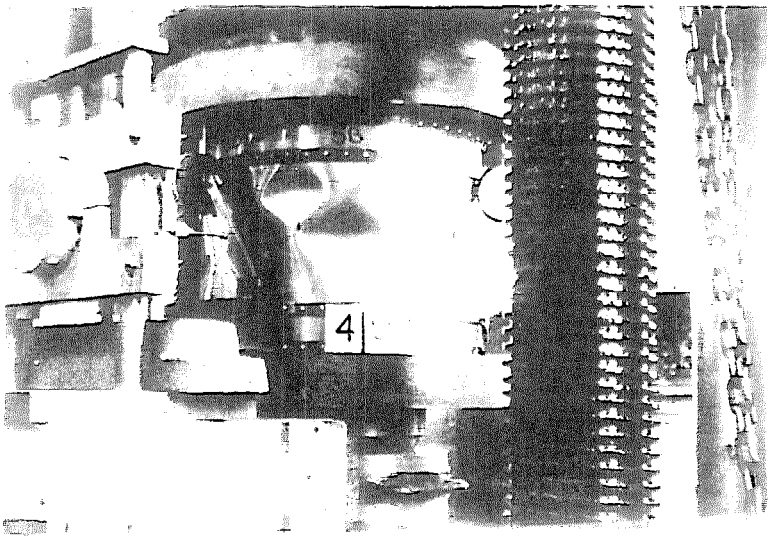

Figure 1

Specimen No. 5 at Buckle State 1

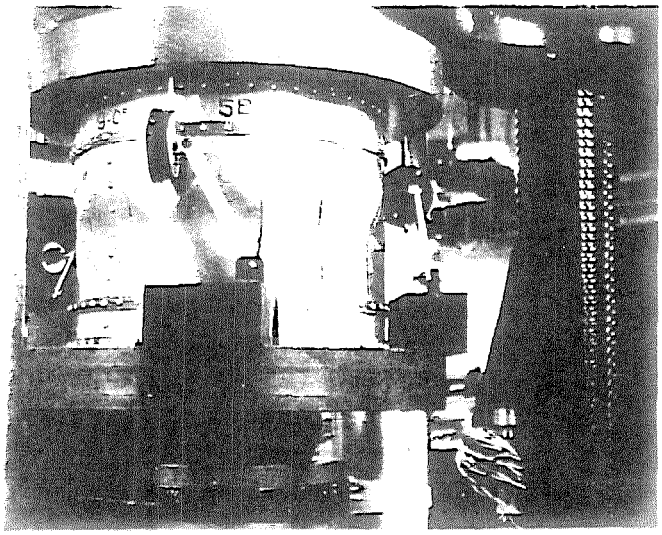

Figure 111

Specimen No. 5B at Buckle State 1

Figure 12

The Effect of Stiffener Spacing on the Buckling Stress

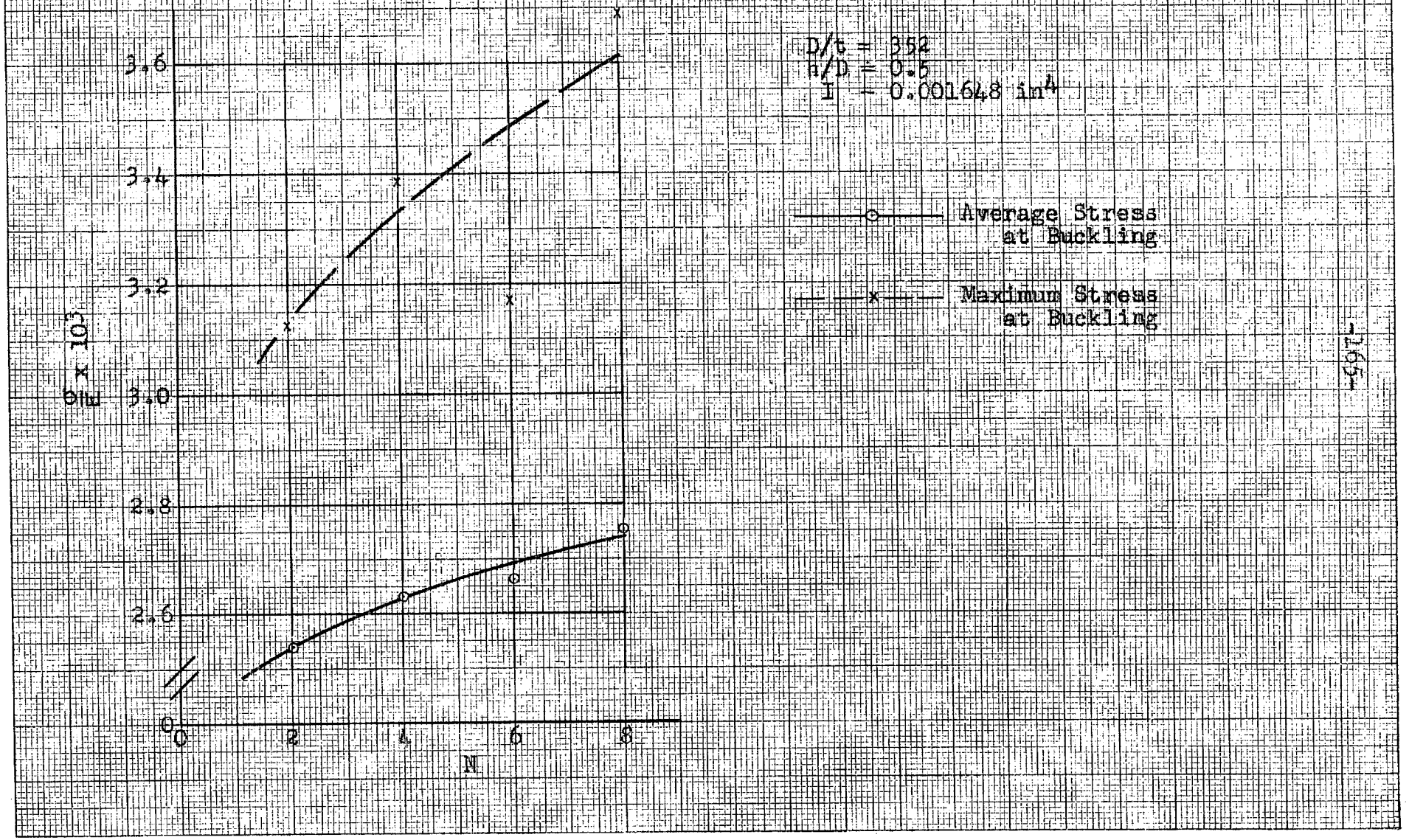

Figure 113

The Effect of Stiffener Spacing on the Buckling Stress

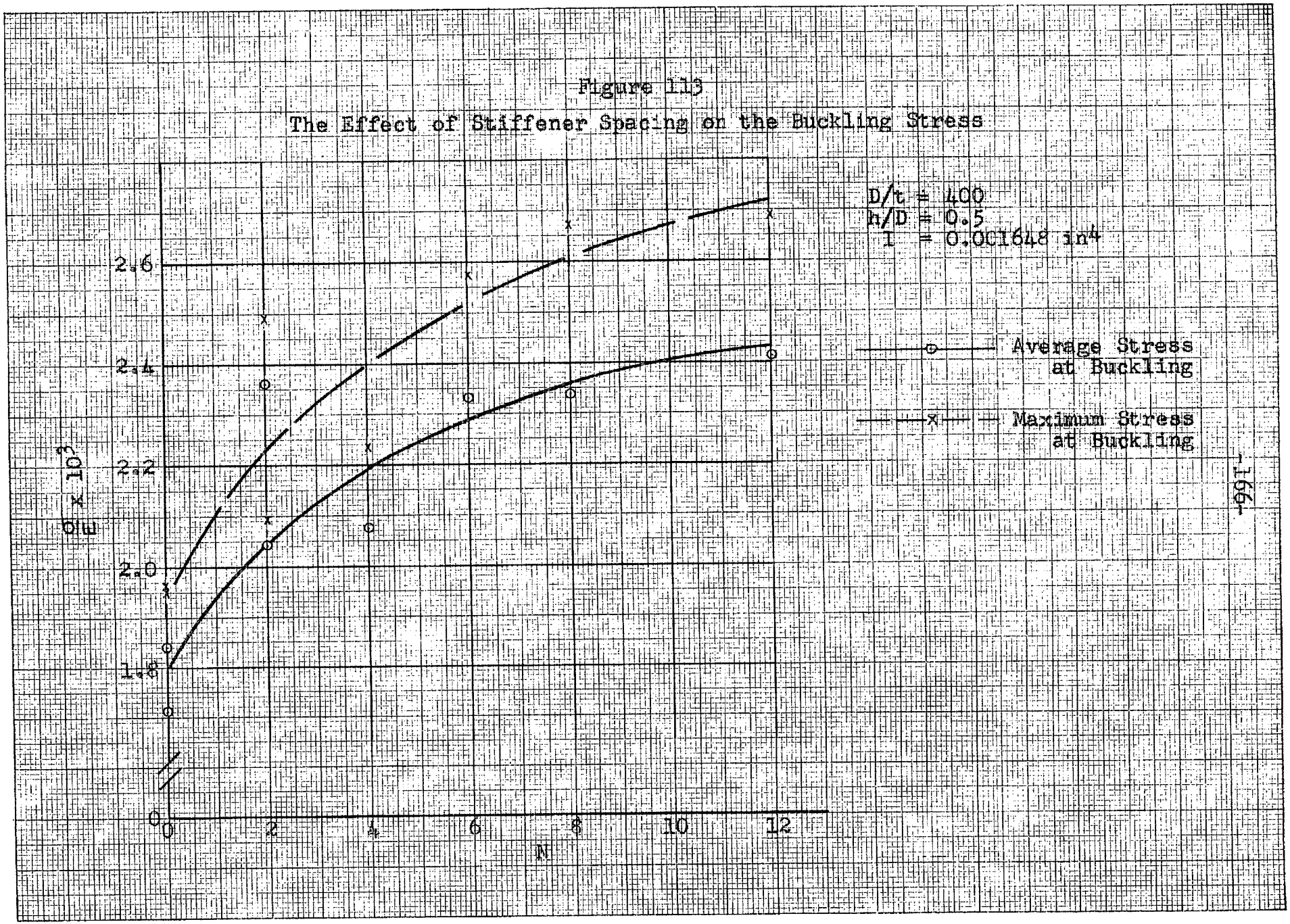

Figure 114

The Effect of Stiffener Spacing on the Buckling Stress

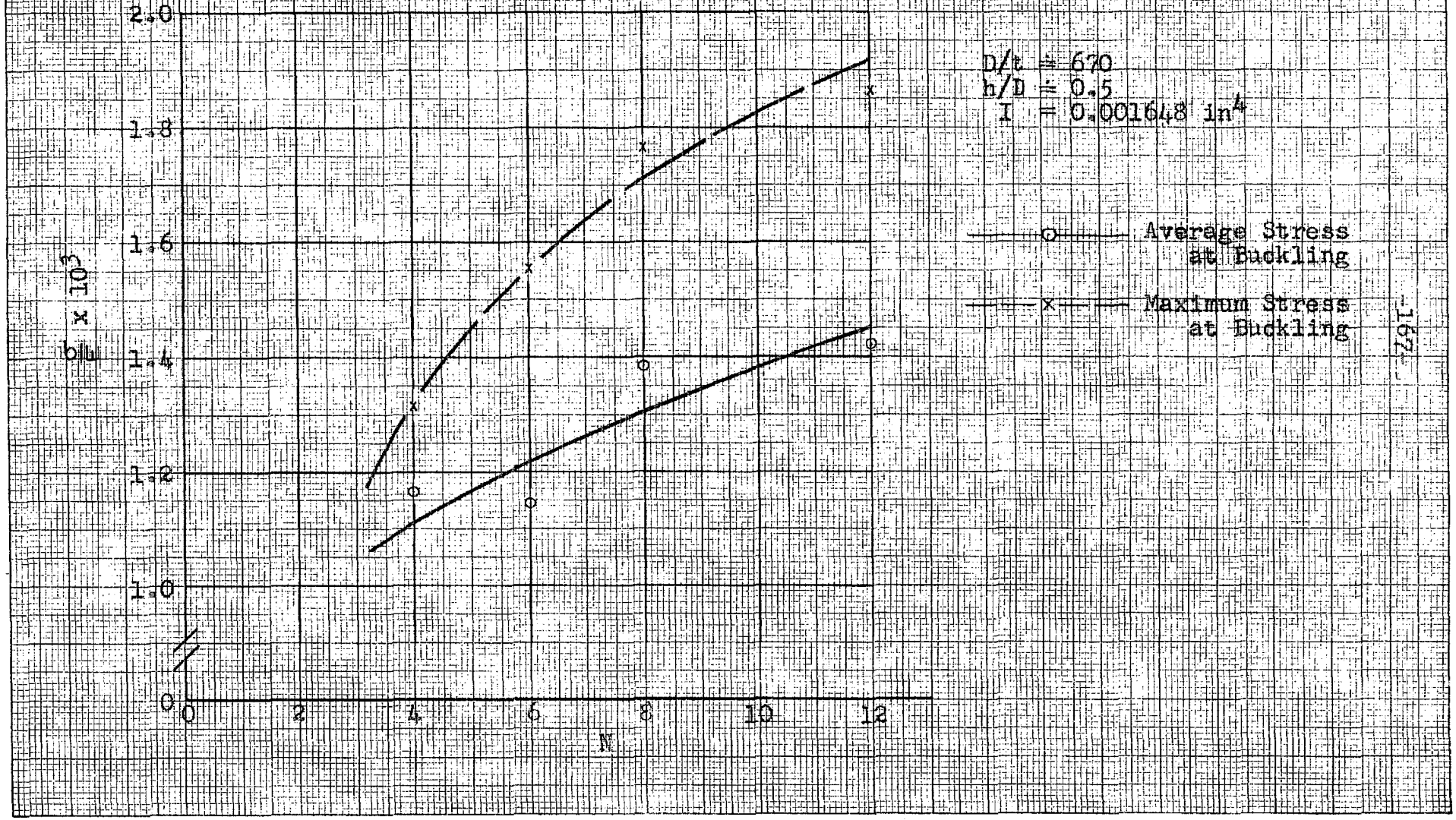

Figure 115

The Variation of Corrected Buckling Stress with D/t and N, Cross Plotted from Paired Experimental Data

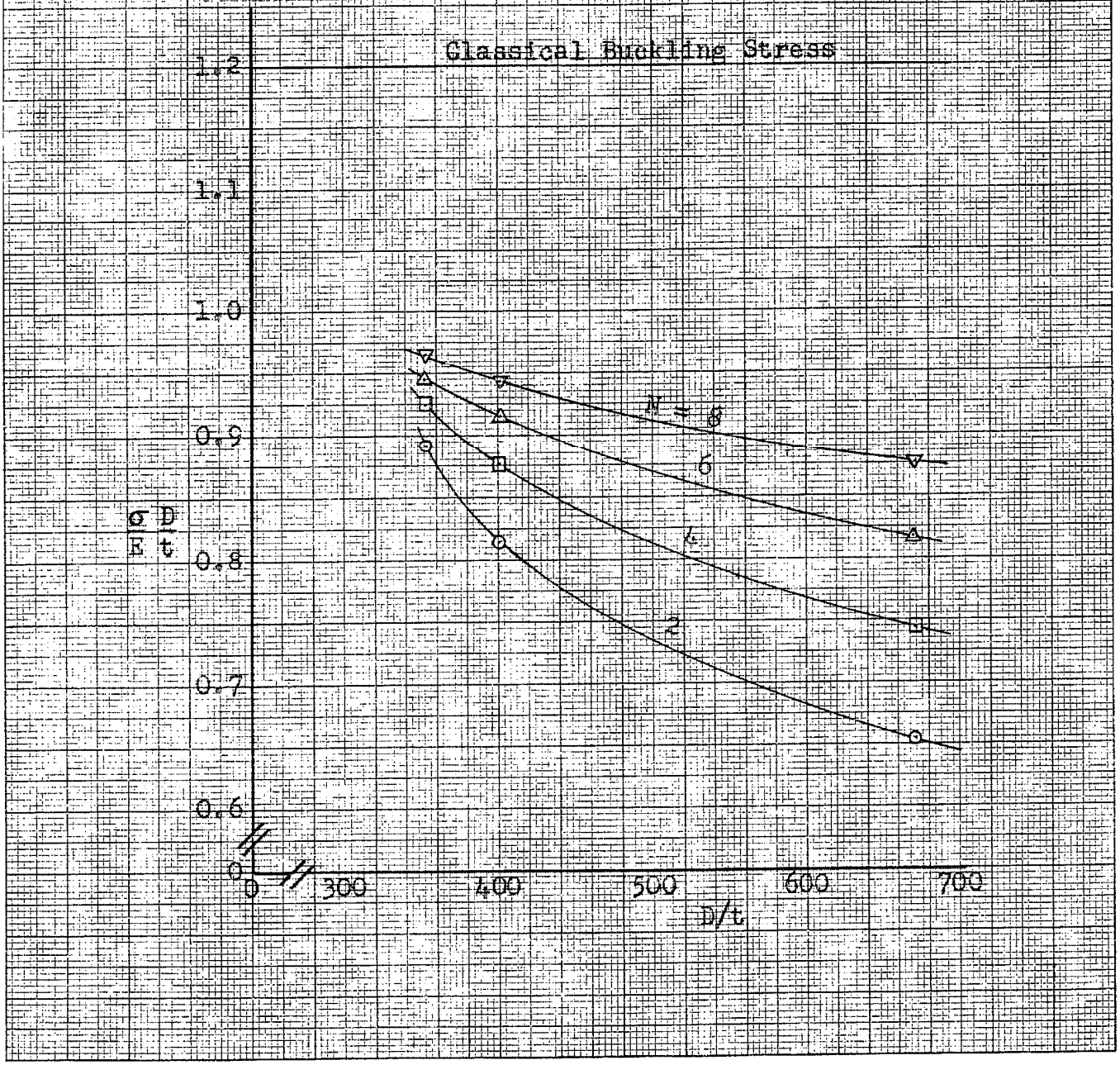

Figure 116

The Effect of Ring Spacing on the Buckling Stress

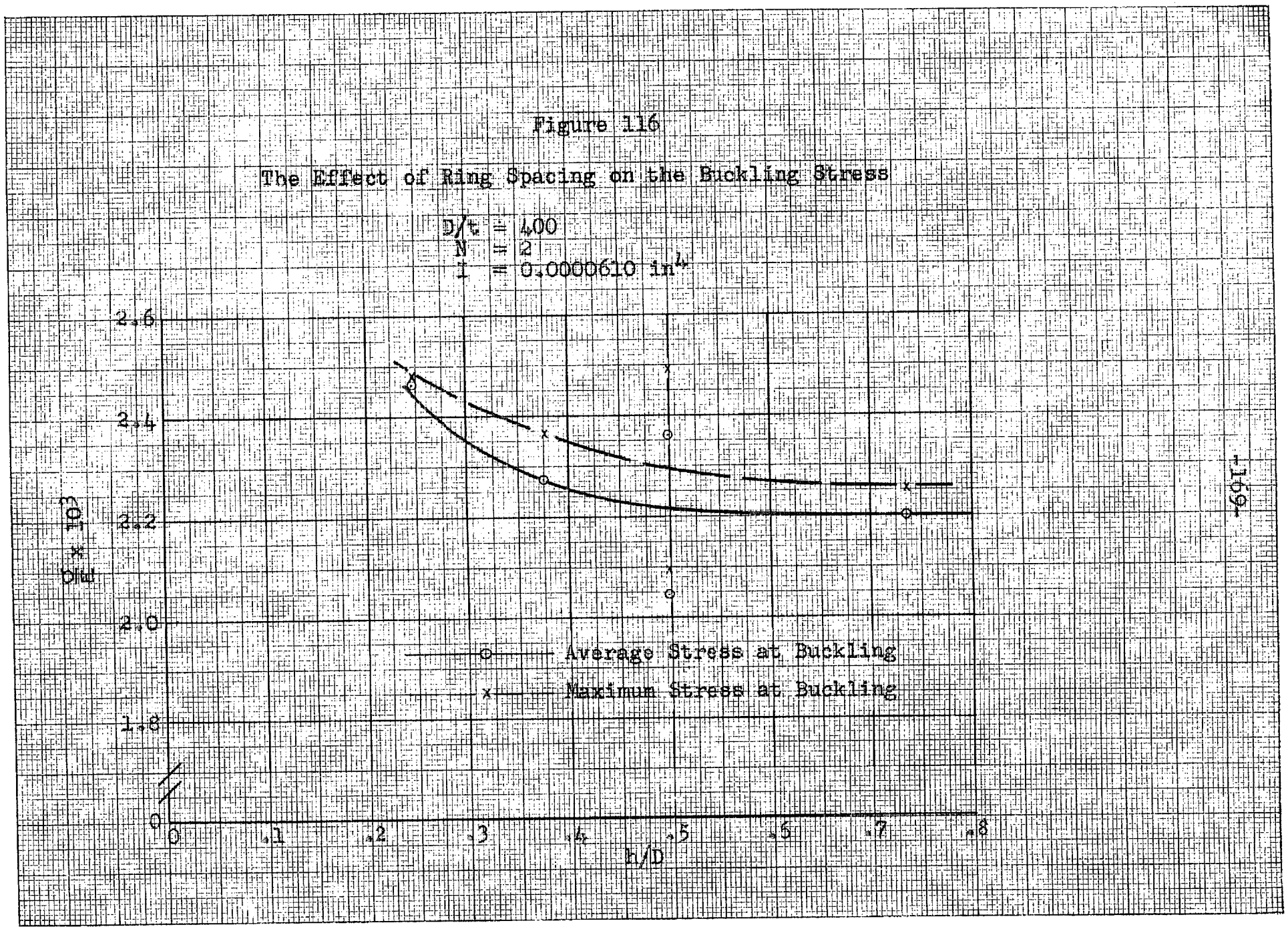

Figure 117

The Effect of Stiffener Moment of Inertia on the Buckling Stress

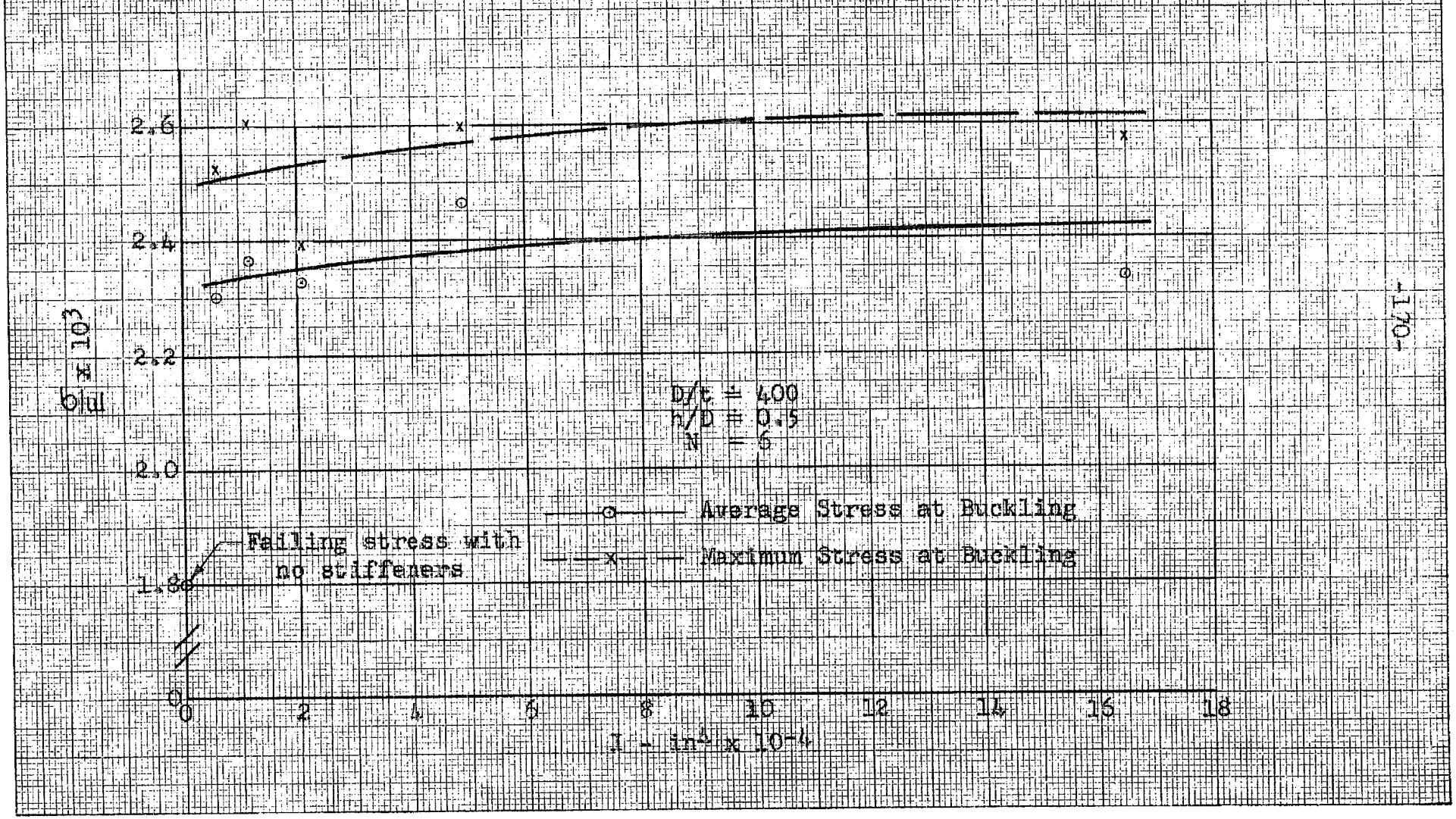

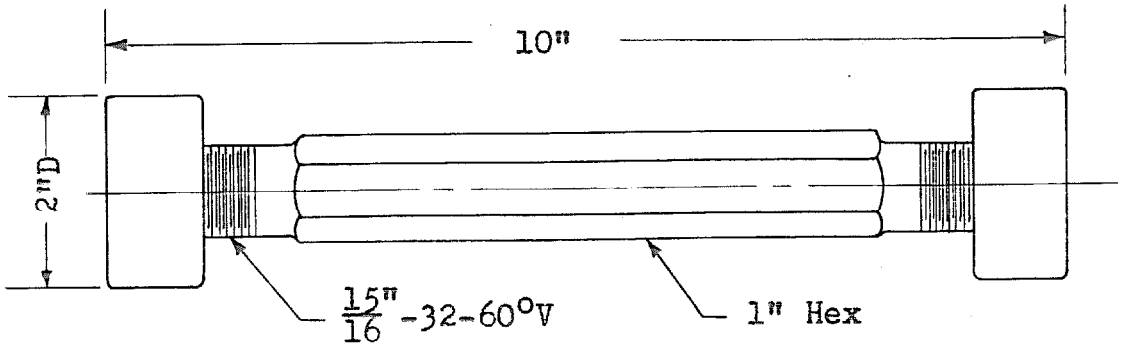

Small Jack

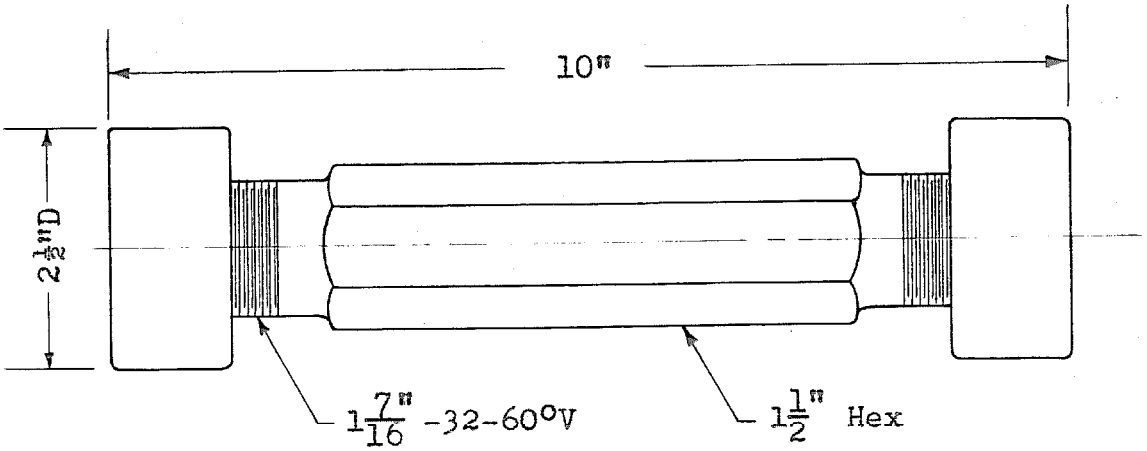

Large Jack

Figure 118

Details of Screw Jacks

Figure 119

Calibration Curve of Jack No. 1L,

Taken After Test of Specimen No. 5A

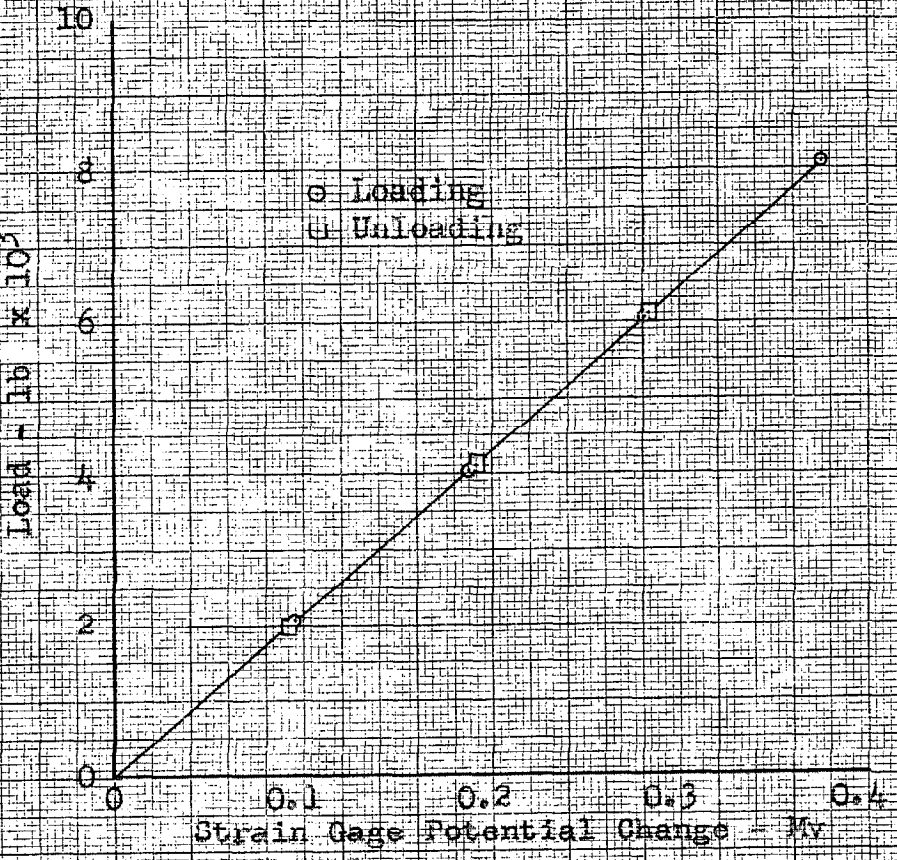

Figure 120

Location of Vibration Nodes on the Mid-Height Cross-Section of Specimen No. 5B, Compared with a Perfect Distribution

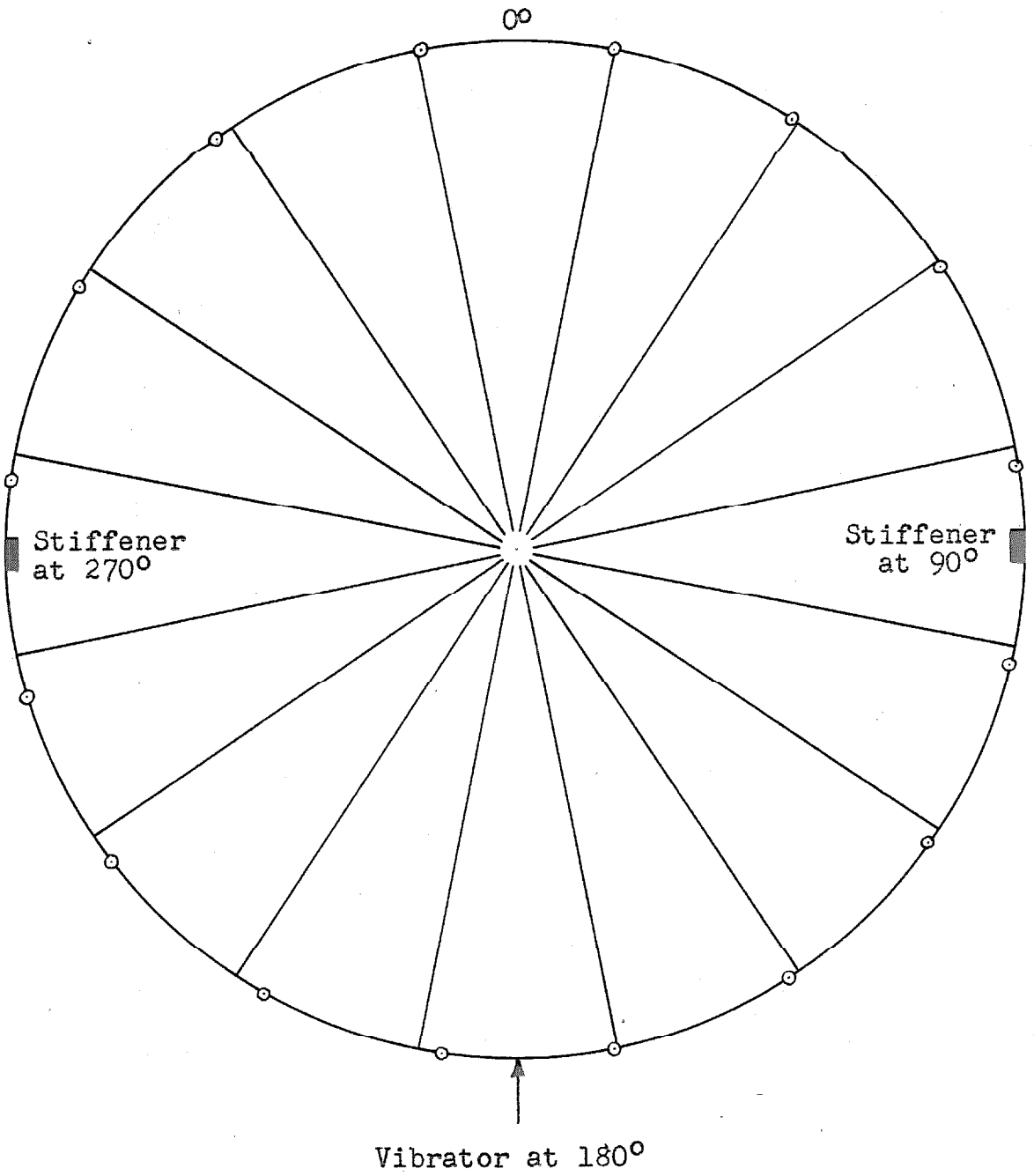

Figure 121

Variation of the Resonant Frequency of Specimen No. 5B with Load